

No.2/2015

# HYDRAULICA

HYDRAULICS-PNEUMATICS-TRIBOLOGY-ECOLOGY-SENSORICS-MECHATRONICS

ISSN 1453 - 7303  
ISSN-L 1453 - 7303

## CONTENTS

<ul style="list-style-type: none"> <li>• <b>EDITORIAL: Ce, De ce, Pentru cine? / What, Why, Whom for?</b> Ph.D. Petrin DRUMEA</li> </ul>	5 - 6
<ul style="list-style-type: none"> <li>• <b>Wireless Remote Control of Electro-Pneumatic Positioning System</b> Prof. Ryszard DINDORF, PhD., Piotr WOS, PhD.</li> </ul>	7 - 13
<ul style="list-style-type: none"> <li>• <b>Aspects Regarding Fluid Viscous Anchoring Systems Used for Vibration Mitigation at Bridge Structures</b> Assistant Professor Fănel Dorel ȘCHEAUA, PhD.</li> </ul>	14 - 17
<ul style="list-style-type: none"> <li>• <b>Designing of Liquid Piston Fluidyne Engines</b> Assistant Professor Sunny NARAYAN</li> </ul>	18 - 26
<ul style="list-style-type: none"> <li>• <b>Kinematic and Dynamic Irregularities of Roller Pumps Part II. Numerical Research, Results and Analysis</b> Prof. MSc. Gencho POPOV PhD., MSc. Yuliyang ANGELOV PhD.</li> </ul>	27- 34
<ul style="list-style-type: none"> <li>• <b>Static Characteristics of the Orifices in a Pilot Operated Pressure Relief Valve</b> PhD. eng. Sasko DIMITROV, PhD. eng. Simeon SIMEONOV, PhD. eng. Slavco CVETKOV</li> </ul>	35 - 39
<ul style="list-style-type: none"> <li>• <b>Experimental Determinations on Improving Dynamic and Energy Performance of Pneumatic Systems</b> PhD. eng. Gabriela MATAACHE, PhD. eng. Radu RADOI, PhD. eng. Gheorghe SOVAIALA, Tech. Ioan PAVEL</li> </ul>	40 - 47
<ul style="list-style-type: none"> <li>• <b>Laboratory Experiments Made on Corrugated Metallic Capsules, for Selecting Optimal Sensitive Elements in Pressure Transducers Used in Modern Mechatronics Systems</b> PhD Eng. Iulian Sorin MUNTEANU, St. PhD Eng. Anghel CONSTANTIN, PhD Eng. Petre MUNTEANU</li> </ul>	48 - 52
<ul style="list-style-type: none"> <li>• <b>Innovative Systems for Incremental Positioning in Pneumatics</b> Prof. Mihai AVRAM PhD, Prof. Constantin BUCȘAN PhD, Prof. Valeriu BANU PhD</li> </ul>	53 - 56
<ul style="list-style-type: none"> <li>• <b>Hydrostatic Transmissions Used to Drive a Collapsible Solar Thermal Collector</b> PhD. eng. Corneliu CRISTESCU, PhD. eng. Radu RADOI, PhD. eng. Catalin DUMITRESCU</li> </ul>	57 - 63

**BOARD****DIRECTOR OF PUBLICATION**

- PhD. Eng. Petrin DRUMEA - Hydraulics and Pneumatics Research Institute in Bucharest, Romania

**EDITOR-IN-CHIEF**

- PhD.Eng. Gabriela MATACHE - Hydraulics and Pneumatics Research Institute in Bucharest, Romania

**EXECUTIVE EDITOR**

- Ana-Maria POPESCU - Hydraulics and Pneumatics Research Institute in Bucharest, Romania

**EDITORIAL BOARD**

PhD.Eng. Gabriela MATACHE - Hydraulics and Pneumatics Research Institute in Bucharest, Romania

Assoc. Prof. Adolfo SENATORE, PhD. – University of Salerno, Italy

PhD.Eng. Catalin DUMITRESCU - Hydraulics and Pneumatics Research Institute in Bucharest, Romania

Assoc. Prof. Constantin CHIRITA, PhD. – “Gheorghe Asachi” Technical University of Iasi, Romania

PhD.Eng. Radu Iulian RADOI - Hydraulics and Pneumatics Research Institute in Bucharest, Romania

Assoc. Prof. Constantin RANEA, PhD. – University Politehnica of Bucharest; National Authority for Scientific Research and Innovation (ANCSI), Romania

Prof. Aurelian FATU, PhD. – Institute Pprime – University of Poitiers, France

PhD.Eng. Małgorzata MALEC – KOMAG Institute of Mining Technology in Gliwice, Poland

Lect. Ioan-Lucian MARCU, PhD. – Technical University of Cluj-Napoca, Romania

**COMMITTEE OF REVIEWERS**

PhD.Eng. Corneliu CRISTESCU – Hydraulics and Pneumatics Research Institute in Bucharest, Romania

Assoc. Prof. Pavel MACH, PhD. – Czech Technical University in Prague, Czech Republic

Prof. Ilare BORDEASU, PhD. – Politehnica University of Timisoara, Romania

Prof. Valeriu DULGHERU, PhD. – Technical University of Moldova, Chisinau, Republic of Moldova

Assist. Prof. Krzysztof KĘDZIA, PhD. – Wrocław University of Technology, Poland

Assoc. Prof. Andrei DRUMEA, PhD. – University Politehnica of Bucharest, Romania

PhD.Eng. Marian BLEJAN - Hydraulics and Pneumatics Research Institute in Bucharest, Romania

Prof. Mihai AVRAM, PhD. – University Politehnica of Bucharest, Romania

Prof. Dan OPRUTA, PhD. – Technical University of Cluj-Napoca, Romania

Prof. Ion PIRNA, PhD. – The National Institute of Research and Development for Machines and Installations Designed to Agriculture and Food Industry - INMA Bucharest, Romania

**Published by:**

**Hydraulics and Pneumatics Research Institute, Bucharest-Romania**

Address: 14 Cuțitul de Argint, district 4, Bucharest, 040558, Romania

Phone: +40 21 336 39 91; Fax:+40 21 337 30 40;

e-Mail: [ihp@fluidas.ro](mailto:ihp@fluidas.ro); Web: [www.ihp.ro](http://www.ihp.ro)

**with support from:**

**National Professional Association of Hydraulics and Pneumatics in Romania - FLUIDAS**

e-Mail: [fluidas@fluidas.ro](mailto:fluidas@fluidas.ro); Web: [www.fluidas.ro](http://www.fluidas.ro)

**HIDRAULICA Magazine** is indexed by international databases:



## EDITORIAL

### Ce, De ce, Pentru cine?

In ultimul timp am fost surprins sa aud cateva intrebari care exprima o mare deruta la nivelul cercetarii si invatamantului superior, totul pornind se pare de la situatia precara a numarului si calitatii specialistilor, precum si a perspectivei nu prea incurajatoare privind viitorul hidraulicii in Romania.

In continuare voi incerca si eu un raspuns cat de cat logic si sper ca destul de la obiect.



Dr.ing. Petrin DRUMEA  
DIRECTOR DE PUBLICATIE

Prima intrebare este “Ce sa cercetam in Romania”. Intrebarea porneste de la numarul mic de firme productive ramase in domeniu, de la numarul mic de cercetatori activi si de la faptul ca se importa atat produse cat si sisteme intr-o proportie foarte mare. Primul impuls este sa raspundem in logica intrebării, adica NIMIC. Analizand situatia reala si perspectivele care se intrevad, raspunsul se nuanteaza si se poate afirma ca sunt cateva domenii de mare interes, dintre care sunt relevante urmatoarele:

- Cercetari privind cresterea eficientei energetice a echipamentelor si sistemelor hidraulice;
- Cercetari privind productia si utilizarea industrială a unor noutati cum ar fi hidraulica digitala, fluidele ecologice si tribologia sistemelor hidraulice;
- Cercetari privind mentinerea si chiar ridicarea performantelor functionale ale echipamentelor si sistemelor hidraulice printr-o mentenanta adecvata;
- Cercetari privind realizarea unor produse hidraulice de nisa.

A doua intrebare este “De ce sa mai facem cercetare” si are raspunsul rapid si inadecvat NU MAI ESTE CAZUL, insa si un raspuns serios care spune ca e nevoie de cercetare in domeniu pentru ca:

- Exista inca un mare numar de specialisti, o reala crestere a cercetarii universitare, precum si o buna traditie in domeniu;
- Exista multe cereri venite din industrie;
- Exista multa hidraulica in tara;
- Mentenanta si cercetarea de nisa trebuie asigurate la un nivel tehnico-stiintific ridicat.

A treia intrebare este “Pentru cine trebuie facuta cercetarea in tara” si are doar un raspuns serios si logic si anume “Pentru economia nationala”, pentru ca:

- A crescut complexitatea utilajelor si echipamentelor industrial;
- A crescut numarul si tehnicitatea utilajelor mobile existente in exploatare in tara;
- A crescut cererea internationala de munca de cercetare in domeniu.

Numarul intrebărilor de acest fel este mai mare, raspunsurile pot fi mai multe si mai nuanțate, insa ideea generala este ca cercetarea in hidraulica va mai exista si se va mai dezvolta, probabil pe anumite domenii si in anumite structuri, care astazi nu sunt relevante. Exista sperante.

## EDITORIAL

### What, Why, Whom for?

Lately I've been surprised to hear some questions expressing a great confusion in the research and higher education areas, all starting apparently from the precarious situation related to the number and quality of specialists, and also to the not so very encouraging perspective on the future of Hydraulics in Romania.

In the following lines I will try to give a somewhat logical, and hopefully focused enough, answer.



Ph.D. Eng. Petrin DRUMEA  
DIRECTOR OF PUBLICATION

The first question is “What to research in Romania?” This question starts from the small number of productive companies still existing in the field, the small number of active researchers and the fact that both products and systems are imported in a large proportion.

The first impulse is to answer in the logic of the question, namely NOTHING. Analyzing the real situation and foreseeable prospects, the answer gets more shades, and it can be said that there are some areas of great interest, of which the following are relevant:

- Research on increasing energy efficiency of hydraulic equipment and systems;
- Research on industrial production and use of novelties such as digital hydraulics, green fluids and tribology of hydraulic systems;
- Research on maintaining and even raising the functional performance of hydraulic equipment and systems through proper maintenance activities;
- Research on development of niche hydraulic products.

The second question is “Why bother do research work?”, and it has the quick and inadequate answer IT IS NO LONGER NECESSARY, but also a serious answer saying that there is necessary to be conducted research in the field because:

- There are still a large number of specialists, a real increase in university research, and also good tradition in the field;
- There are many requests from industry;
- There is a great deal of Hydraulics in our country;
- Maintenance and niche research must be provided at high technical and scientific standards.

The third question is “Whom for should there be done research in our country?”, and it has only one serious and logical answer, namely “For the national economy“, because:

- Complexity of industrial machines and equipment has increased;
- The number and technicality of mobile machinery existing in operation in our country have also increased;
- International demand for research work in the field has increased as well.

The number of questions of this kind is larger, the answers might be more and more sophisticated, but the general idea is that research in Hydraulics will exist and will continue to develop, perhaps in certain areas and in certain structures, which are not relevant today. There are hopes.

## Wireless Remote Control of Electro-Pneumatic Positioning System

Prof. Ryszard DINDORF, PhD.<sup>1</sup>, Piotr WOŚ, PhD.<sup>1</sup>

<sup>1</sup> Kielce University of Technology, Poland, dindorf@tu.kielce.pl

**Abstract:** *Constant development of wireless networks increases possibilities of their application in the industry. Popular wireless computer networks WLAN (Wireless Local Area Network) can be used not only for data transfer between computers, but also for remote control of electro-pneumatic positioning systems based on the application running on the mobile computer. In order to examine the practical effect of the application the laboratory stand was built for wireless control of the electro-pneumatic servo drive. For that purpose the microcomputer board was used, whose task was to connect the wireless card, input/output port and the application for the operator. The input/output port for the controller was a selected module for data acquisition equipped with analog inputs and outputs. A wireless card was used for wireless communication with the computer operator. Servo drive was built based on the proportional pressure valve, pneumatic positioner, pneumatic actuator of double-sided action, convertor of linear transfers and measure of linear transfers.*

**Keywords:** *wireless control, pneumatic systems, servo-drives*

### 1. Introduction

Pneumatic positioning systems have been developing rapidly in recent years. Some of the many applications of pneumatic positioning are: handling of workpieces (such as clamping, positioning, separating, stacking, rotating), packing, filling, metal-forming, stamping [1]. With advancements in micro-computer and servo-valve technology, pneumatic systems are now being considered for industrial applications that involve a control system for positioning of a workpiece. Development of automation and robotization in manufacturing process stimulates interest in pneumatic systems whose advantages include low manufacturing costs, high dynamics and reliability. Unsatisfactory positioning accuracy of multi-axis pneumatic systems considerably reduces their application in manipulating machines, manipulators and robots. Rapid advance in parallel pneumatic manipulators imposes a lot of demands on controllers of pneumatic servo-drive concerning positioning accuracy, resistance to alternating parameters of state and disturbing signals. The problem of positioning accuracy of electro-pneumatic systems is difficult to solve when no sufficient information on the process of conversion of the compressed gas energy into mechanical energy of pneumatic cylinder is available. Therefore, new control methods based on wireless remote control were introduced.

### 2. Wireless network

Wireless networks have become more and more popular in the recent years. Owing to constant development they become faster, safer and more reliable. Since it is easy to install wireless communication it is very common among private users and in industry. Computer networks can be used not only to access the Internet, but also in the communication with devices used in the industry. The aim of this paper is to present the possible use of WiFi wireless network in the servomechanism of electro-pneumatic control system. For that purpose we constructed a laboratory test stand of wireless controlled pneumatic positioning and wrote the application for the communication between operator and pneumatic positioning system. The communication between devices via network must be conducted according to strictly defined principles so-called protocols, which are specific for every applied communication. The task is to define such features as the format and structure of sent message, ways of message exchange between network devices, methods of the system information exchange and errors between network devices as well as to establish and finish connections. Protocols don't usually describe how to carry out a determined function so the implementation of a given protocol is independent of specific technology. Successful communication in the network requires sharing of many different protocols. Such

connected group of protocols is called the protocol suite, which is often presented as the stack [2]. There are two basic models of the network. TCP/IP (protocol model) and OSI model (reference model) [3]. The reference model and protocol model along with their layers are presented in Figure 1. TCP/IP is regarded as the model of Internet network. It defines four layers, which are responsible for correct communication network. The Network Access Layer is responsible for control of physical devices and media forming the network. Next layers are responsible for determining the best route of packages in the network, communication between different devices in different networks and reading data from the user. While sending data they go from the upper layer to the lowest, but the receipt of data is a reverse process. In the first layer of the TCP/IP model it is possible to distinguish three types of media transmission, connecting devices and providing data transmission: metal cables, fiber-optic and wireless communication. The advantages of cable networks include providing adequate signal power on the entire cable length, protection against external signals effects as well as lack of local regulations and standards concerning the use of frequency band. For wireless networks the advantages of cable networks will be their defects, because without additional legal standards it is possible to use only some frequency bands. The useful signal is susceptible to external interferences and it is hard to ensure the appropriate quality of signal far away from its source. Advantages of wireless networks are undoubtedly easy access to the medium transmission as well as the ease of structure and expansions. [4], [6]. A popular access wireless method is WLAN (Wireless Local Area Network). Frequency range of the radio waves used by the standard doesn't require the concession; therefore it is possible to use this standard without special licenses. Standard 802.11 determines the outline of division bands into channels for the frequency range between 2.4 GHz and 2.483 GHz, where distance between individual channels are 5 MHz and width of channel is 22 MHz. This band does not require licensing and is divided into 11 channels for North America and 13 channels for Europe.

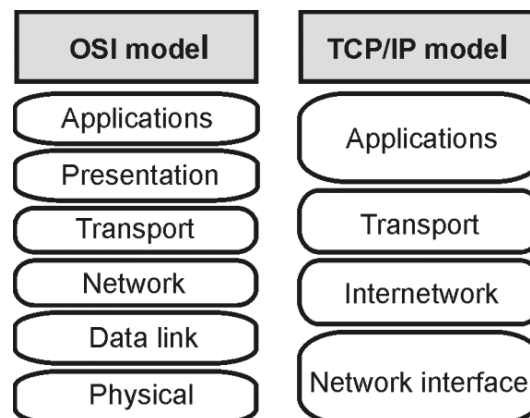


Fig. 1. OSI and TCP/IP models

Network layer is responsible for the exchange of data fragments via network between some determined terminal devices. This layer is responsible for addressing, encapsulation, routing and decapsulation of transmitted data. The most popular protocol used in the network layer is IP protocol (Internet Protocol). Currently it is used in version 4 and in version 6. Moreover, the network layer includes the following protocols: IPX (Internetwork Packet Exchange), Apple Talk or connectionless service CLNS/DECNet network. IP protocol is a connectionless protocol, which makes communication faster and flexible, but also unreliable. The reliable transmission is dependent on layers of the high level in network model. In the IP protocol in version 4 addressing is hierarchical. An IPv4 address consists of a 32-bit number, divided into a host part and a network part. The host part uniquely identifies a given host on a given physical network. The network part identifies the network to which the host is connected. The entire pool of addresses ( $2^{32} = 4294967296$ ) is divided into classes A, B, C, D and E, where classes from A to C are addresses of the unicast type should be allocation for the addressing network devices [2]. Transferring large and constant data bands could make it impossible to make other transmission in the same time because the entire transmission channel is seized. Another problem would be rectifying transmission errors and retransmitting damaged data. Therefore, data are divided into

smaller fragments (segmentation), which are transmitted between devices in the network. Such process also allows for many different applications for simultaneous work in the network by placing a part of messages coming from different applications (multiplexation) in one transmission channel. The tasks of segmentation, merging data and multiplexing communication fall to the transport layer [5]. Depending on requirements concerning data transmission, two basic transmission protocols are distinguished: TCP and UDP. The TCP Protocol is a protocol which guarantees reliable provision of data to the recipient by tracking transmitted data, confirmation of data receipt and repetition of lost data. It is the interconnection protocol, which means that before data is transmitted by the network, the connection is established between the communicating devices. Second protocol which is simpler is UDP. It is faster than TCP, doesn't require confirmations and doesn't provide lost data for the retransmission, and thus doesn't ensure reliability. Where reliability of the data transmission is required the TCP is applied (database applications, electronic mail, websites). In case of less sensitive data, where applications are tolerant to loss of small amounts of data the UDP protocol is applied (video or voice transmission) [2]. The task of protocols layer is to provide an interface between the user of the network device and network data. In this layer it is possible to distinguish two types of the software: applications and services. Services of the application layer are usually transparent for the user and are responsible for connecting the application with network as well as sending data. The application provides interface for the user as well as initiates the process of data transmission by the network. The application layer like the remaining layers of the network contains protocols of different type defined by standards and data formats. FTP can be an example of the application, service and protocol, which constitutes the interface for user (application), supporting program connections for transmission files (service) and interchange standard of network communications (protocol). Protocols of the application layer define the way of data exchange between applications and services, which are started on devices participating in the communication. They carry it out by determining the type and format of an exchanged message as well as by determining the way in which the message is sent and received.

### 3. Wireless controller of servo-drives

The wireless controller of pneumatic positioning system was built on the basis of the TCP/IP model (Fig. 2) [7], [8]. The wireless controller contains the ALIX.1D microcomputer board (Fig. 3a). The board is equipped with AMD Geode 500 MHz processor and 256 MB memory RAM. It is powered with 12 V and characterized by small current intensity of 0.4 to 0.5 A. The task of board is to connect wireless card, input/output port and application for the controller. For that purpose operating system Windows XP was installed on the memory card. This system was chosen, because the ALIX.1D system board meets the minimal requirements and there are no major problems with detection of additional devices and drivers installed in it.

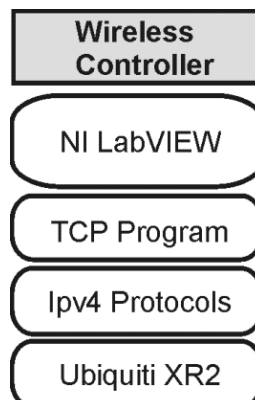
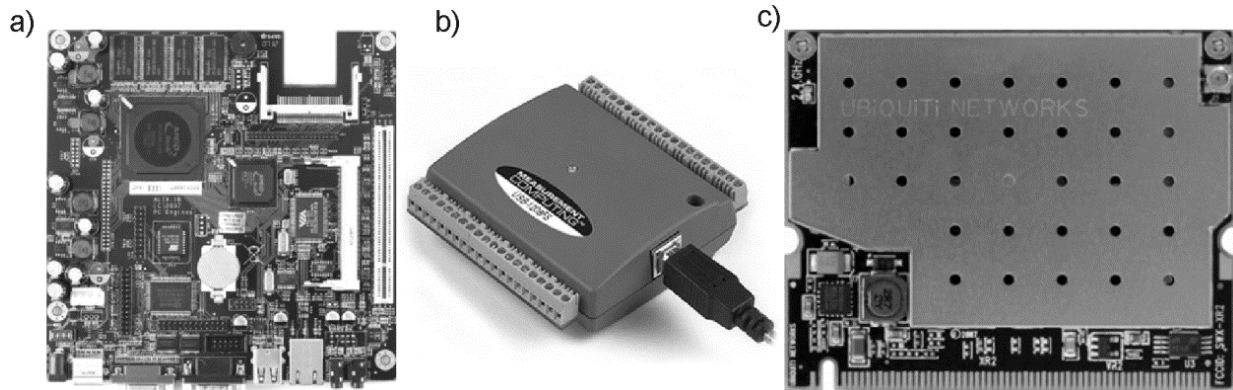


Fig. 2. Wireless controller scheme



**Fig. 3.** Elements used for construction of the wireless controller: a) ALIX 1D microcomputer board, b) module of the acquisition data MicroDAQ USB-1208FS, c) wireless card Ubiquiti XR2

As input/output port for the driver was a chosen module for the data acquisition MicroDAQ USB-1208FS (Fig. 3b). This system has 4 analog inputs in the symmetrical system (differential) and 8 - inputs in the asymmetrical system. Inputs have resolution of 12 bits in the symmetrical system or 11 bits in the asymmetrical system. In the asymmetrical system there is a possibility of voltage measurement which is  $\pm 10$  V, while in the differential system it is  $\pm 20$  V. The module is characterized by sample frequency of up to 50 kS/s while using hardware scanning. For generation of output signals 2 analog outputs are available with resolutions of 12 bits. Output voltage range amounts to 0–4.096 V at maximum load capacity of 15 mA. Analog data are sent with the frequency to 10 kS/s for one channel or 5 kS/s for two channels using the hardware method. This module is connected to the driver board by USB interface. For the communication with operator the Ubiquiti XR2 card is used (Fig. 3c). The card is equipped with MMCX connector which provides a better connection card (pigtail), than the one popular miniPCI cards UFL connectors. The advantages of this card are 802.11b and 802.11g standards, large output power (26 dB) and sensitivity of the receiver to -95 dB. The card is recommended for applications, where the highest reliability and quality of transmission is required. Depending on aerial inside the premises it is possible to obtain the space up to 200 m, however in the open space it is about 50 km. The proper operation of TCP/IP requires that the devices in network be assigned a unique network addresses. For that purpose the pool of addresses IPv4 from class B was divided into subnet consisting of two hosts. The division into smaller subnet was achieved by such a change of the mask that only 2 least significant bits were used for appointing addresses of devices. The output address was network address 172.16.0.0/16. The remaining address in the subnet (172.16.2.3) is a reserved broadcast address. Such addressing increases safety before a “strange device” is connected to the network, since the next address 172.16.2.4/30 is already an address of other subnet,. Consequently the devices will not be able to communicate directly with each other. In order to provide the reliability of transmission and due to small amounts of data which are sent by the network TCP was chosen as the transport protocol. For the communication between the driver and the operator two applications were written, one for the controller and the other for the operator. The application of controller performs the role of the service. Its task is to listen attentively and wait for the operator to indicate the connection on a chosen port. When connection is detected the service starts to collect and send data. When operator finishes the connection, the application again turns into the state of listening and waiting. Both programs were written using LabVIEW software (Fig. 4) which allows one to write program with the use protocols like TCP, UDP, Bluetooth or IrDA. The applications capable of sending data via TCP protocol must use blocks to open and close connection for a determined IP address and port, a blocks to listen for incoming connections as well the blocks that record and read data from the TCP connection. In the figure below an example of the client application and server created with the use of LabVIEW is presented. Apart from the basic TCP blocks a loop was applied. Its task was a constant sending of data from the client application and a constant reception of data from the server.

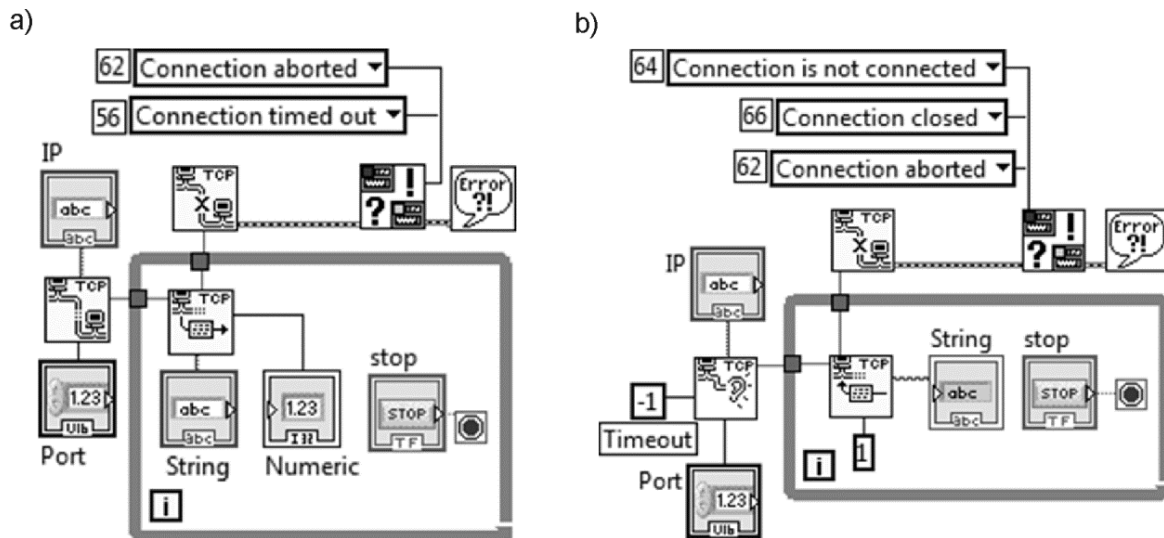


Fig. 4. NI LabVIEW software: a) client application, b) server application

A laboratory test stand of the wireless controlled pneumatic positioning systems and a panel controller view of the wireless communication are presented in Figure 5. Proportional pressure valve SMC of VEP3141 type controls the outlet pressure steplessly according to current [9]. The task of proportional valve pressure is to ensure a set pressure proportional to the value of control voltage on its output. It is possible control the valve in order to obtain on it the output pressure between 5 kPa and 0.15 MPa, at maximum working pressure 1 MPa. It is characterized by flow control of pressure and response time of 0.05 s. Proportional pressure valve is connected to the pneumatic positioner responsible for establishing an appropriate actuator position on the pressure base controlled by the valve. The positioner of the A705 type is designed to cooperate with a 2-side pneumatic-piston-type actuator in the systems of automatic adjustment of the industrial processes in the chemical, foodstuff, energetic industry, etc. [10]. The pneumatic positioner of A 705 type is designed to increase useful force of actuator ensuring precise actuator mandrel positions. Its mechanism of maneuverable tensing ensures fast and accurate setting of the piston actuator, proportional to the value of control signal. Pneumatic positioner can be controlled by the input pressure signal of about 20-100 kPa, at the supply pressure of 0.25-1 MPa. The displacement measurement LVDT of PLx200 type (in the range of 1-200 mm) converting linear displacement of cylinder piston to voltage  $\pm 10$  V [11].

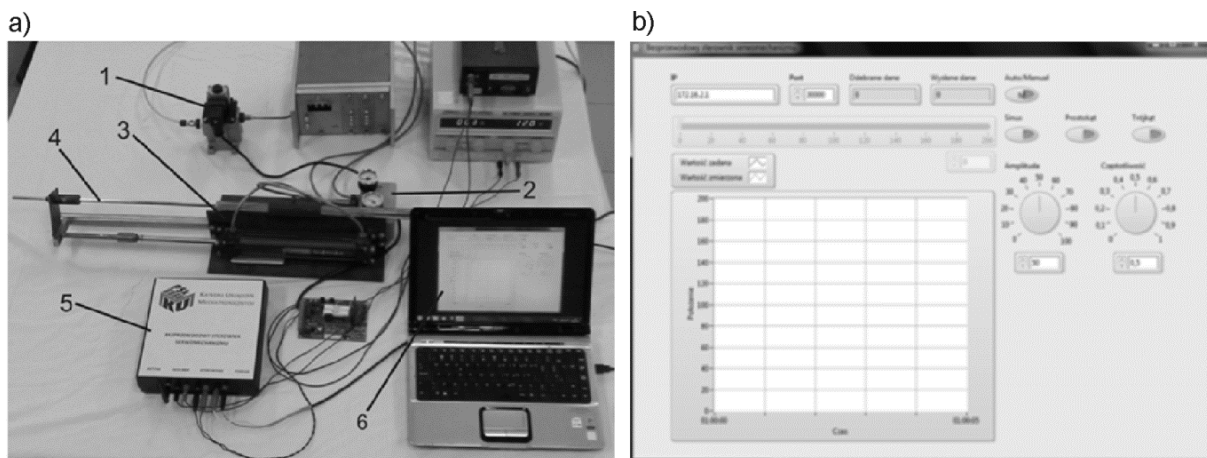
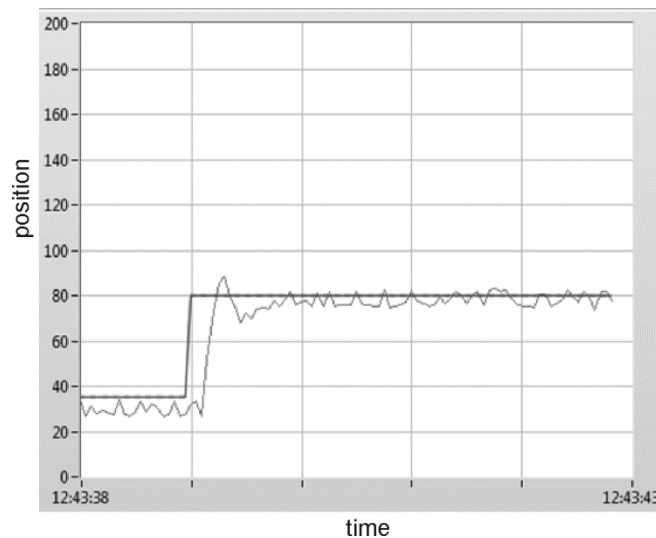


Fig. 5. Laboratory test stand: a) wireless controlled pneumatic positioning systems: 1 – proportional pressure valve SMC VEP3141, 2 – pneumatic positioner type A705, 3 – pneumatic actuator, 4 – displacement measurement LVDT of PTx200, PTx200, 5 – controller to MPL102 type , 6 – driver of the wireless communication, b) computer panel of the controller

#### 4. Results of experimental tests

The experimental tests of electro-pneumatic systems were conducted mainly to check the operation of the designed wireless controller for positioning of pneumatic actuator at various load mass [7], [8]. A transpose control and follow-up control of pneumatic positioning system was carried out. Some graphs showing position tracking of pneumatic actuator are presented in Figures 6-8.



**Fig. 6.** Position tracking of pneumatic actuator for a step input

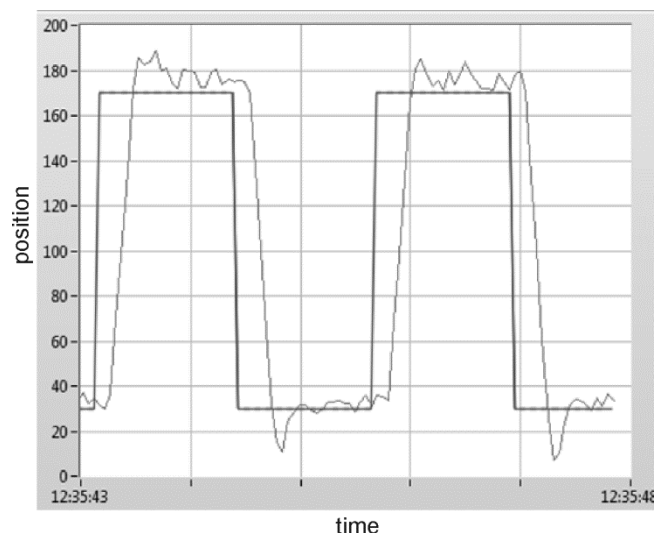


**Fig. 7.** Position tracking of pneumatic actuator for a rectangular pulse input

From the analysis of above graphs it results that there is a delay between the value of a set signal and actuator position. As the driver performs only the role of control system the delay isn't significant in the process of regulation. Pneumatic positioner is responsible for the regulation process. Small values of delay occur in the process of manual control, but larger delays appear in automatic control, where changes of the control signal are faster. The reason of such delays may be transport protocol, which due to quality transmission assurance imposes delays. The next stage in control of the pneumatic positioning system involves change from TCP to UDP in order to check, whether the simpler transports will also impose delays in the data transmission. In spite of the fact that he studied controller causes delays between the control and read signal, which disqualifies it as the adjuster, it can be used for simple control of the servo drive in systems that do not require high precision and in places dangerous to operator of the servomechanism.

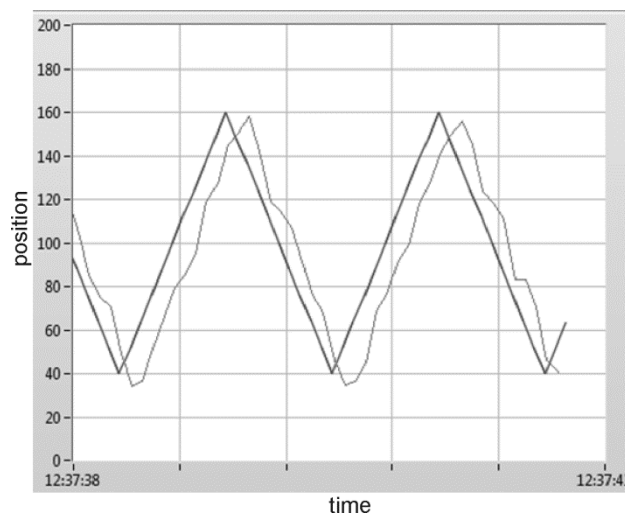


Fig. 8. Position tracking of pneumatic actuator for a triangular pulse input

## 5. Conclusions

The development of computer networks, particularly wireless networks increases their efficiency and safety, which makes them useful in industry. Wireless communication in spite of its limitations, such as susceptibility to disruptions or delays in transmission can be used where cable networks cannot be applied. Wireless control can significantly improve security of the operator and reduce the costs of the network infrastructure. The simulations conducted in the laboratory confirm that it is possible to use the wireless computer network WiFi for communication of the operator with the remote device without obstacles. Moreover, it should be noted that after the replacement of the software it is relatively easy to adopt the controller to other tasks.

## References

- [1] G. Prede, D. Schulz, „Servopneumatics”. Festo GmbH, Denkendorf 2002;
- [2] M. Dye, R. McDonaals, A. Rufi, “Network Fundamentals”, CCNA Exploration Companion Guide, Cisco Press, Indianapolis, Indiana, 2008;
- [3] W. Lewis, “LAN Switching and Wireless”, CCNA Exploration Companion Guide, Cisco Press, Indianapolis, Indiana, 2008;
- [4] D. Meyer, „TCP/IP versus OSI”, IEEE Potentials, 1990, Vol. 9, Issue 1, pp. 16–19;
- [5] W. Charfi, M. Masmoudi, F. Derbel “A layered model for wireless sensor networks”, SSD’2009 - Systems, Signals and Devices, 6th International Multi-Conference, pp.1-5;
- [6] B. Mindang, “Core Technology and Analysis of 802.11N”, ICEICE’2011 - International Conference on Electric Information and Control Engineering IEEE, 2011, pp. 978-982;
- [7] S. Mazur, R. Dindorf, P. Woś, “Wireless control of the electro-pneumatic servo drive”, Information Systems Architecture and Technology. System Analysis Approach to the Design, Control and Decision Support. Wrocław 2012, pp. 231-240;
- [8] S. Mazur, R. Dindorf, P. Woś, „System komunikacji bezprzewodowej w sterowaniu serwonapędów elektropneumatycznych”, Pneumatyka, nr 2, 2012, pp. 46-51;
- [9] SMC Electro Pnuematic Proportional Valve series VEP;
- [10] Technical product documentation of the positioner Type A706, CONTROLMATICA ZAP-PNEFAL Sp. o.o. Ostrow Wilkp., Poland;
- [11] Peltron [http://www.peltron.pl/przetworniki\\_przemieszczen1-ang.html](http://www.peltron.pl/przetworniki_przemieszczen1-ang.html)

## Aspects Regarding Fluid Viscous Anchoring Systems Used for Vibration Mitigation at Bridge Structures

Assistant Professor Fănel Dorel ȘCHEAUA, PhD.<sup>1</sup>

<sup>1</sup>"Dunărea de Jos" University of Galați, Romania, fanel.scheaua@ugal.ro

**Abstract:** During the last period are increasingly used hydraulic devices attached to building structures in order to achieve energy dissipation during earthquakes but also as anchoring systems being interposed between structural frameworks. An anchoring system is a hydraulic device consisting of a cylinder with piston having inside a working fluid with special viscosity properties. The anchor device can be connected to both ends making a connection between the bridge pier and superstructure. This special positioning between structural frames is made in order to ensure vibrations mitigation and increased stability at high stress requests. The device piston can perform translation displacements inside the cylinder by means of a hydraulic circuit which allow working fluid flow between the two chambers of the cylinder. Due to high viscosity values of the working fluid and small diameter of crossing orifices, the relative slow movements between structural frameworks are allowed, but when a dynamic request of major intensity occurs the system becomes rigid assuring the safety connections between structural frameworks. This article shows a method of modelling a three-dimensional model for a hydraulic anchoring system and numerical analysis to highlight the working principle for such a device.

**Keywords:** fluid device, anchoring, structural system, bridge, vibration mitigation, energy dissipation

### 1. Introduction

Special mechanical systems are used at the construction of new bridge or viaduct structural types or rehabilitation of existing ones, that work as anchoring safety connections between structural elements (pier and superstructure) when significant dynamic requests are occurring. Such safety systems are based on a hydraulic fluid having special properties in terms of viscosity.

In the absence of active control equipment are considered passive systems, being velocity dependent, because they respond to relative movements between the structural frames where they are located. In the event of an earthquake there is a tendency of relative motion between frameworks, but by changing the anchoring systems rigidity it is ensured a rigid connection between the superstructure and bridge pier.

The working fluid used is a high viscosity silicone oil which can be used in a wide temperature range (  $40 + 50^{\circ}C$  ) and showing no change in properties over time.

### 2. Modeling aspects for viscous fluid anchoring system

A viscous fluid anchoring system is composed of a cylinder with a piston that divides the interior of the cylinder body in two chambers. The interior volume of the cylinder body is filled with fluid and the movement of the piston is made possible by a special circuit that allows the fluid flow.

Due to the diameter value of the passage orifices, low-velocity movements are allowed for the piston but when a dynamic request occur the hydraulic system is activated acting as a safety device. Increasing rigidity is ensured based on the working fluid due to their high viscosity value but also to valve system that can be adjusted to face high levels of forces arising from the dynamic requests.

A three-dimensional model for viscous fluid anchoring device was developed and presented in Figure 1.

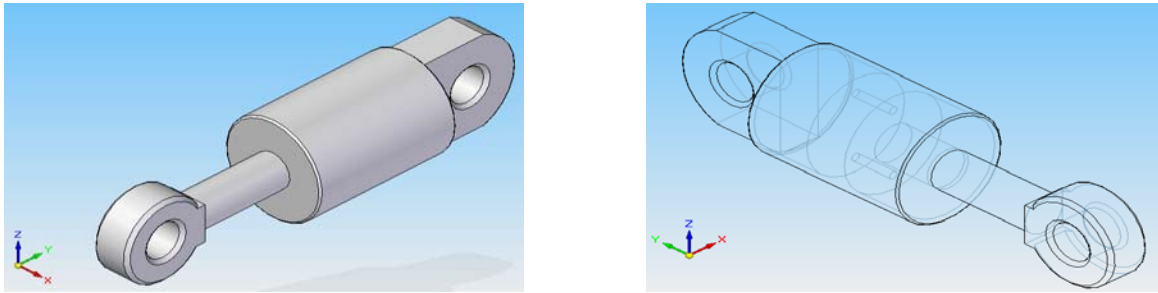


Fig. 1 Fluid viscous anchoring device model assembly

### 3. Theoretical approaches regarding fluid dynamics inside the anchoring system

The fluid viscous anchoring system is connected to the resistance structure of a bridge or viaduct by means of clamping flanges at both ends being positioned between the superstructure and the support pier. In normal working conditions when the system receives small oscillations due to traffic conditions, the piston movement within the cylinder is relatively free without forced circulation of the working fluid within the orifices.

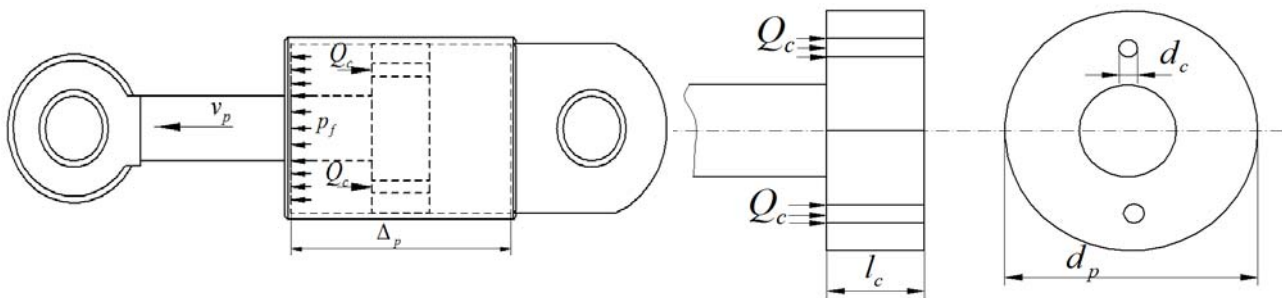


Fig. 2 Anchoring model efforts distribution

When a seismic event is occurring, the anchoring system is activated by the forced relative movement achieved at the device ends, while the piston is moved inside the cylinder by forcing the viscous fluid to pass through the orifices made inside the piston head. The efforts distribution created in this situation it is presented in Fig. 2. The fluid flow rate that is circulated through the orifices can be calculated using the following relation:

$$Q_c = \pi \frac{d_c^2}{4} v \quad (1)$$

Where:

- $Q_c$  - fluid flow rate;
- $d_c$  - orifices diameter;
- $v$  - piston velocity.

The pressure created inside cylinder, performing piston motion braking can be assumed by the relation:

$$p = \frac{\xi \rho}{2} \left( \frac{A}{a_d} \right)^2 \cdot v^2 \quad (2)$$

Where:

- $p$  - pressure;
- $\rho$  - fluid density;
- $A$  - piston area;
- $a_d$  - orifice area.

From pressure relation shall be deduced that the braking pressure is even higher as the momentary piston velocity is higher and the orifices opening area is smaller.

**4. Computation fluid dynamics analysis for anchoring model**

Two different cases were analyzed for the fluid viscous anchoring system three-dimensional model. In the first case it has been considered two circulation orifices for the fluid having a diameter of 20 mm and for the second case the orifices diameter has been reduced to 10 mm. The working fluid is silicone oil having characteristics which remain constant when are changes in temperature or over time. The results are shown in the following, (Fig. 3, Fig. 4).

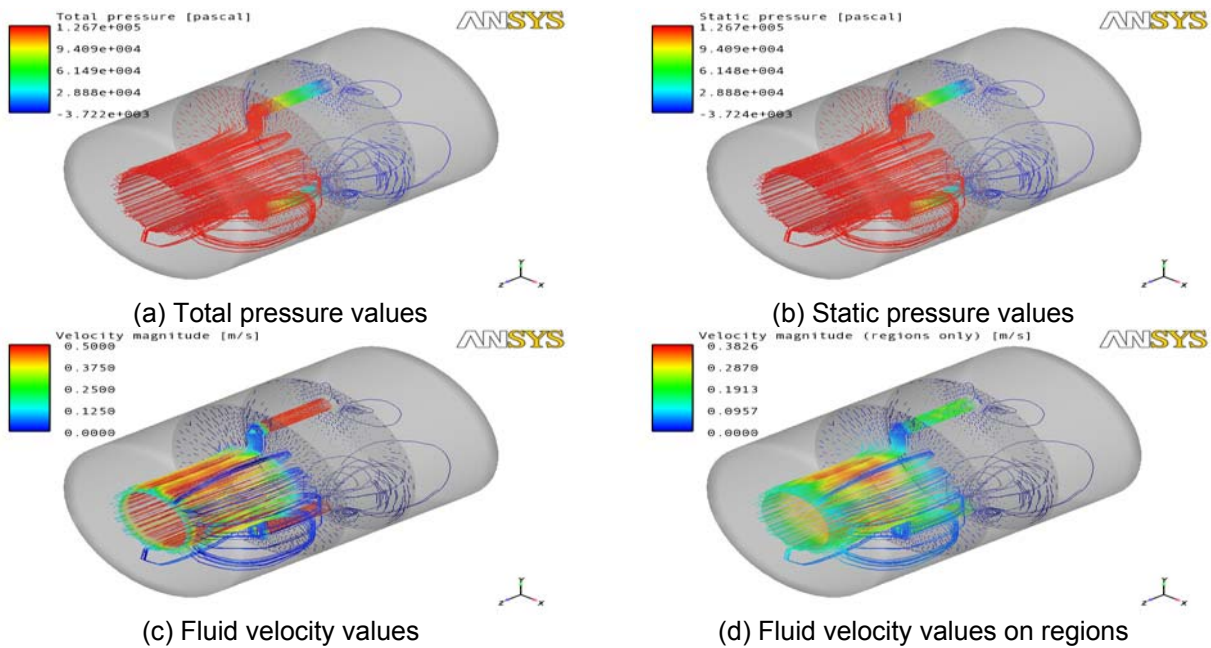


**Fig. 3** The obtained results for anchoring model having diameter orifices of 20 mm (case 1)

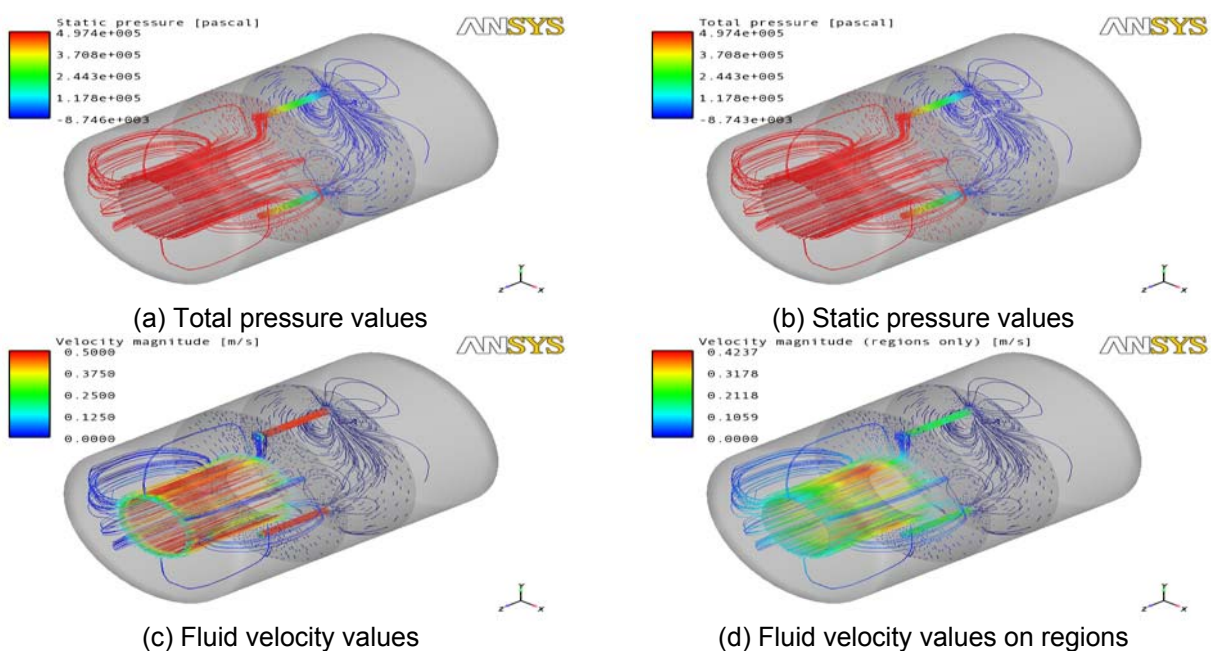


**Fig. 4** The obtained results for anchoring model having orifices diameter of 10 mm (case 2)

The values obtained for the force at piston rod and total pressure for the two analyzed cases are presented in TABLE 1.

**TABLE 1** Result values obtained for total pressure and force

Case 1 – 20 [mm]		Case 2 -10 [mm]	
Force [N]		Force [N]	
Boundary	Z-Component	Boundary	Z-Component
Piston	5575.33	Piston	22171.65
Net	5575.33	Net	22171.65
Pressures (Total) [Pa]		Pressures (Total) [Pa]	
Boundary or Region	Maximum	Boundary or Region	Maximum
Piston	125744.54	Piston	497369.64
Cylinder wall	125744.54	Cylinder wall	491981.75
Fluid	126692.76	Fluid	497369.64

**Total Pressure Values (case 1)**

[Pa]

**Total Pressure Values (case 2)**

[Pa]

## 5. Conclusions

The fluid viscous anchoring system are considered as dissipation devices acting on the passive principle that reacts at relative movements between the structural frames where they are mounted and behave like real safety devices for the bridge or viaduct structural types where there are attached. At this kind of structures the vehicle emergency braking and also the seismic actions can determine the entry into operation of the anchoring devices and make a stiff connection between structural frameworks.

The use of these special fluid viscous anchoring systems shows benefits regarding the high efforts transferred and proper distribution of seismic forces in horizontal plane in the same time with displacement limitation resulted from earthquakes of considerable magnitude.

Following the analysis results made for the three-dimensional model it can be said that while reducing the diameter for the passage orifices with 50% it is obtained an increase in pressure and force values at the piston of nearly four times (400 %), when using silicon oil having a medium value for kinetic viscosity of 30 [cSt] as working fluid.

## References

- [1] G. Axinti, A. S. Axinti, “Acționări hidraulice și pneumatice”, Vol III, Editura Tehnica-Info, Chișinău, 2009;
- [2] S. Nastac, “Non-Linear Stiffness Influences About the Dynamics of the Anti-Vibrational Passive Isolation Systems”, Romanian Journal of Acoustics and Vibration (RJAV), anul, 1.
- [3] S. Nastac, A. Leopa, “Structural optimization of vibration isolation devices for high performances”, International Journal of Systems Applications, Engineering and Development, 2(2), 66, 2008;
- [4] F. D. Scheaua, “Seismic protection of structures using hydraulic damper devices”, Annals of the University Dunarea de Jos of Galati, Fascicle XIV, Mechanical Engineering, 14, 2010;
- [5] F. D. Scheaua, F. Nedelcut., “Energy dissipation device using fluid dampers”, The Annals of Dunarea de Jos, University of Galati Fascicle XIV Mechanical Engineering, Galați, Romania, 2012;
- [6] F. D. Scheaua, A. S. Axinti, G. Axinti, “Mathematical model analysis on hydraulic energy dissipation devices”, Hidraulica Magazine, 2012;
- [7] [http://www.google.ro/Seismic\\_Protection\\_Systems](http://www.google.ro/Seismic_Protection_Systems)

## Designing of Liquid Piston Fluidyne Engines

Assistant Professor **Sunny NARAYAN**<sup>1</sup>

<sup>1</sup> Indus International University, Himachal Pradesh, India, rarekv@gmail.com

**Abstract:** Engines and pumps are common engineering devices which have become essential to the smooth running of modern society. Many of these are very sophisticated and require infrastructure and high levels of technological competence to ensure their correct operation, for example, some are computer controlled, others require stable three phase electrical supplies, or clean hydrocarbon fuels. This work focuses on the identification, design, construction and testing of a simple, yet elegant, device which has the ability to pump water but which can be manufactured easily without any special tooling or exotic materials and which can be powered from either combustion of organic matter or directly from solar heating. The device, which has many of the elements of a Stirling engine is a liquid piston engine in which the fluctuating pressure is harnessed to pump a liquid (water). A simple embodiment of this engine/pump has been designed and constructed. It has been tested and recommendations on how it might be improved are made. The underlying theory of the device is also presented and discussed.

**Keywords:** Liquid Piston Engines; Novel Pumps

### 1. Introduction

Water is an important basic amenity to sustain life on our planet. Out of the total water resources on earth, just 3% of water is available around us as fresh water in form of rivers, lakes, streams etc. [1]. Rest 97% of water available is saline thus unfit for direct use. On an average a human being needs about 20-25 litres of water for daily use. Growth of human population has caused extreme shortage of available resources on our planet. Given that the amount of fresh water available on this planet is very less in percentage, human population has been subjected to acute shortage of water. This problem is more severe in developing nations of Asia and Africa. Figure no1 presents a glimpse of water crisis amongst human population living in African nations:

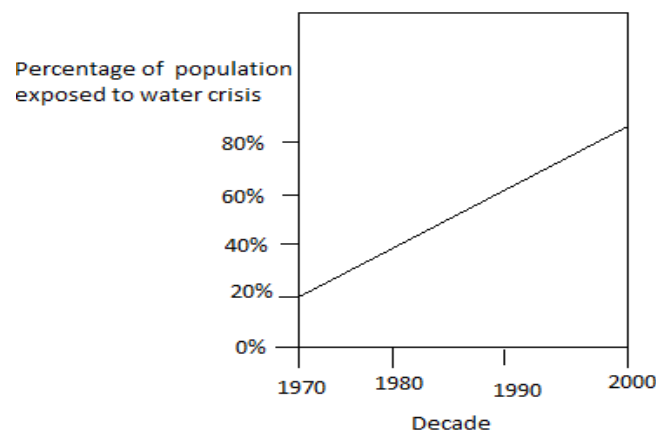


**Fig. 1.** Water crisis in Africa [2]

A major percent of fresh water bodies are being contaminated by industrial or human activity making fresh water available scarce for human use. This has also led to water borne disorders amongst human population. In such a scenario ground water presents an excellent option for human use as it is available as a source of pure water. About 31% of fresh water sources available on earth is in form of ground water. It is available in form of porous rock known as aquifer. This source of water needs to be pumped using suitable mechanical machines. Extent of ground water withdrawal is shown in the following figure.

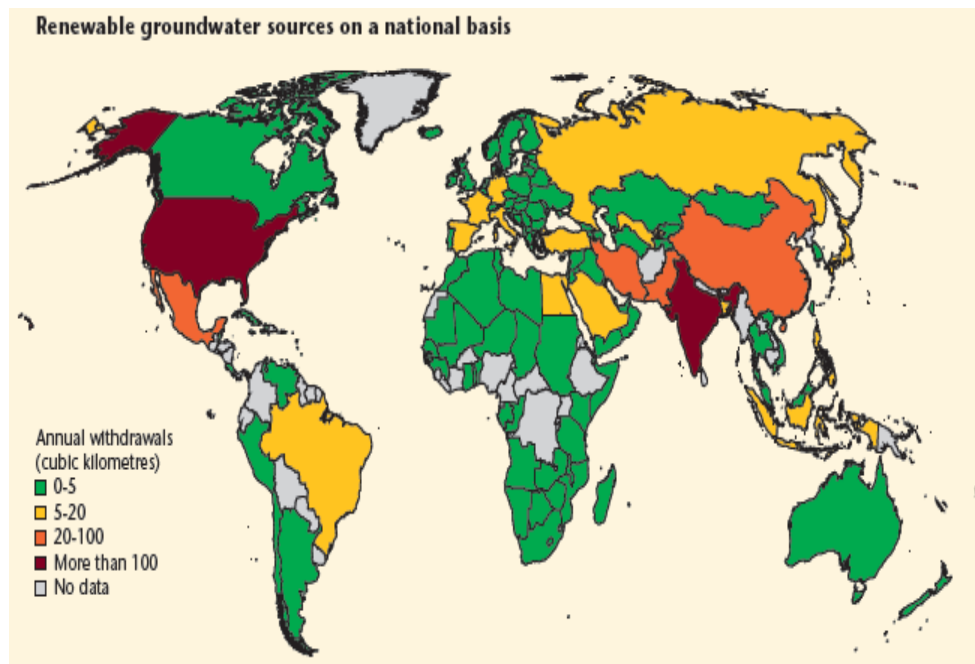


Fig. 2. Global withdrawal of ground water [3]

Solar energy is an important source of renewable energy available around us. Earth receives about 174 PW of solar flux daily, of which about 30% is reflected back into space. The remaining 70% is used to heat up surface of earth [4]. This energy has been utilized for various commercial purposes. The heat from solar energy can be used to run novel liquid piston fluidyne engines which in turn can be used to withdraw ground water for human use.

## 2. Novel pumps

There are several examples of natural pumps found around us. Some of these pumps are discussed in the next section of this work. These pumps are based on clever natural mechanisms and work without use of external power sources.

a) Capillary Action - This mechanism is found in plants and is based on bonding between cellulose cells found in Xylum tissues of plants and water present in the soil.

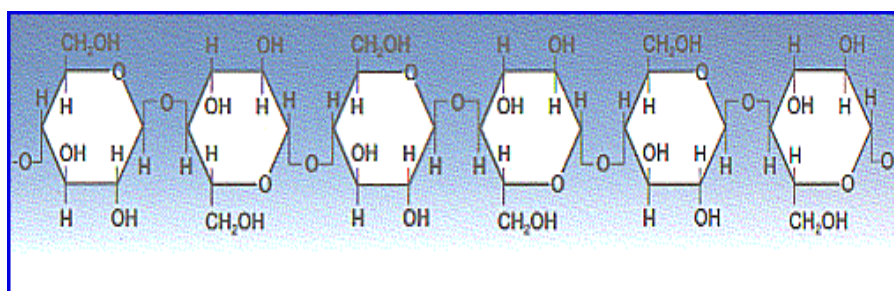


Fig. 3. Water cellulose bonding [5]

b) Human Heart - Human heart is an excellent example of a natural pump. It has four chambers known as auricles and ventricles.

Impure blood flows from right atrium to right ventricle through tricuspid valve and is sent to lungs for oxygen enrichment. From lungs the enriched blood flows to left atrium and then to left ventricle through mitral valve. Pure blood is then distributed to all parts of human body through aorta.[6]

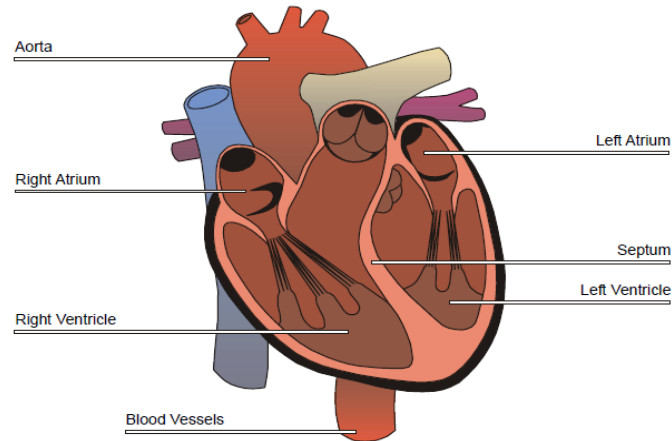


Fig. 4. Human heart [6]

c) Human Neurons - Human nerve cells are based on a sodium potassium pump known as Na-K-ATPase system. This system pumps 3 sodium ions into cell & 2 potassium ions out of a cell which causes excitation leading to human stimuli [7].

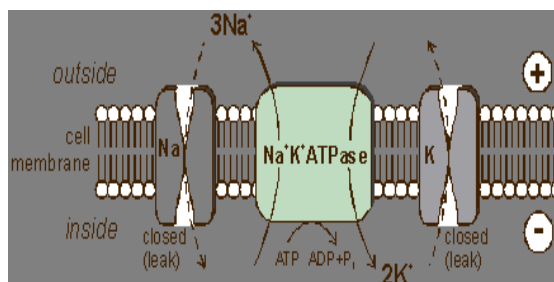


Fig. 5. Human neuron pumps

### 3. Liquid piston fluidyne pump [8]

A liquid piston engine is a novel engine working on Stirling engine cycle. A gas confined in a closed space expands when heated and contracts on cooling. This expansion and contraction can be used to generate pressure fluctuations which can be used to do useful mechanical work. The working of this pump is reviewed in next section of this work. Initially piston is at central and gauge is neutral indicating equal pressures on both sides. When gas present in hot end of arrangement expands, it pushes piston towards extreme left and moves towards cold end by means of connecting tube increasing pressure at cold end as indicated by gauge. As the gas comes in contact with cold end, it contracts and pressure falls hence pushing piston towards extreme left end. Figures 6-8 indicate this operation.

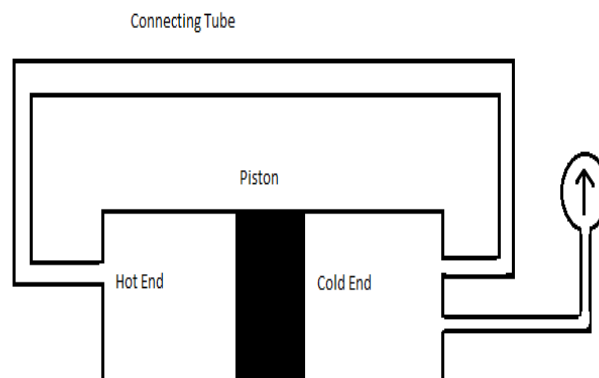


Fig. 6. Neutral position [8]

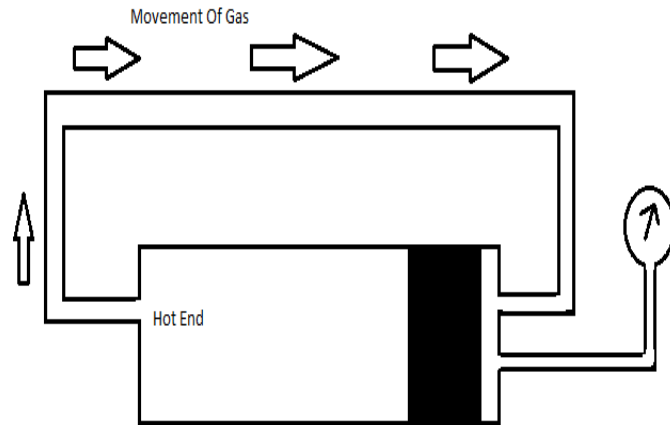


Fig. 7. Expansion phase [8]

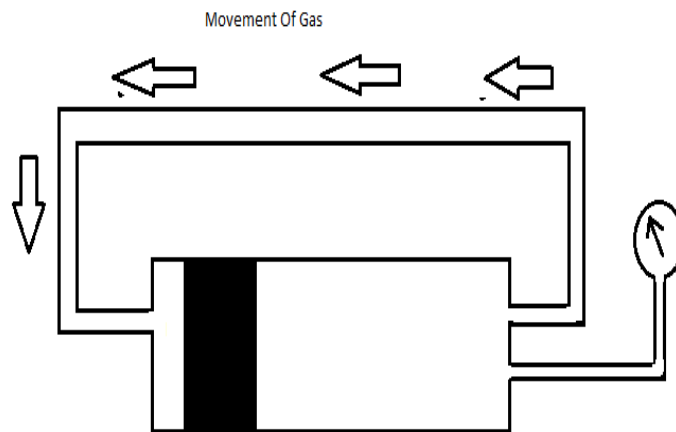


Fig. 8. Contraction phase [8]

The motion of gas causes pressure fluctuations which can be used to drive another engine for extracting useful work, as shown in figure 9. When pressure is high during expansion stroke, piston moves out and vice versa during the contraction stroke. Reciprocating motion of piston can be used to drive a crank shaft for engine motion. A regenerator can be used to increase efficiency of this system, as shown in figure 10. This consists of suitable arrangements of heat exchangers which store heat during expansion phase and release heat during contraction phase of gas.

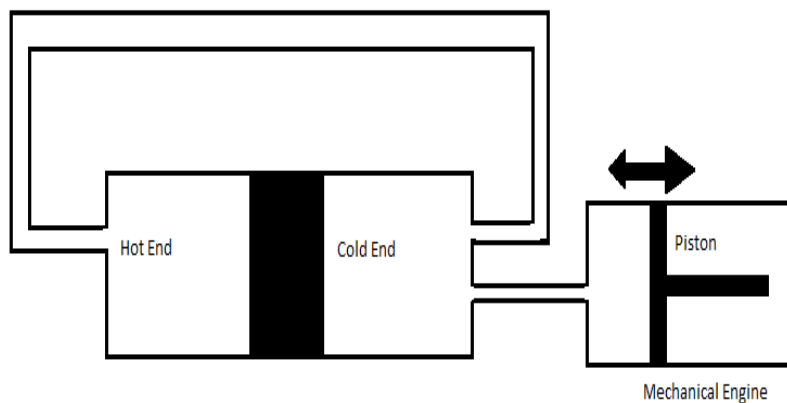


Fig. 9. Extraction of useful work [8]

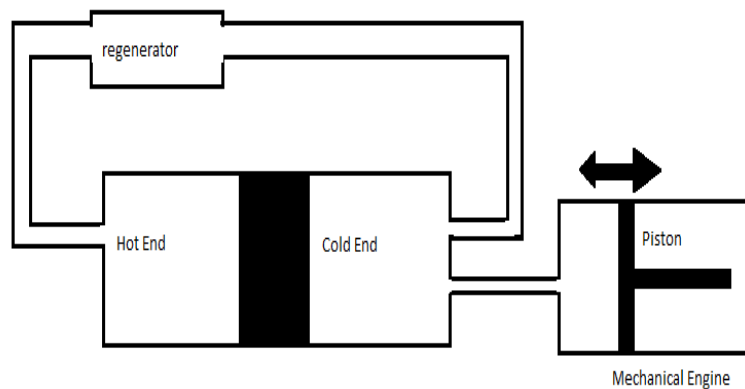


Fig. 10. Regenerator mechanism [8]

**4. Motion analysis**

Consider a U-tube connected by water space at bottom and air space at top. One end of this arrangement is heated and the other end is held cold.

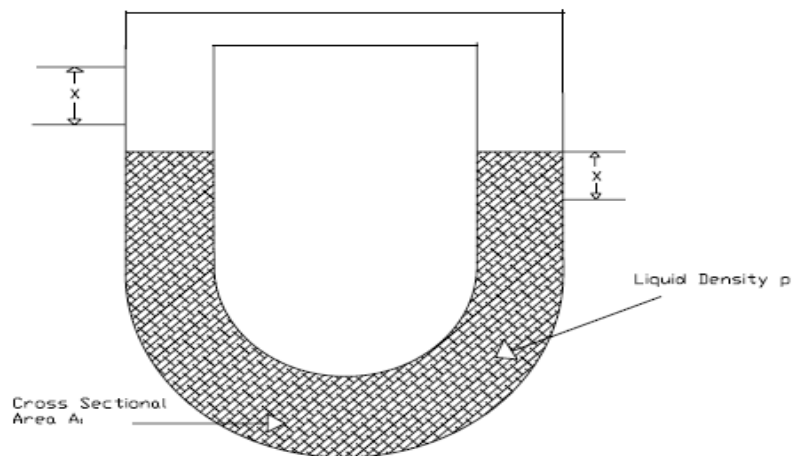


Fig. 11. U Tube arrangement [8]

If the fluid at one end falls by a distance X, then it rises at other end by same distance so that net difference between volumes is  $2 \rho AX$ . Net force acting on column is equal to  $\rho ALX''$ .

Also

$$\rho ALX'' = 2\rho AXg \tag{1}$$

where L is total length of pipe.

Acceleration of fluid is given:

$$X'' = 2X \frac{g}{L} \tag{2}$$

$$\omega = \frac{\sqrt{2g}}{L} \text{ rad/s} \tag{3}$$

Frequency of oscillations is given by  $f = \frac{\omega}{2\pi}$  (4)

**5. Experimental set up**

A test rig was designed and developed to gather more information about working of fluidyne engine. This setup used a displacer pipe of 45cm length (L) and 1.2 cm in diameter (D). Pumping line used had 15 cm height (H) & 0.78 cm in diameter (d). Methanol spirit was used as a fuel to heat up hot end. A typical layout of system is shown in fig 12.

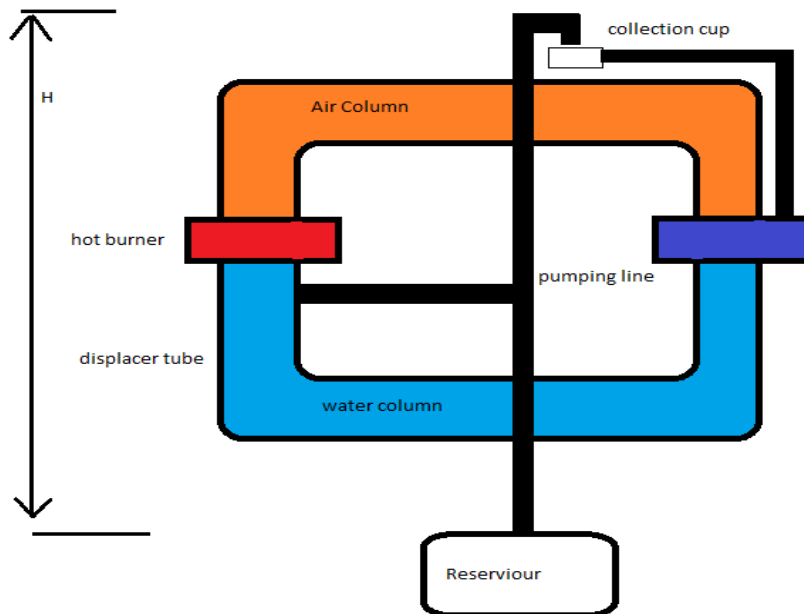


Fig. 12. Layout arrangement

Frequency of oscillations was found to be 1.57Hz using equation no 4. Volume of water pumped from pumping column is given by Q:

$$Q = A \times \sqrt{2gH} = 8.19 \text{ cm}^3/\text{s} = 8.19 \times 10^{-6} \text{ m}^3/\text{s}$$

$$\text{Power needed to pump water} = \rho \times Q \times g \times H = 1000 \times 8.19 \times 10^{-6} \times 9.8 \times 0.15 = 0.012 \text{ W.}$$

**6. Results**

Heat was supplied at hot end by ignition of methanol soaked wick. Open end manometer and thermo meter was used to note the pressures & temperatures at both hot ends after regular time intervals.

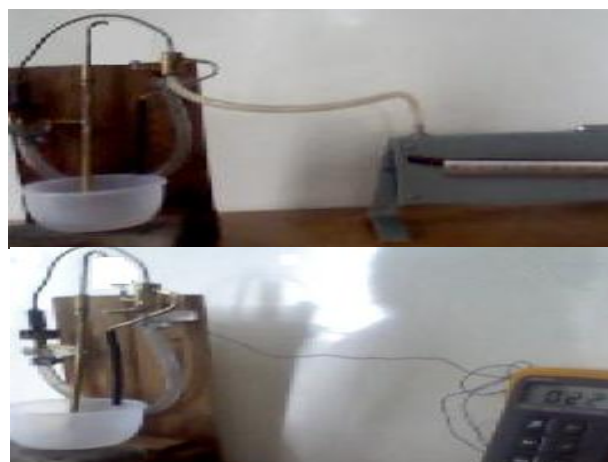


Fig.13. Pressure & temperature measurements by manometer & thermo couple

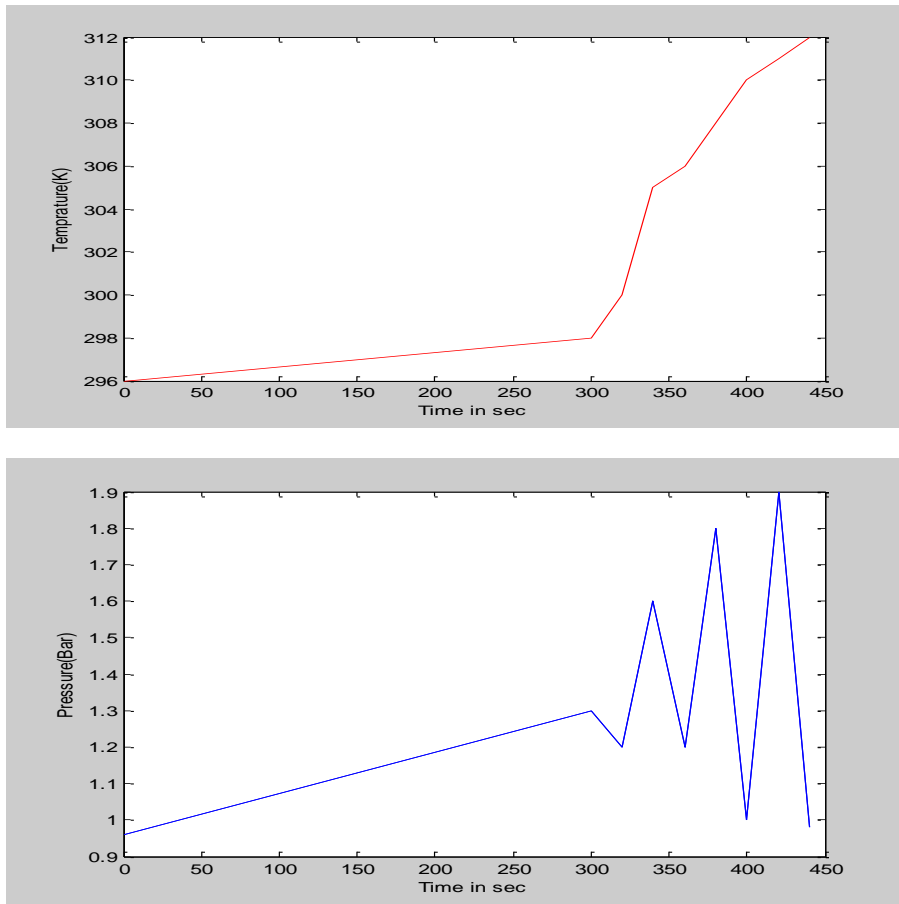


Fig. 14. Variation of pressure & temperatures

Practically it was difficult to observe the stroke length, however using ideal gas laws it was easier to find the theoretical stroke length visualizing the device as a wobbling column of fluid, as shown in figure no 15. Assuming air occupying connecting tube as ideal gas we have:

$$V_1 = \frac{\pi D^2}{4} \tag{5}$$

$$\frac{P_1 V_1}{T_1} = \frac{P_2 V_2}{T_2} \tag{6}$$

$$V_d = V_1 - V_2 = 2 \left( \frac{\pi D^2 S}{4} \right) \tag{7}$$

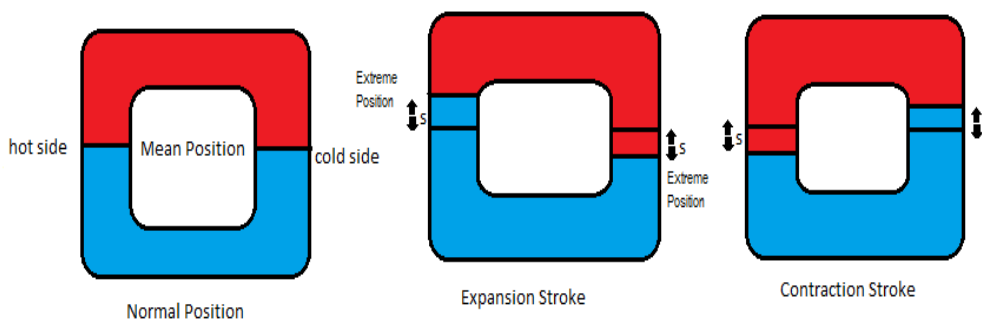


Fig. 15. Wobbling fluid column

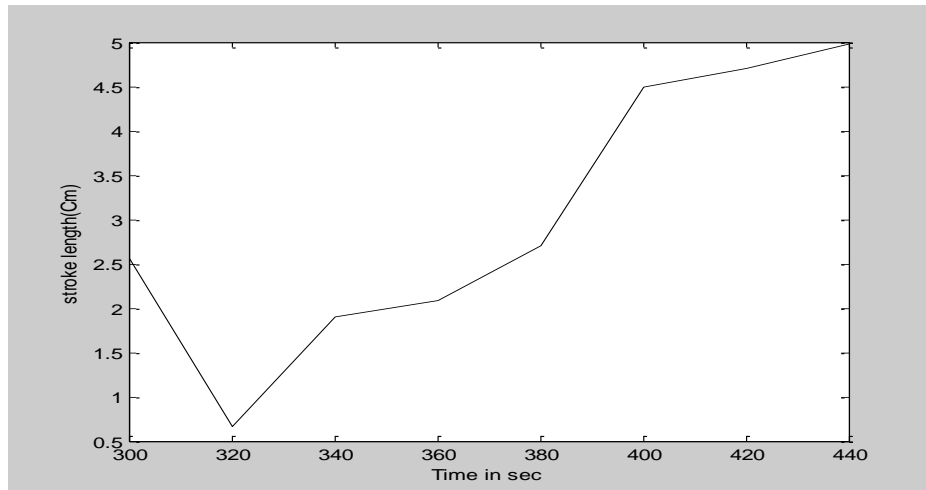


Fig. 16. Variation of stroke length

TABLE 1: Recorded values of pressures &amp; temperatures

Pressure (mm of Hg)	Pressure (Bar)	Temperature (K)	Time(s)
730	0.96	296	0
988	1.3	298	300
912	1.2	300	320
1216	1.6	305	340
912	1.2	306	360
1368	1.8	308	380
760	1	310	400
1444	1.9	311	420
745	0.98	312	440

TABLE 2: Calculation of stroke length

P <sub>1</sub> (mm of Hg)	V <sub>1</sub> (Cm <sup>3</sup> )	T <sub>1</sub> (K)	P <sub>2</sub> (mm of Hg)	T <sub>2</sub> (K)	V <sub>2</sub> (Cm <sup>3</sup> )	V <sub>1</sub> -V <sub>2</sub> (Cm <sup>3</sup> )	S (cm)	Time(s)
733	22.6	296	988	29S	16.8	5.8	2.56	300
988	16.8	298	912	300	18.32	1.52	0.67	320
912	18.32	300	1216	305	13.96	4.36	1.9	340
1216	13.96	305	912	306	18.68	4.72	2.085	360
912	18.68	306	1368	308	12.53	6.15	2.7	380
1368	12.53	30S	760	310	22.7	10.17	4.5	400
760	22.7	310	1444	311	11.99	10.71	4.7	420
1444	11.99	311	745	312	23.31	11.32	4.98	440

## 7. Conclusion

Both temperature & pressure of air in the fluidyne rose with time as it gains more and more heat from the burning fuel. Pressure fluctuated & peak pressure was found to be around 1400 mm of Hg, whereas the peak temperature was found to be around 39°C indicating poor heat transfer to the working gas (air). In order to reduce heat losses, the connecting column can be covered with an insulation covering of polytetrafluoroethylene tape. Further in order to improve the heat transfer rate, bigger connections can be used so that more mass of air is able to gain heat from the burning fuel. Commercial form of such fluidyne engines can be developed by using solar energy as source of heat to create pressure oscillations, thus pumping ground water from a certain depth.

## References

- [1] Ground Water (June 2010), retrieved from [http://en.wikipedia.org/wiki/Ground\\_water](http://en.wikipedia.org/wiki/Ground_water);
- [2] Water Resources (June 2013), retrieved from [http://en.wikipedia.org/wiki/Water\\_resources#Sources\\_of\\_fresh\\_water](http://en.wikipedia.org/wiki/Water_resources#Sources_of_fresh_water);
- [3] The United Nations world water development report 3 (June 2013), retrieved from [http://webworld.unesco.org/water/wwap/wwdr/wwdr3/case\\_studies/pdf/WWDR3\\_Case\\_Study\\_Volume.pdf](http://webworld.unesco.org/water/wwap/wwdr/wwdr3/case_studies/pdf/WWDR3_Case_Study_Volume.pdf);
- [4] Earths energy budget (June 2013), from [http://en.wikipedia.org/wiki/Earth's\\_energy\\_budget](http://en.wikipedia.org/wiki/Earth's_energy_budget);
- [5] Trees & Capillary action (June 2010), from <http://www.davidnelson.md/Cazadero/Trees&CapillaryAction.html>;
- [6] Human Heart (June 2010), retrieved from <http://www.webmd.com/heart/picture-of-the-heart>;
- [7] Nerve impulses (June 2010), from <http://www.biologymad.com/nervoussystem/nerveimpulses.html>;
- [8] C. D. West, “Liquid Piston Stirling Engine”, Van Nostrand Reinhold, New York, 1983.

## Kinematic and Dynamic Irregularities of Roller Pumps

### Part II. Numerical Research, Results and Analysis

Prof. MSc. Gencho POPOV PhD.<sup>1</sup>, MSc. Yuliyang ANGELOV PhD.<sup>1</sup>

<sup>1</sup>University of Ruse “Angel Kanchev”, Bulgaria, gspopov@uni-ruse.bg, julian@uni-ruse.bg

**Abstract:** In this work some theoretically found results, concerning typical irregularities of roller pumps, are given. The impact of some main geometric sizes on the character of changing of a given working camera's flow rate, as well as the possibility for using approximate equations for the determination of the coefficient of kinematic flow rate's irregularity, are indicated. The phase characteristics of a roll's rotation, indicating the existing of a transitional and unsteady periodical process, depended by the kinematic characteristics of rotation, have been presented. Graphs, representing the change of the existing forces, acting on the pump's rolls, and adjusted pump's shaft torque, both them limited in the range of one full rotation, have also been given.

**Keywords:** Roller pump, kinematic and dynamic irregularities.

#### 1. Introduction

In the first part of this work the equations, describing some of the main irregularities of roller pumps: kinematic – determining the flow rate's irregularity; dynamic – determining the loading on the main working elements of these pumps, have been established. These equations ensure the providing of theoretical research, concerning the evaluation and analysis of the work processes of this type of pumps. The main purpose of this work is to use the already established (in the first part) theoretical models and equations, so that numerical research, concerning the determination of the character and parameters of the appeared and periodically existing processes, as well as the change of the occurred irregularities of a roller pump's working characteristics, to be accomplished.

#### 2 Numerical research and results, concerning the kinematic irregularities

In fig. 1 it is given the change of the dimensionless volume of a working camera, for different values of the eccentricity and radiuses of the rolls (with  $r^*$  the roll's radius is indicated), while it has been connected to the high pressure pump's canal.

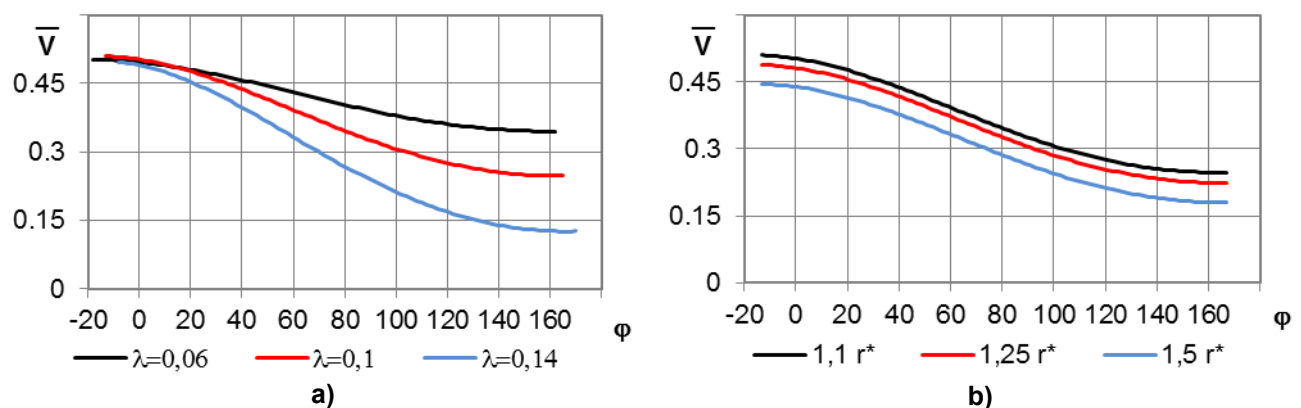


Fig. 1. Change of a working camera's volume as a function of the rotor's angular of rotation

In fig. 1a it can be clearly seen that the character of the volume's changing stays similar for different values of the eccentricity  $\lambda$  and with the increasing of  $\lambda$  the change of the relative volume also start to increase, which can be considered as a result of the increased pump's total working

volume. If the roll's radius is being increased, while the other geometric sizes stay constant, the line  $\bar{V} = f(\varphi)$  moves down, which is a result of the decreased pump's total working volume.

In fig. 2 it can be seen the change of the dimensionless flow rate of a given working camera, while it has been connected to the high pressure zone.

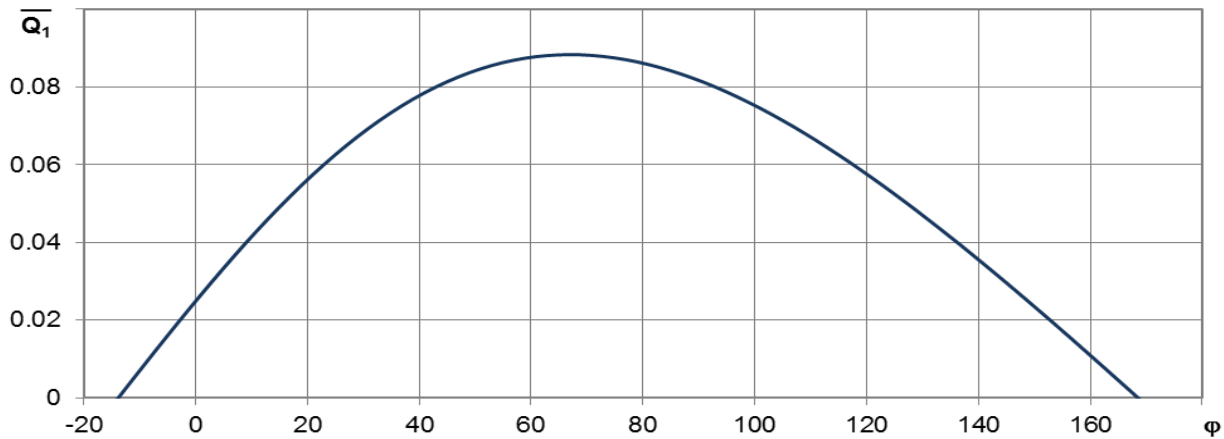


Fig. 2. Change of a given working camera's flow rate

It can be seen that the flow rate, ensured by a working camera, is characterized by too high irregularity, which has a significant impact on the total flow rate's kinematic irregularity for the investigated type of roller pumps. The location of the function's maximum is not exactly in the middle of the high pressure move, and it is dislocated in left. The increasing of the pump's flow rate to  $\bar{Q}_{1,\varphi} = \bar{Q}_{1,\varphi_{\max}}$  becomes more intensive, compared to its decreasing to  $\bar{Q}_{1,\varphi} = 0$ .

It is interesting for the graph, representing the change of the momentary theoretical flow rate -  $Q_{\varphi}$ , for pumps having different number of rolls, to be seen. A well-known fact is that the number of rolls, being even or odd, has a significant impact on the working process for all the volumetric hydraulic machines with analogical kinematic of their main working elements. The graphs, given in fig. 3, show the change of a pump's momentary flow rate, when the pump consists of an odd ( $z = 5$ ) or even ( $z = 6$ ) number of rolls. It can be seen, that for the odd number of rolls the difference between the maximal and minimal flow rate has a significantly less value than in case the pump is with an even number of rolls. This is the main reason for the less kinematic irregularity of the theoretical flow rate in case of a pump with an odd, instead of even, number of working cameras.

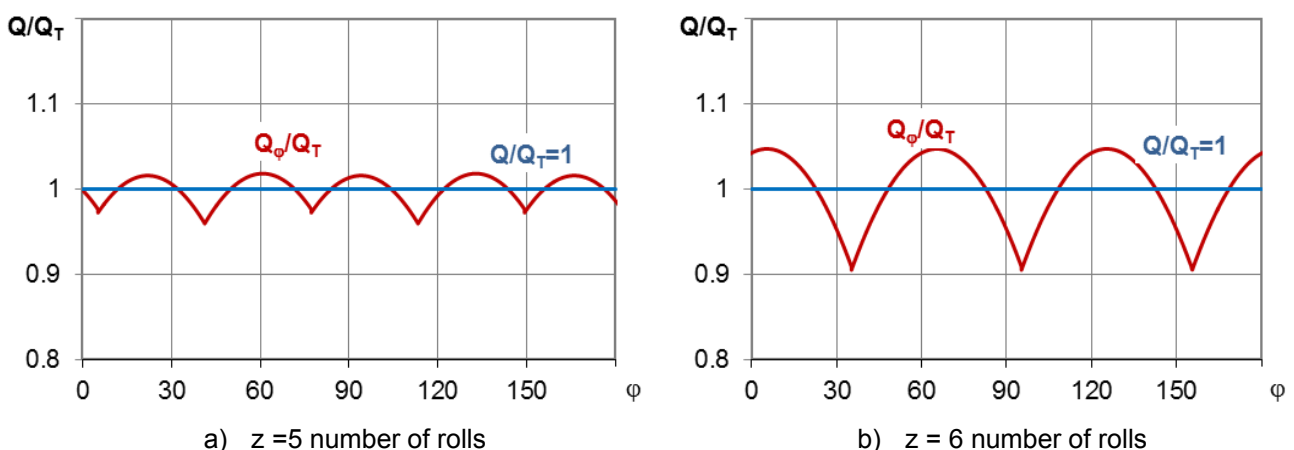


Fig. 3. Change of the momentary theoretical flow rate of a roller pump with an odd and even number of rolls

As it can be expected, the number of rolls has the most significant impact on the pump flow rate’s irregularity. For an even number of the working cameras the coefficient  $\delta$  of the flow rate’s kinematic irregularity has a significantly higher value than in case of an odd number of these cameras. The impact of the main geometric parameters – relative eccentricity and diameter of the rolls, on the coefficient of irregularity is minor. Practically, the roll size doesn’t influence the flow rate’s irregularity. With the increasing of the pump’s relative eccentricity, for a given number of rolls, the kinematic irregularity of the flow rate will also increase. The value of this increase will be limited in a given range, however it will be higher (given as an absolute value) for the pump with less number of rolls. For pumps with more than 10 rolls, when the relative eccentricity is being increased the coefficient of irregularity will also increase, but this increase (given as an absolute value) will be less than 1%.

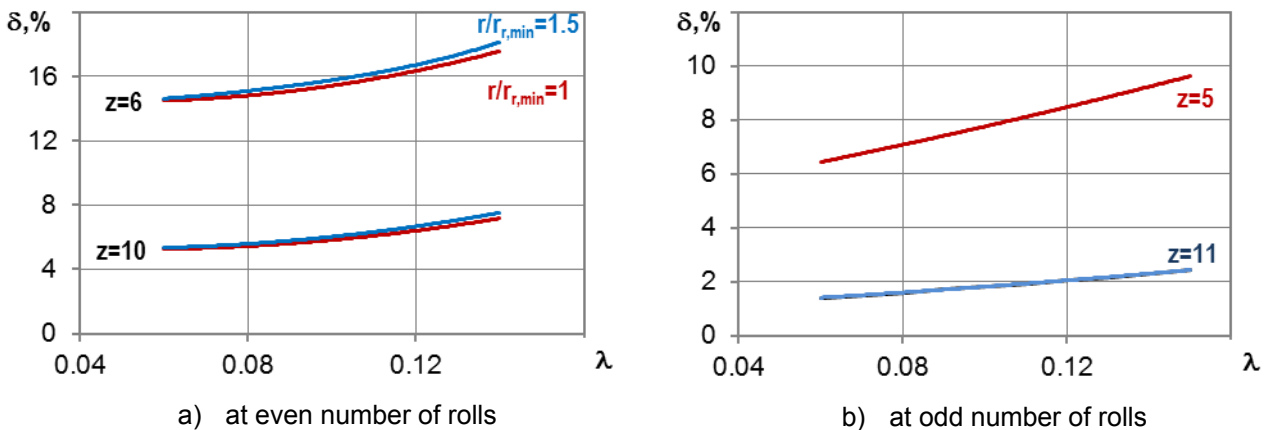


Fig. 4. Change of the coefficient of irregularity of the theoretical flow rate of roller pumps with an odd and even number of rolls

The evaluation of the kinematic irregularity (in finding a solution of engineering problems) can be accomplished by using approximate equations, ensuring the estimation of  $\delta$ . For rotary volumetric pumps with similar kinematic of their main working elements (pistons, vanes, etc.), it is recommended that:  $\delta \approx \frac{500}{z^2}$  - for pumps with an even number of rolls;  $\delta \approx \frac{125}{z^2}$  - for pumps with an odd number of rolls. This can be clearly seen in fig. 5.

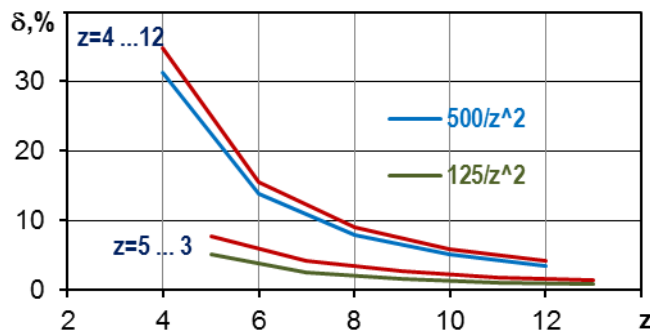


Fig. 5 Comparison between the values of the coefficients of kinematic irregularities, found by using the established precise and approximate equations

### 3. Numerical research and results found for the investigated dynamic processes

This part of the work consists of results, found for given concrete problems and having different level of coherence between each other, but both are based on the established in the first part equations - (16)-(21). For finding a solution of these problems the required algorithms, programs

and numerical procedures, used to accomplish the simulation and to investigate the existing processes, have been developed in Matlab. The accomplished numerical experiments represent the next stage of progress to the research given in [2], where the investigated roller pump has the following parameters:  $z = 6$ ,  $\Delta p = 0.4$  MPa,  $k = 0.01 r_r$  Nms/rad,  $g = 9.81$  m/s<sup>2</sup>,  $m = 0.02$  kg,  $R = 0.045$  m,  $r = 0.0415$  m,  $r_r = 0.009$  m,  $b = 0.0381$  m,  $e = 0.003$  m,  $\omega = 500\pi$  rad/s,  $\mu_1 = \mu_2 = 0.02$ .

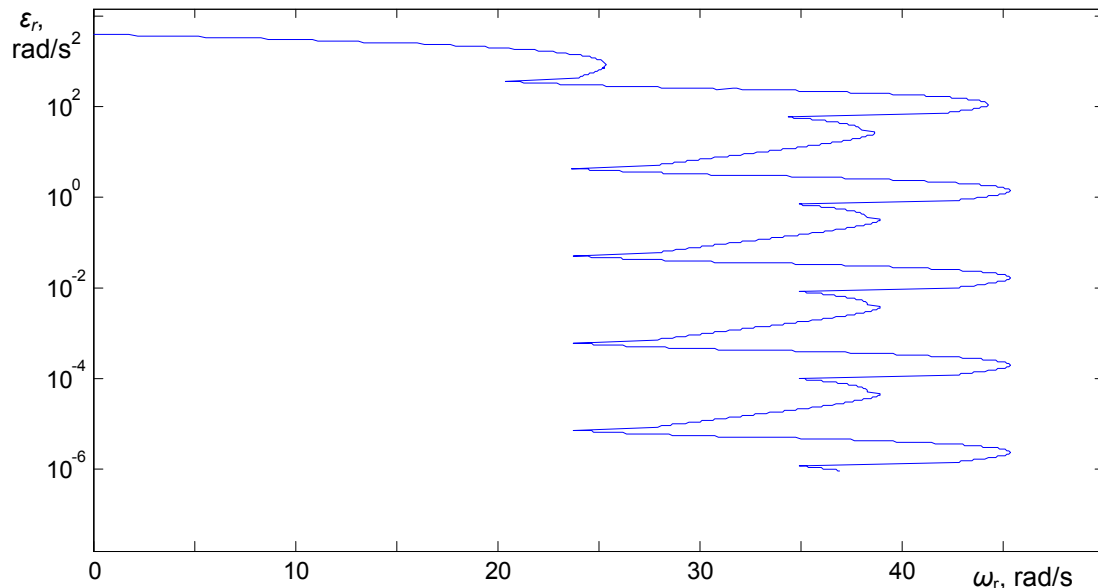


Fig. 6. A phase characteristic  $\omega_r = \omega_r(\varepsilon_r)$

A significant part of the investigation of a given dynamic process is the structuring and analyzing of its phase characteristics. Fig. 6 shows the relation between the angular velocity and acceleration, and fig. 7 – the relation between the angular of rotation and angular velocity. Looking at the graphs, it can be seen that a transitional process and steady periodical process of changing the roll's angular velocity exists.

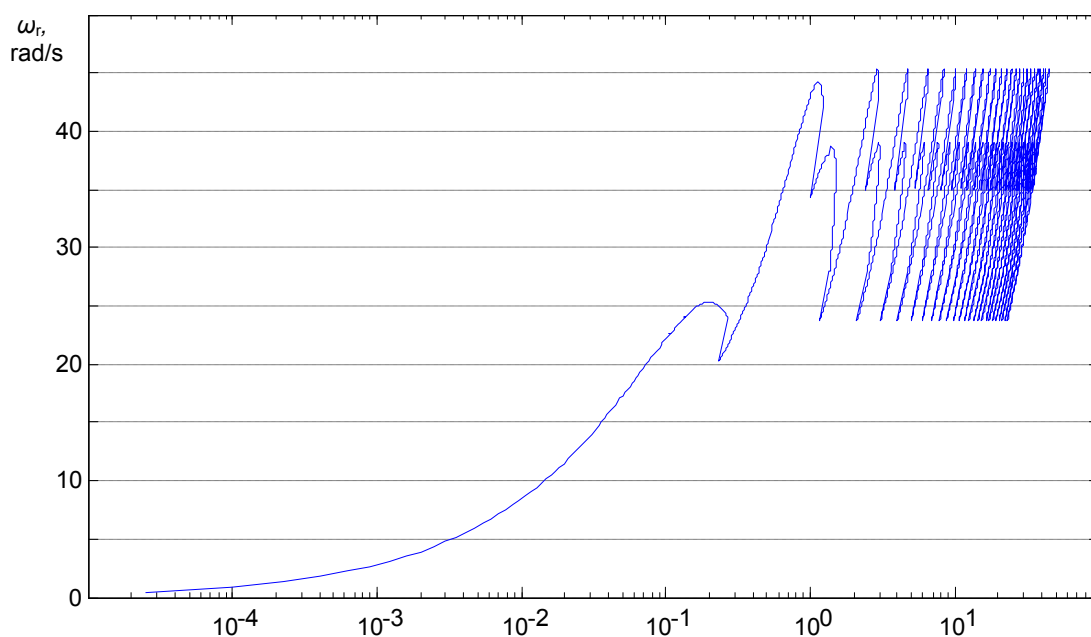
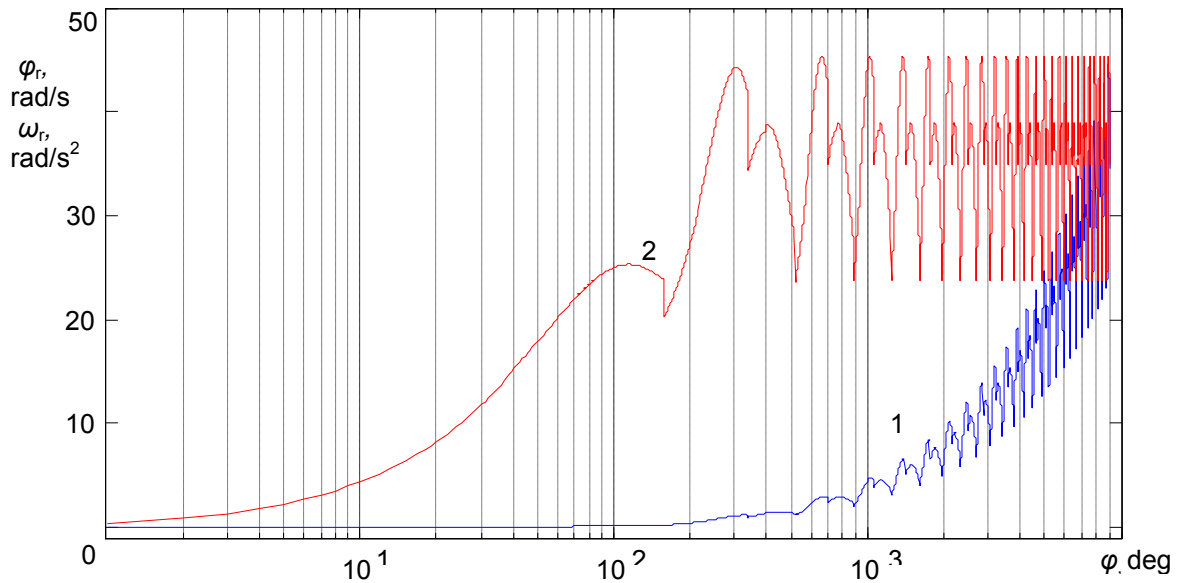


Fig. 7. A phase characteristic  $\varphi_r = \varphi_r(\omega_r)$

For the visualization of the transitional process the angular acceleration (in fig. 6) and the angular of rotation (in fig. 7), are given together in a same logarithmic scale. The periodicity of changing to the angular velocity, in the defined regime, is being characterized with a constant value of its amplitude. The angular acceleration, found for different significant values of the initial velocities (fig. 6), get steady rapidly to the levels of keeping the fluctuations of the roll's angular velocity  $\omega_r$  in a given constant interval. This leads to the ensuring of a periodicity of the roll angular of rotation's value -  $\varphi_r$ , achieved at the same speed of rotation (fig. 8), but belonged to a range of values with continuous one-direction increase (fig. 7).



**Fig. 8.** Change of the angular of rotation  $\varphi_r$  (1) and roll's angular velocity  $\omega_r$  (2) according to the rotor's angular of rotation  $\varphi$

The graphs, given in fig. 9, represent the normed, in terms of the maximal force of pressure -  $F_{\max}$ , equations, concerning the forces with the most significant impact on the mechanical state of the pump rolls:

$$\bar{F} = \frac{F}{F_{\max}}, \quad \bar{N}_1 = \frac{N_1}{F_{\max}}, \quad \bar{N}_2 = \frac{N_2}{F_{\max}} \quad \text{and} \quad \bar{\Phi} = \frac{\Phi}{F_{\max}},$$

when the rotor is being rotated three times.

For the same period of time it is given and the graph representing the relation between the roll's angular velocity -  $\omega_r$ , normed with respect to its maximal value:

$$\bar{\omega}_r = \frac{\omega_r}{\omega_{r,\max}}.$$

The so given dimensionless equations, ensuring the accomplishment of a scale overlay (fig. 9), where parameters, having different dimensions, can be implemented. This will lead to the simplification of studying and analyzing the investigated processes. The results, found in this research, confirm the results found in [2], according to which the change of the angular velocity -  $\omega_r$ , for a steady pump's work regime, has a cyclic character with a period of  $2\pi$  and a phase, which is coincident to the centrifugal inertia force -  $\Phi$ . As a significant element in the graph of  $\omega_r$ , the "jumping" decrease of the angular velocity's value, during the incursion in sealing sections and the "jumping" increase - during the leaving of these sections, can be recognized. It has to be indicated that, if the roll's mass inertia moment has a constant value, the periods of incursion and leaving are related (respectively) to the exporting and importing of kinetic energy. In the graph of  $\omega_r$ , given in fig. 9, the additional possibilities for ensuring of a quantitative view for the values of "jumps" - the decreases in the velocity's value are significantly higher, compared with the increases, can be seen. In terms of mathematical considerations the interruptions in the graph of

the function  $\omega_r = \omega_r(\varphi)$  represent ambiguities, implementing an additional cyclic irregularity of the work processes in the investigated pump. Their studying is being an object of an additional research, which does not correspond to the purpose of this work.

The “jumping” change of the reactions  $N_1$  and  $N_2$  is presented in [2], where it has been defined as a shock/hit interaction between the roll and respectively the stator and rotor. Applying the hypothesis for the existing of ideal plasticity, i.e. the velocity of reflection, occurred after the hit’s realization, is equal to zero, then during the roll’s incursion through the sealing sections the relative velocity of the hit interaction between the roll and stator will be twice bigger than the one between the roll and the rotor.

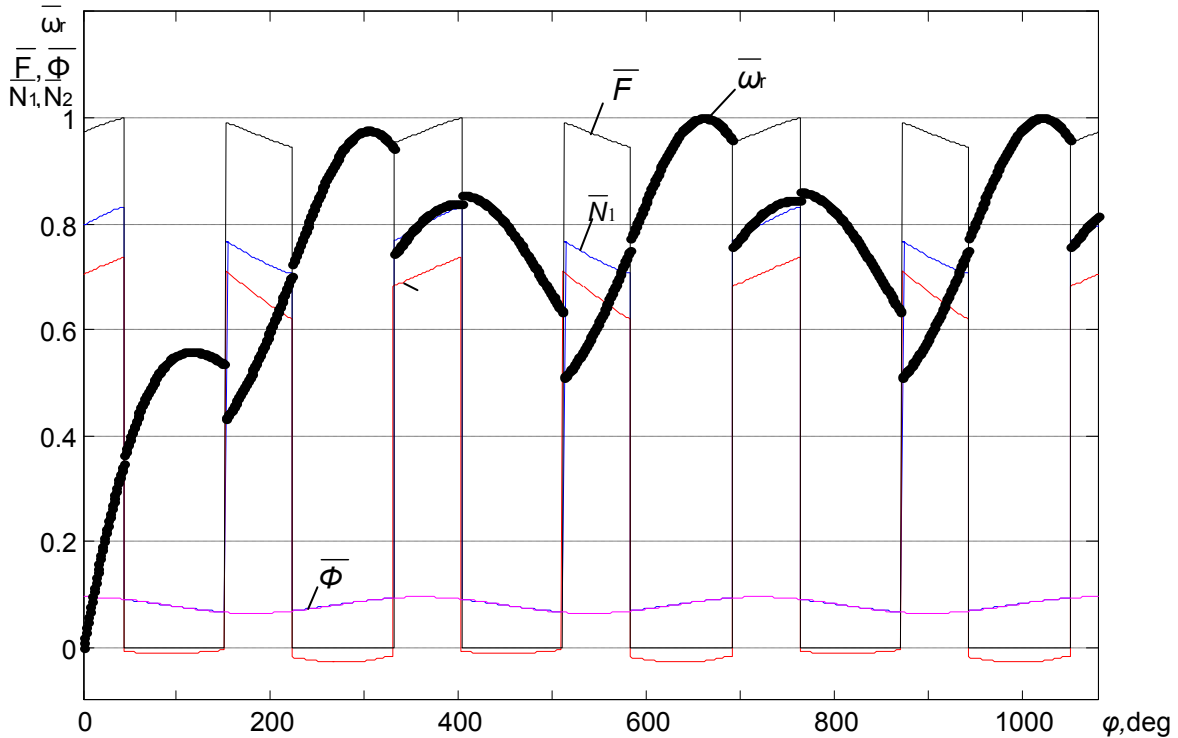


**Fig.9.** The change of the normed values of the roll’s angular velocity  $\bar{\omega}_r$  and the forces  $\bar{F}$ ,  $\bar{N}_1$ ,  $\bar{N}_2$  and  $\bar{\Phi}$  belonging to the first three rotations of the rotor.

During the pump is working, the occurred irregularities will not only affect the rolls, but they can also be referred to other pump’s main working elements. The irregularities, concerning respectively the stator and rotor, represent the appearance of dynamicity in the reactions of the pump’s fastening elements and the torque’s characteristic -  $M_R = M_R(\varphi)$ . The rotor torque’s degree of irregularity can be evaluated by the coefficient of dynamicity:

$$k_d = \frac{M_{R,max} - M_{R,min}}{M_{R,mid}},$$

where  $M_{R,max}$  and  $M_{R,min}$  are respectively the maximal and minimal values of the function  $M_R = M_R(\varphi)$ , and  $M_{R,mid}$  is the function’s average value:

$$M_{R,mid} = \frac{M_{R,max} + M_{R,min}}{2}.$$

Based on the equations, established in part I of this work, the possibility for accomplishing the graph -  $M_R = M_R(\varphi)$ , is given by the equation, estimating the reduced moments, in terms of the rotor’s axis:

$$M_R(\varphi) = \sum_{i=0}^{z-1} N_{2,i}(\varphi + i\beta) \overline{O_r C_i}(\varphi + i\beta),$$

where  $O_r C_i(\varphi) = e \cos(\varphi) + \sqrt{(R-r)^2 - e^2 \sin^2(\varphi)}$  is the distance between the rotor’s axis of rotation and the  $i^{th}$  number of a roll, and  $N_2(\varphi)$  is the projection of the main vector of forces on the tangent. In figures 10 and 11, the graphs of the functions  $M_R = M_R(\varphi)$ , found for one full rotation of the pump’s rotor, in case of an odd ( $z=7$ ) and even ( $z=8$ ) number of rolls, where all the other main parameters are having fixed constant values, are given.

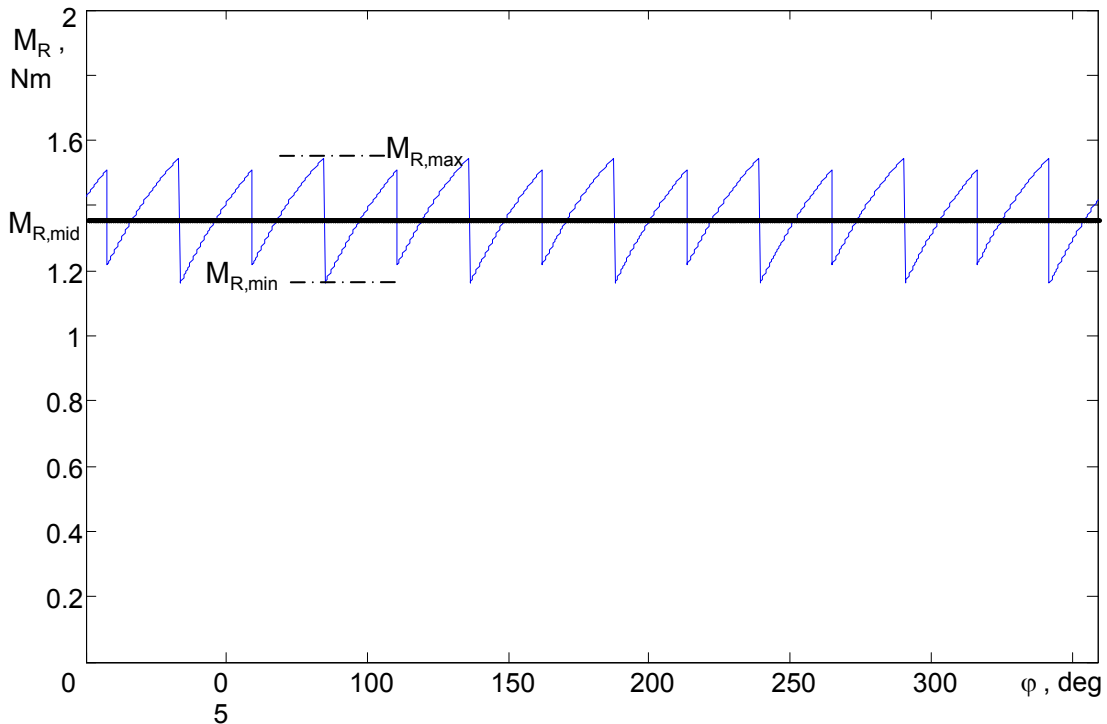


Fig.10. Torque’s characteristics  $M_{R,mid}$  at  $z=7$

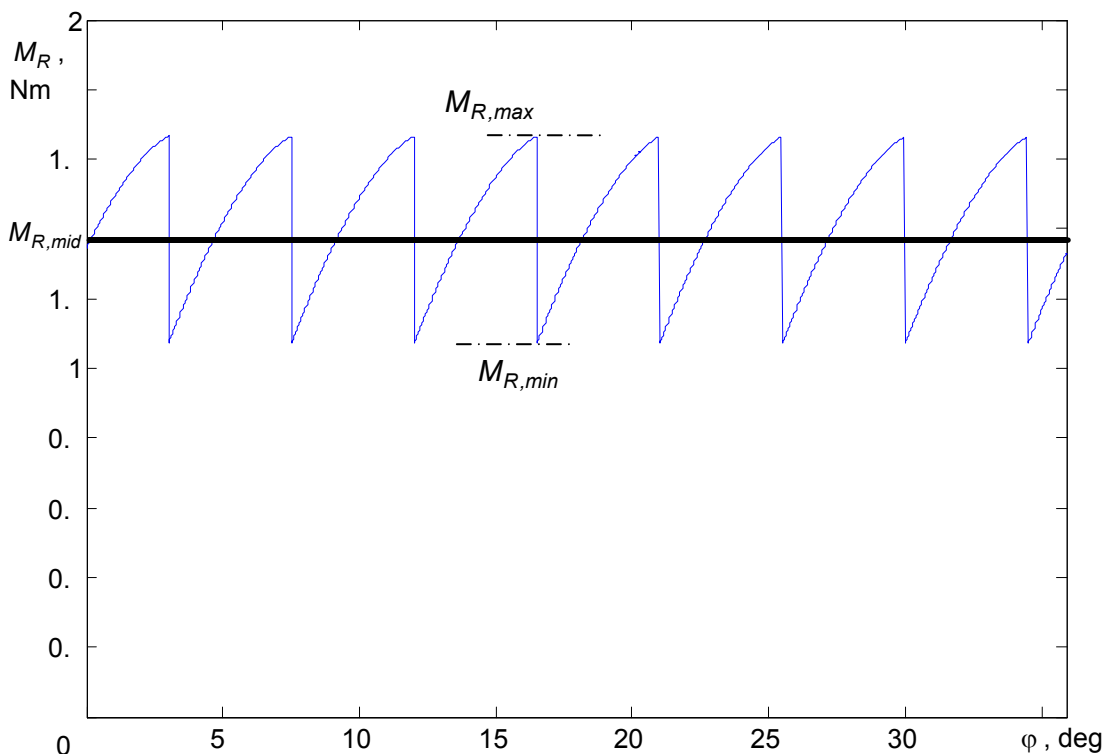


Fig.11. Torque’s characteristic  $M_{R,mid}$  at  $z=8$

The difference in the values of the coefficient of dynamics  $k_d$  is significant, which fully correspond to the information, given in some high-reputed specialized editions. In the case of an odd number ( $z=7$ ) of rolls, it is found that:  $k_d = 0.2844$  - at  $M_{R,max} = 1.5464\text{Nm}$ ,  $M_{R,min} = 1.1614\text{Nm}$  and  $M_{R,mid} = 1.3539\text{Nm}$ , and in case of an even number ( $z=8$ ) of rolls, it is found that:  $k_d = 0.4313$  - at  $M_{R,max} = 1.6659\text{Nm}$ ,  $M_{R,min} = 1.0748\text{Nm}$  and  $M_{R,mid} = 1.3704\text{Nm}$ . As a significant the difference between the frequencies of the existing irregularities, occurred in the range of one full rotor's rotation, can be considered. It is necessary to indicate, that for an even number of rolls the frequency is multiple to the number of rolls  $z$ , while for an odd number of rolls, it is multiple to their doubled number –  $2z$ .

## Conclusions

Analyzing the accomplished theoretical research, concerning some typical for the investigated type of roller pumps irregularities, the following more important conclusions can be given:

- The impact of the relative eccentricity and roll size on the character of changing to the flow rate of a work camera – fig. 1, is determined;
- According to the graph, given in fig. 5, it can be seen that for the approximate evaluation of the flow rate's kinematic irregularity the approximate equations for estimating the coefficient  $\delta$ , can be used. The using of these equations is recommended in case of volumetric pumps with a similar kinematic of their working elements (pistons, vanes, etc.);
- In figures 6 and 7, the phase characteristics of the roll rotation for a given roller pump, are given. The analysis of these results indicates the existing of a transitional and steady periodical process, related to the kinematic characteristics of the roll's rotation (fig. 8);
- According to the graph of the normed forces and angular velocity, given in fig. 9, it can be concluded that the “jumping” ambiguities in the change of the angular velocity will match the ambiguities of the forces, occurred during the roll's transition through the transitional sealing sections;
- By using an appropriate modification of the proposed mathematical model (1), (2) and (3), the diagram of the rotor's torque (fig. 10 and fig. 11) is being found. In addition to that, the coefficient of rotor's dynamic (1), in case of an even and odd number of rolls, is determined.

## References

- [1] Angelov Y., G. Popov Dynamics of the rollers of a roller pump, Part I. Modeling of force load. PROCEEDINGS of the UNIVERSITY OF RUSE “Angel Kanchev” Volume 53, book 2 Mechanics, Mechanical and Manufacturing Engineering, ISBN 1311-3321, Ruse, 2014, 111-115 p.
- [2] Angelov Y., I. Nikolaev Dynamics of the rolls of a roller pump, Part II. Numerical study of the dynamics of rolls. PROCEEDINGS of the UNIVERSITY OF RUSE “Angel Kanchev” Volume 53, book 2 Mechanics, Mechanical and Manufacturing Engineering, ISBN 1311-3321, Ruse, 2014, 116-120 p.
- [3] Popov G., P. Russev. Irregularities in a roller pump's flow rate. PROCEEDINGS of the UNIVERSITY OF RUSE “Angel Kanchev” Volume 37, ser. 9, ISBN 1311-3321, Ruse, 1999, 102-105 p.
- [4] Popov G., P. Russev. About the geometry of the flow rate's distribution in roller pumps. PROCEEDINGS of the UNIVERSITY OF RUSE “Angel Kanchev” Volume 37, ser. 9, ISBN 1311-3321, Ruse, 1999, 106-110 p.

## Static Characteristics of the Orifices in a Pilot Operated Pressure Relief Valve

PhD. eng. Sasko DIMITROV<sup>1</sup>, PhD. eng. Simeon SIMEONOV<sup>2</sup>, PhD. eng. Slavco CVETKOV<sup>3</sup>

<sup>1</sup> “Goce Delcev” University - Stip, Macedonia, sasko.dimitrov@ugd.edu.mk

<sup>2</sup> simeon.simeonov@ugd.edu.mk, <sup>3</sup> slavco.cvetkov@ugd.edu.mk

**Abstract:** In this paper the static characteristics of the sharp edged orifices have been investigated. Mathematical relationship between pressure loss and flow through the orifice has been developed and solved for orifices mainly used in pilot operated pressure relief valves. A CFD simulation of the flowing process has been done. A full CAD model of the volume for orifices with different geometric parameters was created and meshed at finite number of elements. As a result of the CFD computations, few diagrams have been presented and compared to the theoretical ones. The discharge coefficient and the pressure loss coefficient have been obtained.

**Keywords:** orifice, pressure drop, flow, CFD, simulation, discharge coefficient.

### 1. Introduction

Functional drawing of conventional type, most frequently used in industry, pilot operated pressure relief valve is presented on fig. 1 [1]. Inlet parameter of the valve is the flow  $q_1$  and the outlet parameter is the system pressure  $p_1$  set at the pilot valve. When the system pressure is lower than  $p_1$ , both stages, the pilot and the main stage, are closed. When the system pressure reach the set value, pilot stage opens and small amount of pilot flow  $q_y$  is flowing through the orifices 1 and 2 and the pilot stage, but the main stage is still closed because of low pressure drop in the orifices 1, 2 and 3. When the pilot flow increases enough, the orifices 1, 2 and 3 causes enough pressure drop, pressure force in the upper chamber of the main stage is lower than the pressure force of the system pressure. In this case the main stage opens and all the flow is relieving to the tank. So, pressure drop through the valve orifices is the key factor for proper operation of the valve. Those orifices are sharp edged, i.e. short length orifices where linear pressure drop can be neglected, only quadratic pressure drop exist.

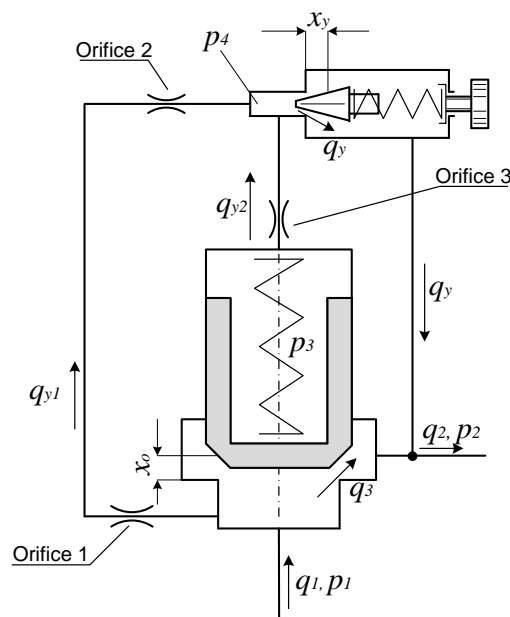


Fig. 1. Functional diagram of a pilot operate pressure relief valve

The flowing and pressure drop through the sharp edged short orifices have been investigated long time ago. In [2] a model for discharge coefficient in the orifice is introduced as a function of the Reynolds number. According to this model, discharge coefficient calculation requires iterative procedure because Reynolds number also depends on the flow rate. To avoid this iterative procedure, in [3] an empirical discharge coefficient model for orifice flow is recommended. Another model for the discharge coefficient is described in [4] by Borutzky. Those models provide a linear relation through the orifice for small velocities while for turbulent flows, they match the conventional square root characteristics. Also, the transition from the laminar to the turbulent regime is smooth [5].

In this paper a CFD method for simulation of the flowing process through the orifice is used, the pressure drop coefficient and the discharges coefficient have been determined and compared with numerical ones.

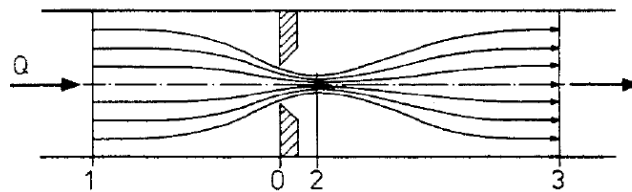


Fig. 2. The sharp edged orifice

## 2. Mathematical modelling

Steady state flowing process through an orifice is presented in fig.2. Well known dependence on flow of the pressure drop is [6]:

$$Q = \alpha_D \cdot A_0 \cdot \sqrt{\frac{2}{\rho} \cdot \Delta p} \quad (1)$$

where:  $Q$  – the flow through the orifice;  $\alpha_D$  – the discharge coefficient;  $A_0$  - the area of the orifice,  $\Delta p = p_1 - p_3$  - the pressure drop in the orifice.

Pressure drop in the sharp edged short orifice can be expressed by the equation:

$$\Delta p = \xi \cdot \frac{\rho}{2 \cdot A_0} \cdot Q^2 \quad (2)$$

Where:  $\xi$  - the local resistant coefficient.

Comparing the eq. (1) and (2), the dependence among the discharge coefficient and the pressure drop coefficient, is:

$$\alpha_D = \frac{1}{\sqrt{\xi}} \quad (3)$$

For  $Re = 10 - 20000$  and  $l/d = 1.5 - 10$ , Lichtarowicz [7] has recommended an expression for discharge coefficient calculation:

$$\frac{1}{\alpha_D} = \frac{1}{\alpha_{Dmax}} + \frac{20}{Re} \cdot \left(1 + 2.25 \cdot \frac{l}{d}\right) \quad (4)$$

Where  $d$  - the orifice diameter;  $l$  - the orifice length.

Experimentally Wobben [8] has determined the maximal value of the discharges coefficient and it is  $\alpha_{Dmax} = 0.83$ .

Reynolds number for circle area is  $= \frac{v \cdot d}{\nu} = \frac{4 \cdot Q}{d \cdot \pi \cdot \nu}$ . Combining the last eq. for  $Re$ , into eq. (4) and introducing the correction factor  $\left[\frac{20 \cdot \nu}{d} \cdot \left(1 + 2.25 \cdot (l/d)\right)\right]^2$ , the final equation for flow calculation in a sharp edged orifice has been obtained:

$$Q = \alpha_{Dmax} \cdot \frac{\pi \cdot d^2}{4} \cdot \sqrt{\frac{2}{\rho} \cdot \Delta p + \left[ \frac{20 \cdot v}{d} \cdot (1 + 2.25 \cdot (l/d)) \right]^2} - \alpha_{Dmax} \cdot 5 \cdot \pi \cdot d \cdot v \cdot \left( 1 + 2.25 \cdot \frac{l}{d} \right) \tag{5}$$

Knowing the geometric parameters of the orifice, applying eq. (5), it is possible to obtain the static characteristic of the orifice, i.e. the flow through the orifice depending on the pressure drop in the orifice.

### 3. CFD simulation of the flowing process through the orifices

To identify the discharge coefficient and the pressure drop in the orifice a series of steady-state CFD computations was performed with commercial CFD software package FLUENT. Three different sizes of orifices have been investigated: 0.6 mm, 0.8 mm and 1.0 mm. CAD model of the fluid volume has been created and it has been divided into around 310000 elements, depending on the size of the orifice. The meshing model of the 0.8 mm orifice is presented on fig.3.

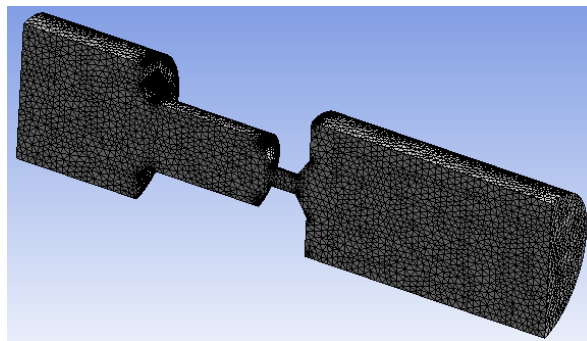
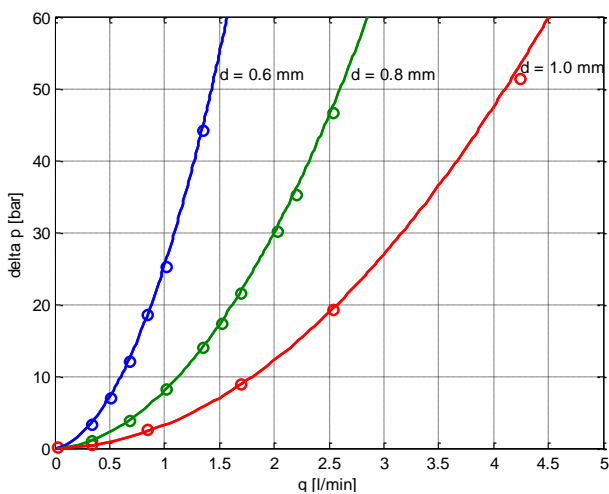


Fig.3. The CFD meshed geometry

As an input parameter was set the flow in the orifice. The output parameter, calculated by FLUENT, is the pressure drop through the orifice.

The results obtained by CFD simulation and the solution of the eq. (5) have been shown on fig.4. It is evident that there is a very good match of the results between CFD simulation and the presented theory.



○ CFD; — eq. ( )  
 Fig. 4. The static characteristics of the orifices

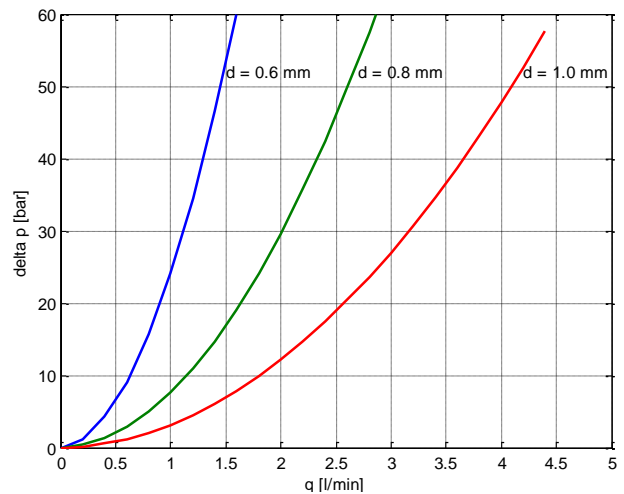


Fig. 5. The theoretical static characteristics of the orifices

For simplicity of calculation, very often the pressure drop in the sharp edged orifice can be approximated by the eq. (2). According to this relation, for the local resistant coefficient  $\xi = 1.48$ ,

the curves on fig. 5 have been obtained. It can be seen that there is good match between CFD simulation and relation (5) (fig.4) and the approximated eq. (2) fig. 5. Applying the eq.(3), the flow coefficient is  $\alpha_D = 0.822$ , i.e. it tends to  $\alpha_{Dmax} = 0.83$ .

The values of the flow coefficient depending on the Reynolds number have been presented on fig. (6). For turbulent regime of flowing the flow coefficient has constant value, but in the laminar regime of flowing, the flow coefficient is not constant, i.e. it varies depending on the average velocity of flowing in the orifice. Usually the pilot flow in the pressure relief valves is around 1.0 – 1.5 [l/min]. So the  $Re$  number does not exceed the value of 1500. For simplicity of calculation, in the dynamic model of the pilot operated pressure relief valve an average value of 0.8 for flow coefficient can be taken.

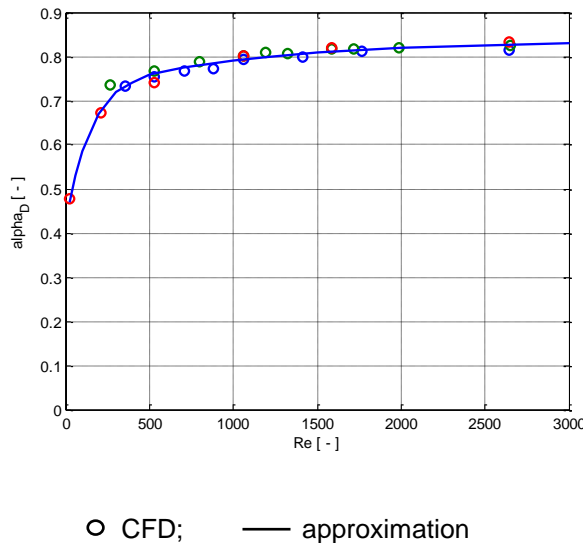


Fig. 6. The discharge coefficient of the orifices

Fig. 7 and fig.8 depict the pressure and velocity distribution for 0.8 mm sharp-edged orifice along the axis of the orifice. The pressure and velocity distribution do not differ qualitatively for different orifice diameters. The pressure drops quickly in the nozzle, then at the end of the nozzle the pressure little increase and then decrease and stay approximately constant. The velocity sharply rises in the nozzle and at the end of the nozzle begins to decrease.

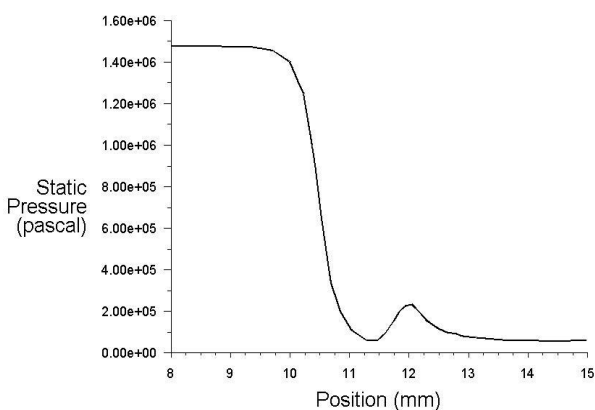


Fig.7. The pressure distribution along the orifice axis

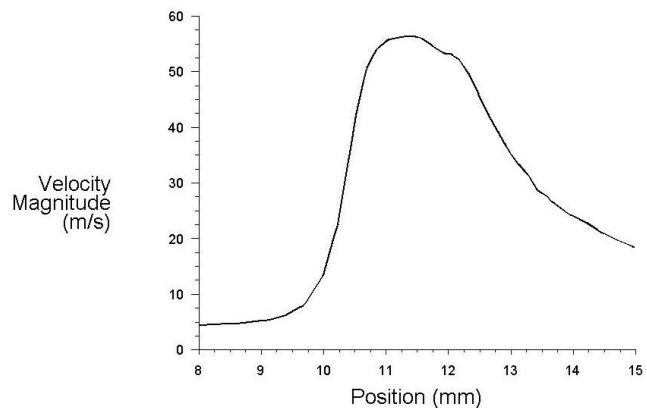


Fig. 8. The velocity distribution along the orifice axis

Typical velocity contour and velocity vectors of 0.8 mm orifice diameter, with 1.35 l/min and 14 bar pressure drop in the orifice is presented on fig. 9 and. Fig.10. The velocity contours and velocity vectors do not differ qualitatively for different orifice diameters. As it is expected, the maximal velocity occurs at the nozzle where the diameter is the lowest.

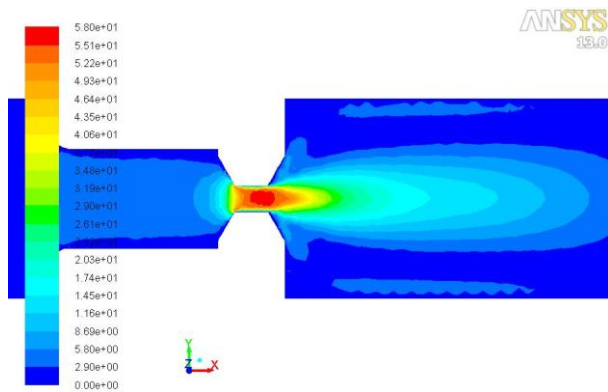


Fig. 9. The velocity contour

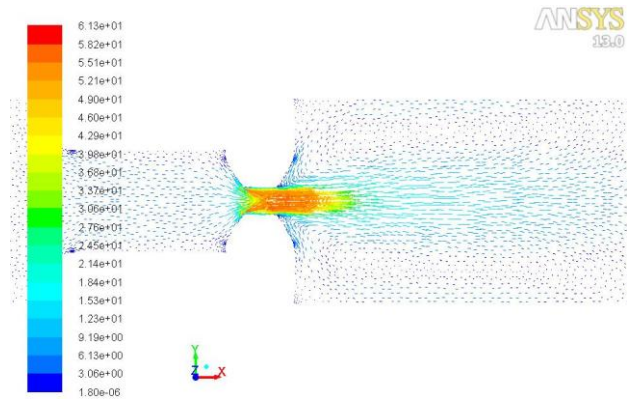


Fig. 10. The velocity vectors

#### 4. Conclusions

Mathematical relationship between flow and pressure loss in the sharp edged orifices has been developed in this paper. This mathematical model was confirmed with CFD simulation. CAD model of the flowing volume was created and simulation of the flowing process has been made. Graphically was compared the results of the CFD simulation and the solution of the eq. (5). The flow coefficient depending on the Reynolds number was obtained and presented graphically on fig.6. The pressure and velocity distribution along the orifice axis was depicted and the velocity contour and velocity vectors were shown (fig. 9 and fig.10).

#### References

- [1] M. Komitovski, S. Dimitrov, “Transient response process of a pilot operate pressure relief valve”, XVIII National Scientific with International Participation, FPEPM 2013, Sozopol, Bulgaria, 2013;
- [2] H. E. Meritt, “Hydraulic Control Systems”, John Wiley and Sons, 1967;
- [3] D. Wu, R. Burton, and G. Schoenau, “An Empirical Discharge Coefficient Model for Orifice Flow”, International Journal of Fluid Power – ISSN 1439-9776, Vol. 3, No. 3, pp. 17-24, 2002;
- [4] W. Borutzky, B. Barnard, J. Thoma, “An orifice flow model for laminar and turbulent conditions”, Simulation Modelling Practice and Theory, Elsevier Science B. V., Vol. 10, 2002. pp. 141-152;
- [5] C. Hos, “Dynamic Behavior of Hydraulic Drives”, Dissertation, Department for Hydrodynamic Systems, Budapest University of Technology and Economics, Budapest, 2005;
- [6] W. Backé, H. Murrenhoff, “Grundlagen der Ölhydraulik. Institut für fluidtechnische Antriebe und Steuerungen“, Technische Hochschule Aachen, 1994;
- [7] A. Lichtarowicz, R. Duggins, E. Markland, “Discharge Coefficients for Incompressible NonCavitating Flow Through Long Orifices”, J. Mech. Eng. Sc. Nr. 2, 1965, pp. 210 – 219;
- [8] G. D. Wobben, “Statisches und dynamisches Verhalten vorgesteuerter Druckbegrenzungsventile unter besonderer Berücksichtigung der Strömungskräfte“, Dissertation, RWTH Aachen, 1978.

## Experimental Determinations on Improving Dynamic and Energy Performance of Pneumatic Systems

PhD. eng. **Gabriela MATACHE**, PhD. eng. **Radu RADOI**,  
PhD. eng. **Gheorghe SOVAIALA**, Tech. **Ioan PAVEL**

<sup>1</sup>INOE 2000-IHP, Bucharest, sovaiala.ihp@fluidas.ro

**Abstract:** *This paper presents the results of tests conducted on a pneumatic system using medium and high pressure actuators. These tests aimed to:*

- *detect the behaviour in dynamic regime of the drive system with medium pressure pneumatic actuators, pneumatic spring type load, achieved by installing throttles on the piston and rod chambers of the pneumatic drive actuator, respectively controlled using the pressure regulator valve, for step, ramp and sine wave signal (plotting the BODE diagrams: attenuation vs. frequency and phase vs. frequency);*
- *identify the methods and ways for optimization of dynamic and energy performance of drive systems with medium pressure pneumatic linear actuators.*

**Keywords:** *pneumatic positioning system, BODE plots*

### 1. Introduction

The pneumatic system with medium and high pressure actuators undergoes two types of tests:

**Static tests**, targeting:

- determining the minimum starting pressure for the piston of the pneumatic actuator driving the system, for both directions of travel (rod chamber and piston chamber);
- determining the pushing / traction forces of the pneumatic drive actuator;
- speed test at predetermined pressure, with pneumatic spring type load;
- speed test at predetermined pressure, with load created by proportional pressure regulator valve;

**Dynamic tests**, targeting:

- the response of pneumatic drive system with double acting actuator to step signal, for different values of the PID controller and pneumatic spring type load;
- the response of pneumatic drive system with double acting actuator to step signal, for different values of the PID controller and load controlled by proportional pressure regulator valve;
- the response of pneumatic drive system with double acting actuator to sine wave signal, for preset values of the PID controller parameters and load controlled by proportional pressure regulator valve; plotting the BODE diagrams (attenuation vs. frequency and phase vs. frequency) [1],[3]

The testing software is developed in LabVIEW. On the input of the USB-6218 data acquisition board there are inserted voltage-type signals from the pressure transducers (corresponding to the two chambers of the drive actuator), force transducer, displacement transducer, proportional pressure regulator valve. One of the two analog signal outputs of the data acquisition board is used for control of the proportional pressure regulator, and the other one for control of the proportional directional control valve in the testing diagram.

The testing device allows for tests on the drive systems with simple pneumatic actuators, namely medium and high pressure servo actuators, both in static and dynamic regime.

Supplying the electromagnets of the proportional equipment and also the sensors, the data acquisition board is made from a two-channel voltage source.

### 2 . Description of the system under tests

The system is made up of a mechanical assembly of two linear actuators, a drive actuator and a load one, and it is equipped with pressure transducers on the chambers of the drive actuator, force transducer between the rods of the two transducers and reflex position sensor to track position of the drive actuator rod.

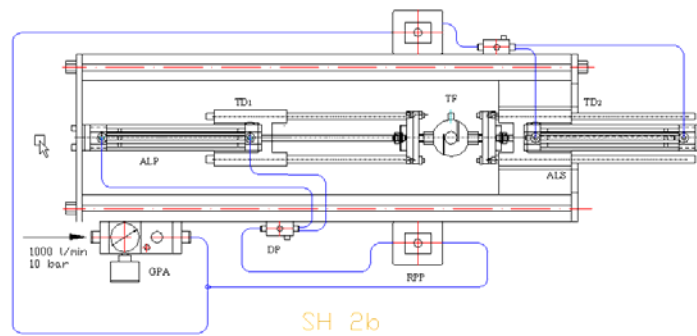


Fig. 1 Drive system with medium pressure pneumatic actuators  
(Schematic diagram of pneumatic connections)

### 3. System structure and functioning

The drive system with medium pressure pneumatic actuators, with load controlled by proportional pressure regulator valve, Fig. 2, is the embodiment of the pneumatic diagram in Fig. 3, and it has the following structure [3]:

-**GPA1 - air preparation group**, which includes the RP1 pressure regulator and the F1 filter; the air preparation group in the system structure is air regulator filter type, FRC-D, version MIDI;

-**RP- MPPE-3-1/2-10-010-B proportional pressure regulator**; the proportional pneumatic pressure regulator is an electro pneumatic interface element, which provides an output pneumatic pressure proportional to the input electrical signal

-**DP1 - MPYE-5-1/8HF-010-B flow proportional directional control valve (regulator)**; the flow proportional directional control valve enables achieving controlled flow rates, by opening the air passage cross-section by the slide valve depending on the amount of voltage type analog signal received by the electromagnet coil; in conjunction with an external position controller and a displacement encoder, enables the development of a highly accurate positioning pneumatic system; it plays the role of air flow controlling, to achieve different speeds of the pneumatic actuator rods, and allows changing the direction of motion.

-**TP<sub>1</sub>, TP<sub>2</sub> - PMP 1400 pressure transducers** read the values of pressure in the chambers of the drive actuators, convert them into voltage type analog signals and convey them to the computer via the USB-6218 data acquisition board; the PMP pressure transducer series 1400 is a resistive transducer and it is designed for use in harsh environments, in many industrial and process applications. The output signal is voltage type, with varying range 0 ... 5 V DC, and it is proportional to the pressure applied on the diaphragm. Precision: 0.15%.

-**ALP - DNCI-32 pneumatic linear drive servo actuator**, equipped with **TD<sub>1</sub> incremental displacement transducer**

-**ALS - DNCI-32 pneumatic linear load servo actuator**, equipped with **TD<sub>2</sub> incremental displacement transducer**

-**CP<sub>1/2</sub> – piston chambers** of pneumatic drive/load actuators;

-**CT<sub>1/2</sub> – rod chambers** of pneumatic drive/load actuators;

-**TF - CTOL 500 force transducer**, is installed between the rods of pneumatic drive and load actuators, and it is designed to allow tests on the thrust / traction force at the drive actuator, and also position and speed tests under load. Combined error of the transducer: < +/- 0.03 %.

The two medium pressure pneumatic actuators are identical, type DNCI 32, manufactured by FESTO, and they are equipped with incremental displacement transducer.

To increase the accuracy regarding the position of the drive actuator rod, a **reflex distance sensor code CP35MHT80** manufactured by WENGLOR has been introduced in the system, the incremental displacement transducers in the structure of the actuators not being connected to the data acquisition board.



**Fig. 2** Pneumatic system with medium pressure actuators, with load controlled by proportional pressure regulator valve

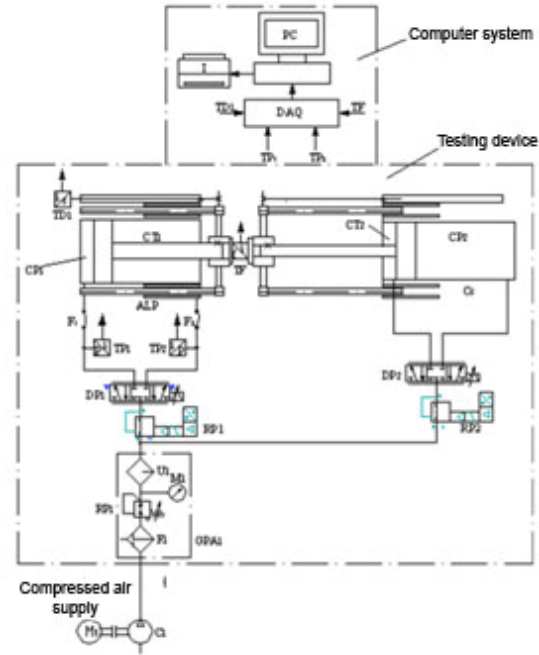


**Fig. 3** Pneumatic diagram of the drive system

**3. Electrical diagram of the data acquisition system**

The five transducers in the system are connected to the data acquisition system according to the diagram in Figure 4, [1].

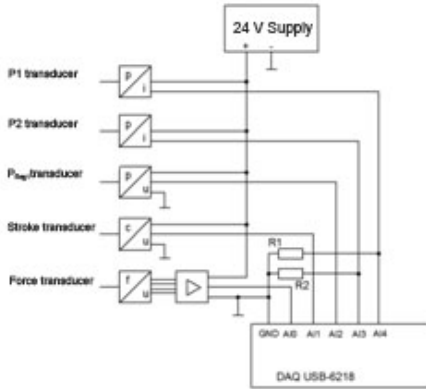


**Fig. 4** Layout of the system for data acquisition from transducers

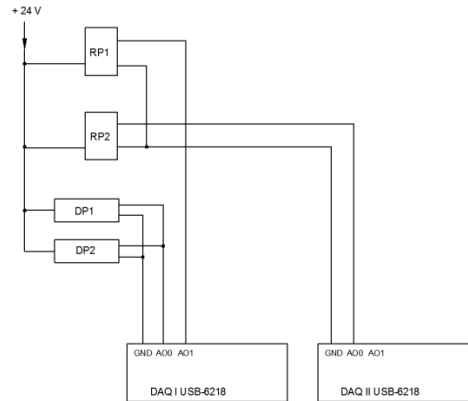


**Fig.5** Control diagram of proportional directional control valves and pressure regulators

Electrical control of proportional directional control valves and proportional pressure regulators is done via the analog outputs of two acquisition boards.

**4. The software for tests to step signal and response in frequency**

To conduct the tests there has been developed the system with medium pressure actuators (Fig. 2), based on the pneumatic testing diagram (Fig. 3) and the diagram of connections between the pneumatic devices used (Fig. 1).

The tests targeted the dynamic behaviour of the drive system with medium pressure pneumatic actuators with controlled load for step, ramp and sine wave signal (plotting the BODE diagrams:

attenuation vs. frequency and phase vs. frequency). In order to test other types of pneumatic systems it is required to create the conditions for functioning and data acquisition (pressure, force, displacement), then there can be used the software developed under this project.

**Performances of the dynamic regime** are described by synthetic quality parameters characterizing the unit step response of the system [2]:

- *override*  $\sigma$ ;
- *period of first maximum* or the period of reaching the maximum deviation of the output parameter in the transient regime  $t_0$ ;
- *period of the transient regime*  $t_t$ , defined as the time that elapses from the moment when applying excitation (the input) on the reference channel till the output parameter enters a range of  $\pm (2 \div 5)\% y_s$ ;
- *oscillation parameter*  $\Psi$  represents the relative variation of the amplitudes of two successive exceedances of the same sign of the steady state value,
- *time of oscillations*  $T$  for the damped oscillatory state;
- *number of oscillations*  $N$  if the response crosses a finite number of times the stationary component.

In addition to these key quality indicators, one can define others as well, such as:

- *time of setting*: the moment when the stationary output value is reached for the first time;
- *time of growing*: value of subtangent to  $y(t)$  at  $0.5 y_{st}$ , the tangent being limited by the axis  $t$  and the axis  $y_s$ .

The testing software developed in LabVIEW consists of flowcharts [2], fig. 6a-f, as follows:

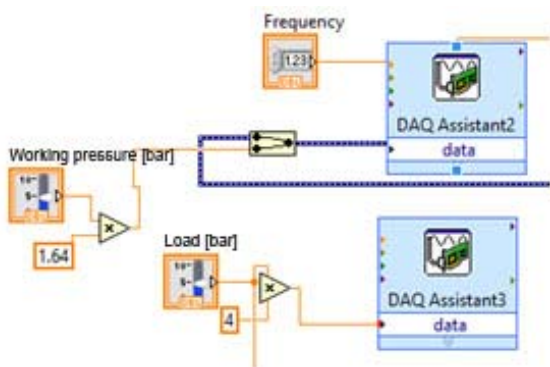


Fig. 6a Control block for proportional pressure regulators

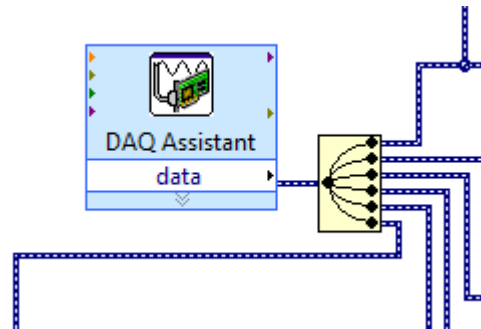


Fig. 6b Block for reading signals from the transducers connected to the inputs AI0...AI4

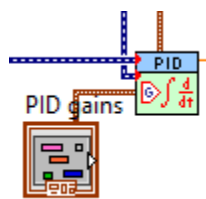


Fig. 6c PID controller block

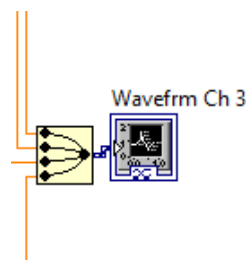


Fig. 6d Block for graphical display of signals

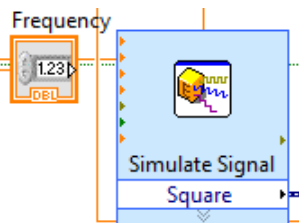


Fig. 6e Step signal generator

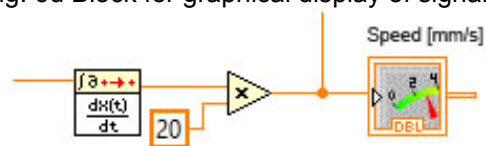


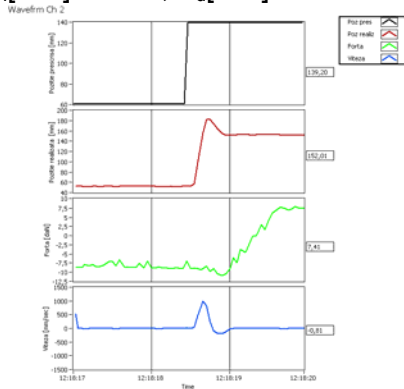
Fig. 6f Speed calculation block

**Fig 6a-f.** Block diagrams of the testing software in LabVIEW

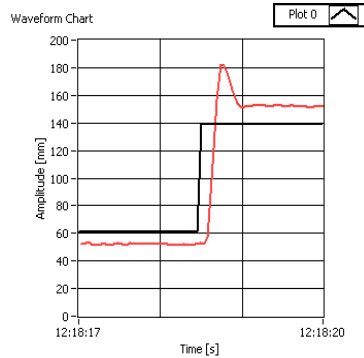
The tests have been carried out in a dynamic regime according to the test methodology, as follows:

**The response of the system to step signal in dynamic regime, with preset load \*the variable parameter  $p_s$ - the pressure generating the load of the drive actuator**

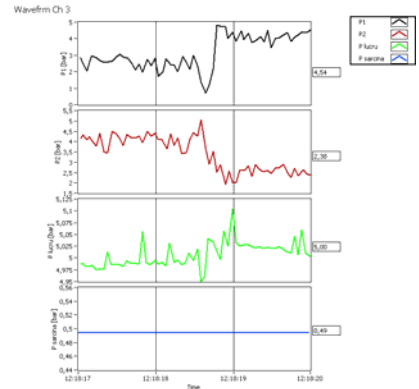
The input parameters of the system for which testing has been carried out were: the load generating pressure  $p_s=0.5$  bar; the parameters of the automatic control system:  $k_c=0.500$ ;  $T_i[\text{min}]=0.500$ ;  $T_d[\text{min}]=0.000$ .



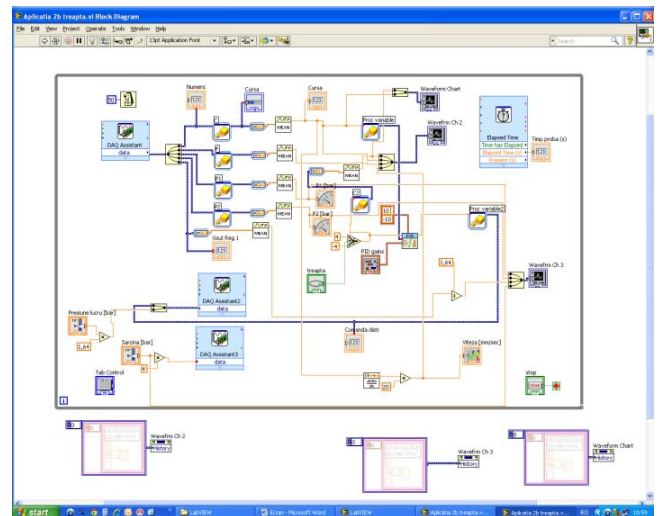
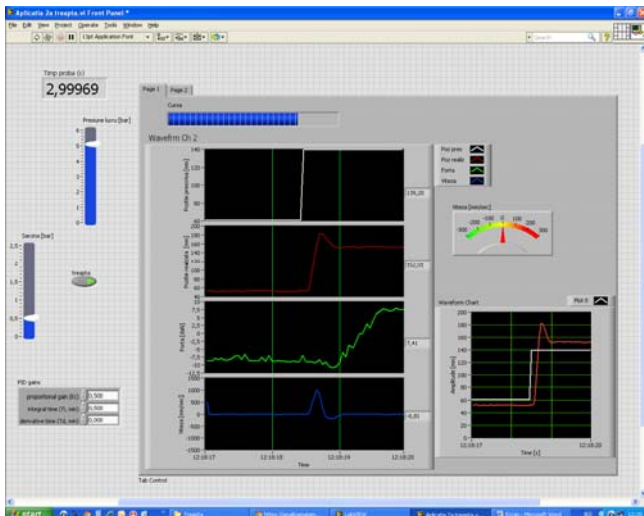
Window displaying prescribed position [mm], achieved position [mm], force [daN], speed [mm/s]



Window displaying amplitude [mm]=f(t) [s]



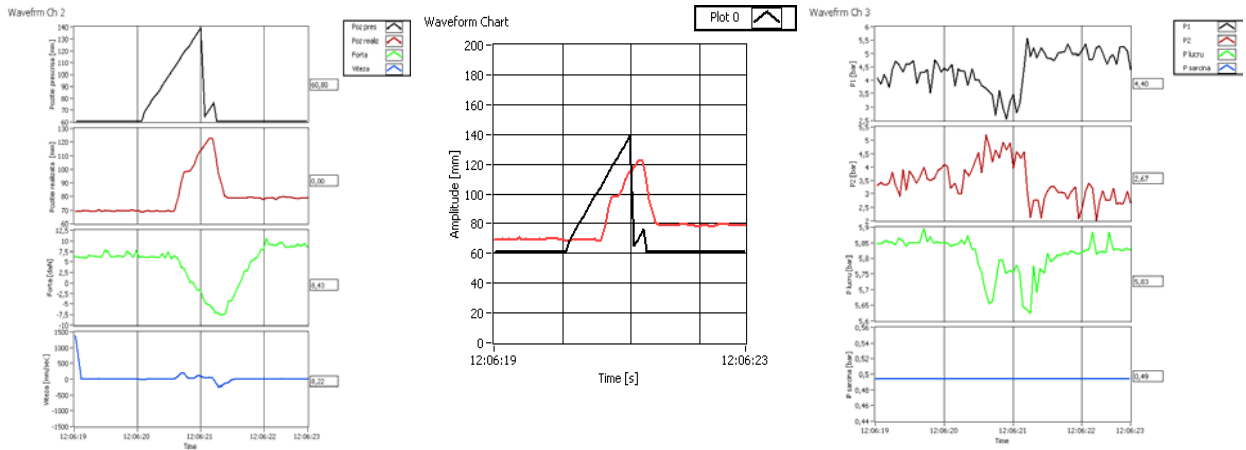
Window displaying the pneumatic parameters of the drive actuator: pressure in piston chamber  $p_1$  [bar], pressure in rod chamber  $p_2$  [bar], working pressure  $p_1$  [bar], load generating pressure  $p_s$  [bar]



Screen capture highlighting the step signal parameters: prescribed position [mm], achieved position [mm], amplitude [mm], pneumatic parameters of the drive actuator: working pressure  $p_1$  [bar], load generating pressure  $p_s$  [bar], parameters of the PID automatic controller:  $k_c$ ,  $T_i$ ,  $T_d$

**The response of the system to ramp signal in dynamic regime, with preset load \*the variable parameter f-signal frequency, Hz**

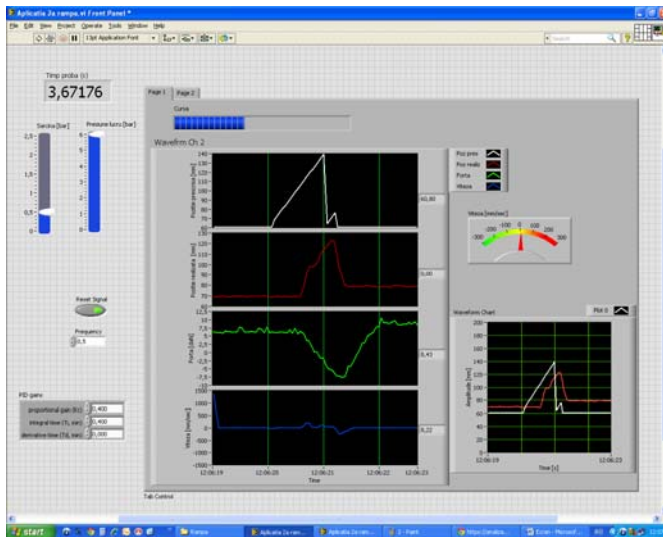
The tests have been carried out for load generating pressure  $p_s=0.5$  bar; working pressure of the drive actuator  $p_1=6$  bar; parameters of the automatic control system:  $k_c=0.400$ ;  $T_i[\text{min}]=0.400$ ;  $T_d[\text{min}]=0.000$ ; f-variable signal frequency,  $f=0.05-0.5$  Hz, with increments of 0.25 Hz.



Window displaying prescribed position [mm], achieved position [mm], force [daN], speed [mm/s]

Window displaying amplitude [mm]=f(t) [s]

Window displaying the pneumatic parameters of the drive actuator: pressure in piston chamber  $p_1$  [bar], pressure in rod chamber  $p_2$  [bar], working pressure  $p_i$  [bar], load generating pressure  $p_s$  [bar]



Screen capture highlighting the ramp signal parameters: prescribed position [mm], achieved position [mm], amplitude [mm], pneumatic parameters of the drive actuator: working pressure  $p_1$  [bar], load generating pressure  $p_s$  [bar], parameters of the PID automatic controller:  $k_c$ ,  $T_i$ ,  $T_d$

**The response to sine wave signal (plotting the BODE diagram)**

Tests are conducted in dynamic regime, on the device set up based on the pneumatic diagram with load controlled by proportional pressure regulator valve, Fig. 3.

The testing software, developed in LabVIEW, consists of block diagrams, Fig. 7, as follows [2]:

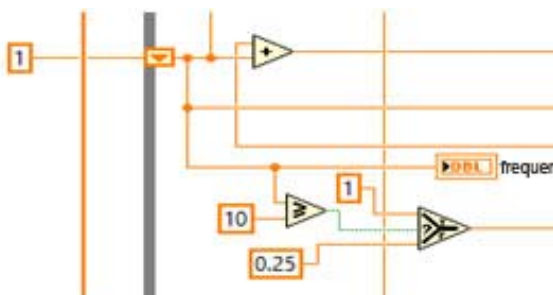


Fig. 7a Generating of frequency pitches (increments) for testing

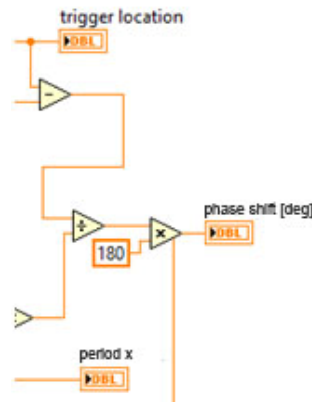


Fig. 7b Phase shift calculation

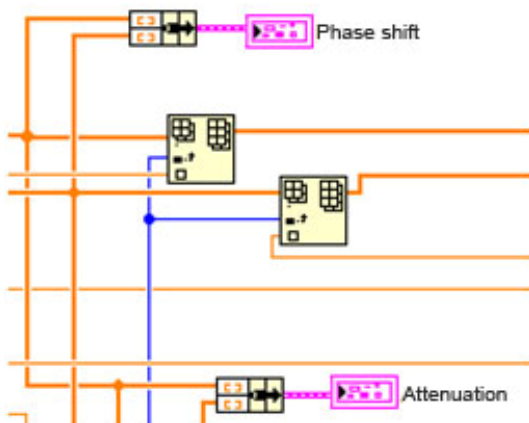


Fig. 7c Displaying of phase shift and attenuation charts

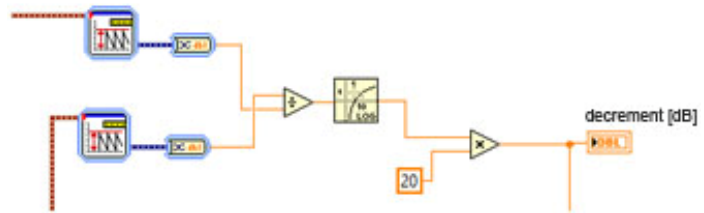


Fig. 7d Decrement calculation

### Attenuation vs. frequency graph (the response to sine wave signal)

It consists in an analysis of the positioning system response when a sine wave variation of the electrical control signal is applied to it, in a relevant frequency range.

a) By means of the signal generator there is applied a sine wave signal of  $\pm 15$  V amplitude and 1-3 Hz frequency, with increments of 0.25 Hz. Using the data acquisition system there is recorded variation over time of the electric signal controlling position and stroke achieved by the rod of the positioning system [3].

b) The attenuation vs. frequency graph is plotted directly on the screen in real time using a software developed in LabVIEW which records on the chart the amplitude values for each frequency incremented in pitches of 0.25 Hz; there is calculated the ratio of amplitude of oscillations of the cylinder rod ( $U_t$ ) and amplitude of oscillations of current signal ( $U_c$ ), and it is introduced in the calculation formula of attenuation to frequency, A:

$$A \text{ (dB)} = -20 \lg \frac{U_t}{U_c}$$

where:

$U_t$  – amplitude of oscillations of the cylinder rod;  $U_c$  – amplitude of oscillations of control signal.

With the resulted values there is plotted the attenuation vs. frequency curve in the BODE diagram.

**Phase shift vs. frequency graph** is plotted like this:

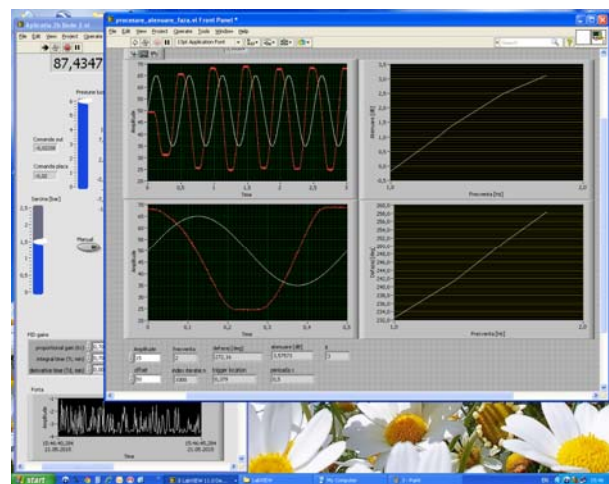
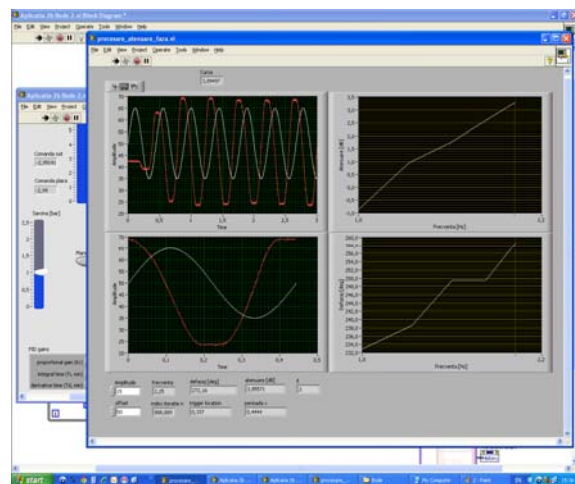
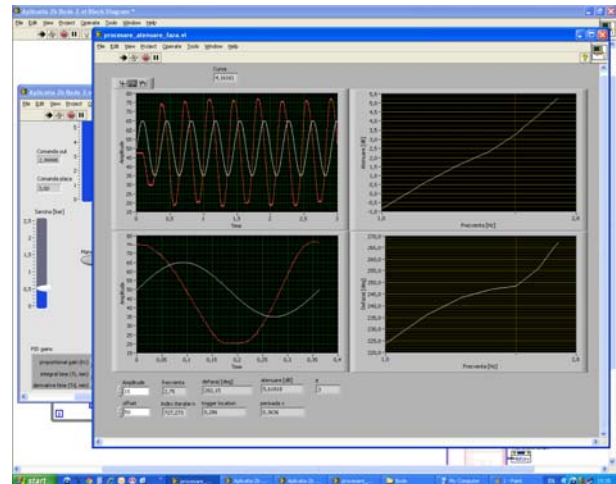
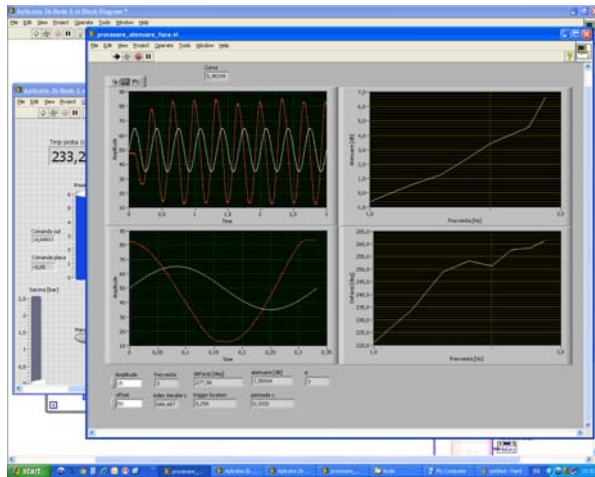
After reading the values  $\Delta t$  and  $T$  on the chart, for each frequency incremented in pitches of 0.25Hz, there is calculated the phase shift between the cylinder stroke and the control signal [1]:

$$\varphi [^\circ] = \frac{\Delta t}{T} \times 360^\circ$$

where:  $\varphi$  - phase shift;  $\Delta t$  – time difference between the intersection of control signal curve with time axis and the intersection of cylinder stroke with time axis on a half period;  $T$  – control signal period.

There are registered points until attenuation decreases by 15 dB or the phase shift exceeds the value of  $120^\circ$ . With the resulted values there is plotted the phase shift vs. frequency curve in the BODE diagram.

The tests have been carried out for values of the load generating pressure  $p_s$  ranging between 0-2 bar, with increments of 0.5 bar; the parameters of the automatic control system:  $k_c=0.700$ ;  $T_i[\text{min}]=0.700$ ;  $T_d[\text{min}]=0.000$ ; amplitude of the sine wave signal  $\pm 15$  [% of the drive actuator stroke]; sine wave signal frequency  $f=1-3$  Hz, with increments of 0.25 Hz.



## 5. Conclusions

Results of these tests highlight the system behaviour for various values of parameters of the PID automatic controller:

- the  $P$  type controller appreciably reduces the overshoot, leads to a short transitional period but introduces a large stationary error  $\varepsilon_{st}$ ;
- by introducing the component  $I$ , the  $PI$  type controller cancels the stationary error at step input, but leads to an overshoot higher than the one at the  $P$  controller and an increased value of response time;
- by introducing the component  $D$ , the  $PD$  type controller improves the dynamic behavior (overshoot  $\sigma$  and duration of transitional period are low), but maintains a large stationary error;
- the  $PID$  type controller, combining the effects  $P$ ,  $I$  and  $D$ , provides superior performance both in a stationary and in a transient regime.

The system under tests had a steady behavior for values of the PID parameters ranging between:  $K_c=4.000-6.000$ ;  $T_i=5.000-6.000$ ;  $T_d=0.001$ .

## References

- [1] R. Radoi, M. Blejan, I. Dutu, Gh. Sovaiala, I. Pavel, Determining the step response for a pneumatic cylinder positioning system, *Hidraulica* no. 2/2014, pp. 25-31;
- [2] A. Drumea, Control of industrial systems using Android-based devices, 36th International Spring Seminar on Electronics Technology ISSE 2013, May 2013, pp. 405-408;
- [3] R. Radoi, I. Dutu, G. Matache, Considerations on the dynamic testing of pneumatic equipment, *Hidraulica* no. 3/2013, pp. 97-100.

## Laboratory Experiments Made on Corrugated Metallic Capsules, for Selecting Optimal Sensitive Elements in Pressure Transducers Used in Modern Mechatronics Systems

PhD Eng. **Iulian Sorin MUNTEANU**<sup>1</sup>, St. PhD Eng. **Anghel CONSTANTIN**<sup>1</sup>,  
PhD Eng. **Petre MUNTEANU**<sup>2</sup>

<sup>1</sup> National Institute of Research and Development in Mechatronics and Measurement Technique, munteanu75@gmail.com; anghel.constantin@incdmtm.ro;

<sup>2</sup> Expert freelance, petre.munteanu@gmail.com

**Abstract:** *This work focuses on laboratory experiments and researches carried out in laboratory environments, in order to obtain the “useful deformations” of the behaviour of corrugated metallic capsules – which are very imported for optimal dimensioning of sensible elements of low pressure transducers. This research provides real information needed in the construction of precision transducers for low pressure, having corrugated metallic capsules as sensitive elements.*

**Keywords:** *low pressures, sensitive elements, corrugated capsules, transducers for low pressures*

### 1. Introduction

A team of specialists made efforts to create a low pressure measuring device with high accuracy class (0.25%), which falls into the category of standard measuring devices which can check less precise measuring devices, in safe and efficient way.

The authors studied the comparative performance of different transducers with pressure sensor type “corrugated capsule”, having incorporate systems of mechanical compensation of errors due to temperature variations, designing and developing a performance constructive solution with competitive and important advantages, such as: stability and better accuracy, sensitivity and high reliability, operating within tolerable error in the range 5°C ... 55°C.

There have been studied and experimented several corrugated metallic capsules (having minimum geometric dimension) that falling within the rigid centre displacement of 1 mm in the range of maximum 1000 mbar (including subdomains 0 ... 40 mbar, 0 ... 80 mbar, 0 ... 100 mbar, 0 ... 160 mbar, 0 ... 200 mbar), based on experimental observation that efficient use of inductive coils into an inductive transducer occurs for a displacement of 1 mm of ferromagnetic core (linear hysteresis area).

### 2. Innovative equipment developed for conducting practical experiments on different types of corrugated metallic capsules

The accumulated experience in several years of research and development has led to the development and creation of an special innovative equipment for experiments (named „MCDR-MM-01”) used when carrying out experiments, and it was designed, assembled and used for precision determinations, according to internal norms and the procedures in accredited laboratories.

The special innovative equipment - MCDR-MM-01 for measuring the useful deformation of corrugated metallic capsules, working at low pressures, has the following components:

- a precision manometer with a maximum of 100 mbar range,
- an instrumental air source,
- a subassembly for mounting watertight capsule,
- a subassembly for reading (showing) deformation of the capsule made up from a micro-meter that ensures a proper visualization of the corresponding deformation for a certain work pressure and a signalling device for instantaneous contact between the prod (feeler pin of micrometric

screw) and the superior membrane of the corrugated metallic capsule (which is tested about maximal deformation obtained on upper surface),

- a digital thermometer for indicating temperature inside the laboratory,
- a barometer – for checking atmosphere pressure.



**Fig. 1. MCDR-MM-01** - The equipment for measuring the deformations of corrugated capsules, when into these capsules are applied low pressures

With the support of MCDR-MM-01 equipment was made more substrings measurements on several types of corrugated capsules in order to determine the best solution of a curled capsule that can provide useful deformation desired, according to pre-calculations made in the design stage for executed a sensitive element with corrugated capsule for a high efficient inductive transducer.

We measured useful deformations for 40 corrugated capsules, but following the centralization of the results obtained, it was found that the optimal output parameters are supplied of the following measures:

- measuring the deformations corresponds to some points of applied low pressures, for corrugated copper-beryllium capsules, having a diameter of 60 mm, a radius of the tightened centre of 6 mm, with 6 sinusoidal corrugations, with height of the first 5 undulations of 1.1 mm, and thickness variables – the row of values in: {0.2; 0.22; 0.25} [mm] – there have been obtained some pairs of values (“p -  $w_{\text{capsule}}$ ”) recorded in the following tables, then we used these results to draw characteristics “pressures - deformations” of the corrugated capsule (“p -  $w_{\text{capsule}}$ ”), in order to examine graphic the differences resulting and make the right decision for stage of practical execution of a precision transducers for low pressure.

Table 1 - contains the values of the pressure needed to displace the rigid centre of the measuring capsule (having a thickness 0.2[mm]) with a “useful deformations” (“offset”) of 0.94 mm, and fig.2 depicts the characteristics “pressures–deformations” for corrugated metallic capsule, within the domain 0... 40 mbar;

**TABLE 1:** Values for “pressures–deformations” into domain 0...40 mbar

<b>p [pressure][bar]</b>	0	0.01	0.02	0.03	0.04
<b><math>w_{\text{capsule}}</math> [mm]</b>	0	0.24	0.46	0.70	0.94

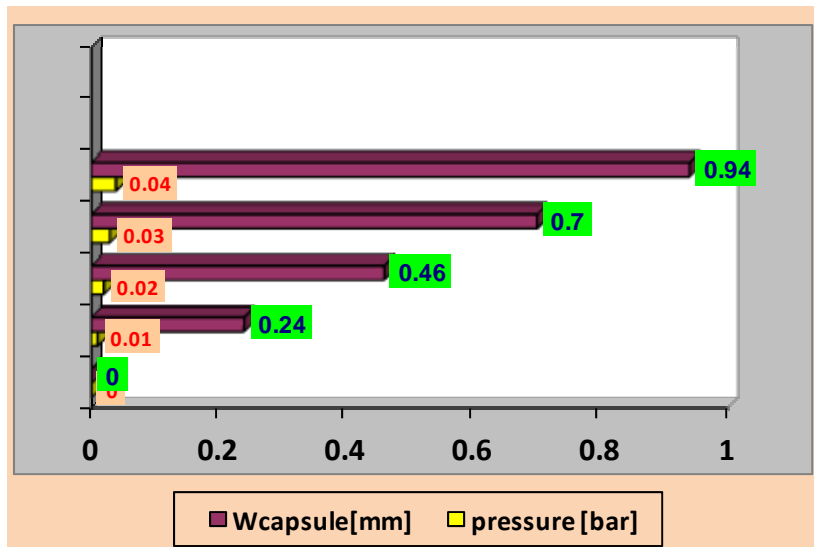


Fig. 2. The characteristics "pressures–deformations" for low pressure applied on corrugated metallic capsule, within the domain 0... 40 mbar

Table 2 contains the values of the pressure needed to displace the rigid centre of the measuring capsule with a “useful deformations” (“offset”) of 1.46 mm, and fig. 3 depicts the characteristics "pressures–deformations" for corrugated metallic capsule, within the domain 0... 60 mbar;

TABLE 2: Values for "pressures–deformations" into domain 0...60 mbar

p [pressure ][bar]	0	0.01	0.02	0.03	0.04	0.05	0.06
w <sub>capsule</sub> [mm]	0	0.24	0.48	0.74	0.98	1.22	1.46

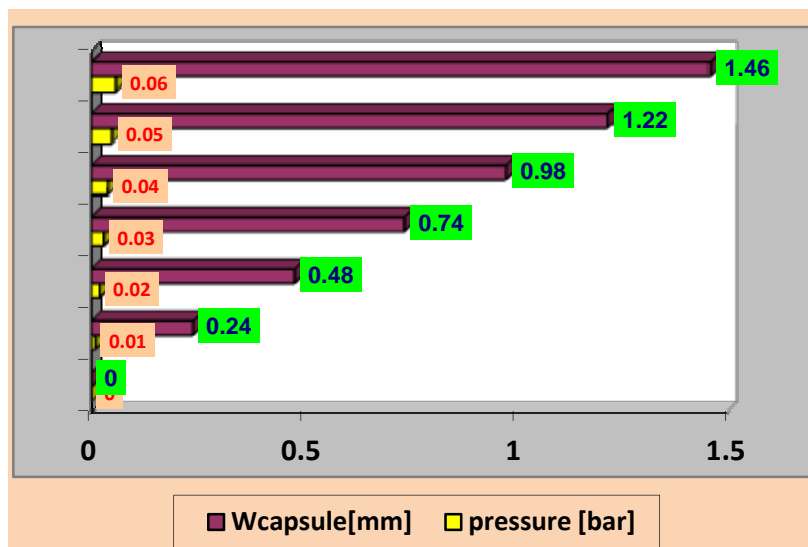
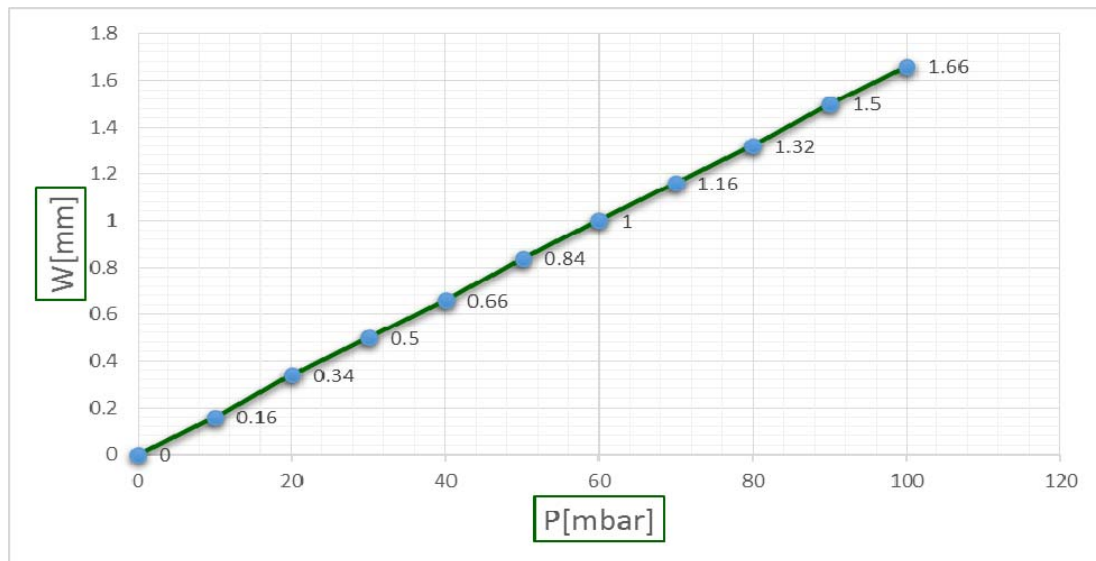


Fig. 3. The characteristics "pressures–deformations" for low pressure applied on corrugated metallic capsule, within the domain 0... 60 mbar

Table 3 contains the values of the pressure needed to displace the rigid centre of the measuring capsule with a “useful deformations” (“offset”) of 1.66 mm, and fig. 4 depicts the characteristics “pressures–deformations” for corrugated metallic membrane/ capsule, within the domain 0...100 mbar;

**TABLE 3:** Values for “pressures–deformations” into domain 0...100 mbar

P [bar]	0	0.01	0.02	0.03	0.04	0.05	0.06	0.07	0.08	0.09	0.1
$W_{cp} = W_{capsule}$	0	0.16	0.34	0.5	0.66	0.84	1	1.16	1.32	1.5	1.66



**Fig. 4.** The characteristics “pressures–deformations” for low pressure applied on corrugated metallic membrane/ capsule, within the domain 0... 100 mbar

Table 4 and fig. 5 contain the values obtained after the experiments took place.

The pressure check was of 100 mbar of a measuring capsule with a 60 mm diameter, a rigid centre radius of 6 mm, with 6 sinusoidal corrugations, wave height of 1.9 mm, with rising and falling pressure.

**TABLE 4:** Different values measured for low pressure into range 0 ... 100 mbar (for increasing pressure and for decreasing pressure)

Pressure [bar] (Pressure rising)	Capsule arrow “Useful deformations”[mm]	Pressure [bar] (Pressure decreasing)	Capsule arrow “Useful deformations” [mm]
0	0	0.1	1.66
0.01	0.16	0.09	1.49
0.02	0.34	0.08	1.32
0.03	0.5	0.07	1.16
0.04	0.66	0.06	1
0.05	0.84	0.05	0.83
0.06	1	0.04	0.65
0.07	1.16	0.03	0.48
0.08	1.32	0.02	0.33
0.09	1.5	0.01	0.16
<b>0.1</b>	<b>1.66</b>	<b>0</b>	<b>0</b>

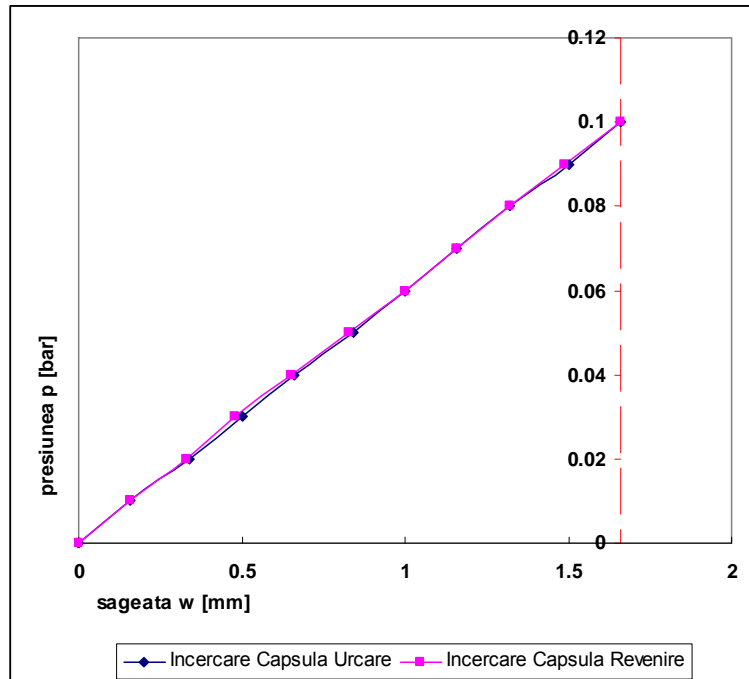


Fig. 5 Values measured for “pressure rising” and “pressure decreasing” for a pressure domain 0 ... 0.1 bar

### 3. Conclusions

After conducting practical experiments on corrugated metallic capsules, with different wall thicknesses, it was desirable a dedicated application software, which can offer an accurate simulation of the behaviour at low pressure applied into corrugated metallic capsules, to compare theoretical and practical results, and finally obtain valuable results, proved technically and mathematically.

This paper focused on laboratory experiments generated results for optimal dimensioning of sensible elements of low pressure transducers. To ensure valuable results, experiments were conducted in rigorously controlled laboratory conditions, with always controlled temperature and maintained at values mentioned in modern standards.

By creating an original device for measuring "useful deformations", real data could be recorded extremely accurately, which subsequently had directed efforts to correct conception of an inductive transducer for low pressures.

### References

- [1] P. Munteanu, I. S. Munteanu, E. Condurateanu, “Independent equipment for measuring, checking and monitoring axle load, using a mechanical weight receiver, generating the increase of safety transportation, in accordance with EU standards”, “Romanian Review Precision Mechanics, Optics & Mechatronics”, No. 27, ISSN 1584-5982, 2005;
- [2] Gh. Gheorghe, I. S. Munteanu, N. Mocanu, S. Sorea, et al., “Sistem mecatronic inteligent de înaltă precizie pentru măsurarea microdeplasărilor liniare în medii industriale și de laborator”, Revista Automatizări și Instrumentație, No. 2, ISSN 1582 – 3334, 2007;
- [3] I. S. Munteanu, P. Munteanu, “Experimental researches regarding compensating errors due to the influence of environment for an apparatus of control and adjustment of pressure”, Proceedings of the Annual Symposium of the Institute of Solid Mechanics and Session of the Commission of Acoustics SISOM & Acoustics 2009, Ed. Mediamira, ISSN 2068-0481, May 28-29, 2009;
- [4] Patent No. 122745 – OSIM, “Micromanometru” / Micromanometer ([http://www.osim.ro/publicatii/brevete/bopi\\_2009/bopi\\_inv\\_1209.pdf](http://www.osim.ro/publicatii/brevete/bopi_2009/bopi_inv_1209.pdf))
- [5] Patent No. 123375 – OSIM, “Presostat cu dispozitiv optoelectronic” / Pressure switch with optoelectronic device ([http://www.osim.ro/publicatii/brevete/bopi\\_2011/bopi\\_inv\\_11\\_2011.pdf](http://www.osim.ro/publicatii/brevete/bopi_2011/bopi_inv_11_2011.pdf) data eliberării 30.11.2011)

## Innovative Systems for Incremental Positioning in Pneumatics

Prof. **Mihai AVRAM** PhD<sup>1</sup>, Prof. **Constantin BUCȘAN** PhD<sup>1</sup>, Prof. **Valeriu BANU** PhD<sup>1</sup>

<sup>1</sup> "Politehnica" University of Bucharest, 313 Spl. Independentei, Bucharest, mavram02@yahoo.com

**Abstract:** The paper presents the structure and functioning of two pneumatic linear incremental positioning systems and the experimental models designed and built in order to determine their performances.

**Keywords:** pneumatics, incremental positioning, positioning accuracy

### 1. Introduction

More and more pneumatic applications require the accurate positioning of the actuated load in certain points of the working stroke. The number of stop points is very important when solving this problem. If the number of stop points increases, the accurate positioning is more difficult to obtain. There are efforts to build some special motors, but the results are not widely used.

It is well known that the accurate positioning of the pneumatically actuated load can be done only in two points of the working stroke: the stroke ends or intermediate positions within the stroke, materialized by mechanical stoppers. Without stoppers, it is difficult to control the stopping of the load in any point within the stroke due to air compressibility [1].

If the number of stop points is limited it is possible to design different actuating systems to accomplish the task. A number of such systems are presented in [2].

### 2. Proposed positioning systems

Two pneumatic linear incremental positioning systems are further presented.

The first pneumatic linear incremental positioning system is based on the principle scheme presented in [3]. In order to build an experimental model, four commercial dosing cylinders were used. Figure 1 shows the functioning scheme of the system.

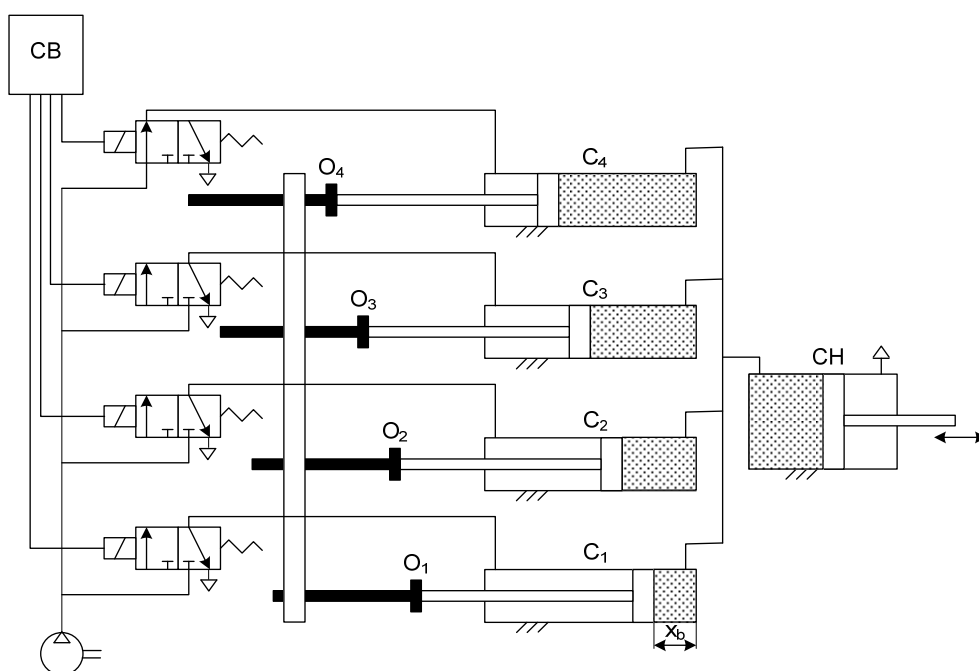
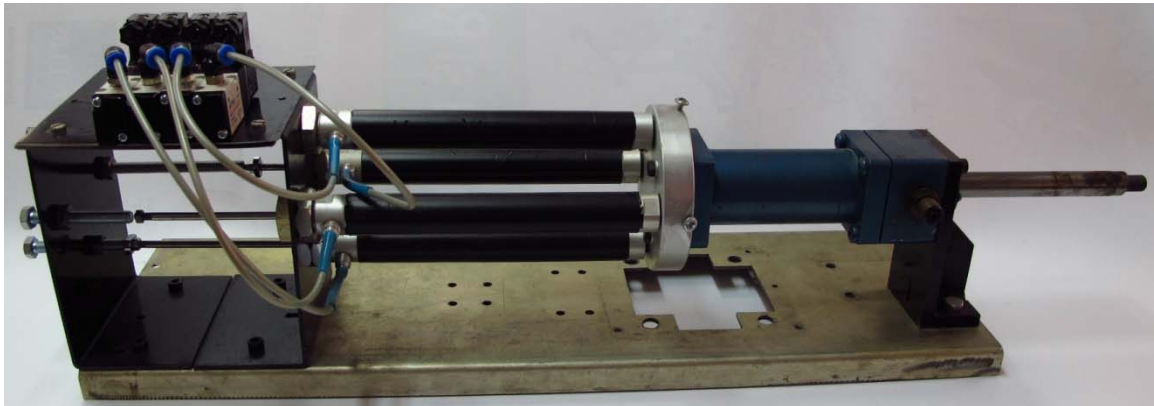


Fig. 1. The functioning scheme of the pneumatic linear incremental positioning system

Based on the scheme in figure 1 and imposing the design parameters, the composing elements of the system (way valves, dosing cylinders, main cylinder, connecting circuits) were dimensioned. The 3D model was designed and the experimental model shown in figure 2 was built.



**Fig. 2.** A view of the experimental model of the pneumatic linear incremental positioning system

The axial positions of the stoppers  $O_1$ ,  $O_2$ ,  $O_3$  and  $O_4$  must be properly adjusted in order to limit the active strokes of the cylinders to the values:

$$\begin{cases} x_1 = 2^0 \cdot x_b \\ x_2 = 2^1 \cdot x_b \\ x_3 = 2^2 \cdot x_b \\ x_4 = 2^3 \cdot x_b \end{cases} \quad (1)$$

If the value of the step has to be changed, a new adjustment must be done, respecting the conditions (1).

The control of system can be performed by various methods: a PC with a data acquisition board and an adapting electronic circuit, a programmable automaton or a microcontroller.

The experimental model tested in the Control and Robotics Laboratory of the Mechatronics and Precision Mechanics Department was controlled using a PC and an interface based on dedicated I/O Field Point modules. The working program was developed using the LabView software.

The performed tests showed that the positioning accuracy highly depends on the machining accuracy of the mechanical structure and on the way the volumes  $V_1$ ,  $V_2$ ,  $V_3$ ,  $V_4$ , and  $V$  and the connecting circuits are filled with oil.

The main advantage of the system is the possibility to adjust the step increment  $\Delta$ .

The second system is a pneumatic linear incremental positioning system using a pneumatic step by step turning motor [3,4] and a screw and nut mechanism to transform the rotation in translation movement.

The linear step  $x_p$  depends on the angular step of the motor  $\varphi_p$  and on the pitch  $p$  of the screw:

$$x_p = p \cdot \varphi_p / 360^\circ \quad (2)$$

Equation (2) shows that the positioning accuracy is better as the pitch of the screw is smaller.

The average moving speed is lower because the maximum working speed of the motor is limited.

The elements of the system structure - motor, screw and nut mechanism, guiding, coupling - have direct influence upon the positioning accuracy, repeatability and maximum speed.

The main characteristics of the system are:

- linear increment lower than 1 mm;
- high positioning accuracy;
- average moving speed;
- medium or short strokes (lower than 1000 mm);
- high reliability.

Figure 3 shows the experimental model of the system, with the following structure: the pneumatic step by step rotational motor 1, the coupling 2, the mobile slide 3, the screw 4, the guiding 5, the body 6, the control panel 7, the electronic block 8 and the air supply 9.

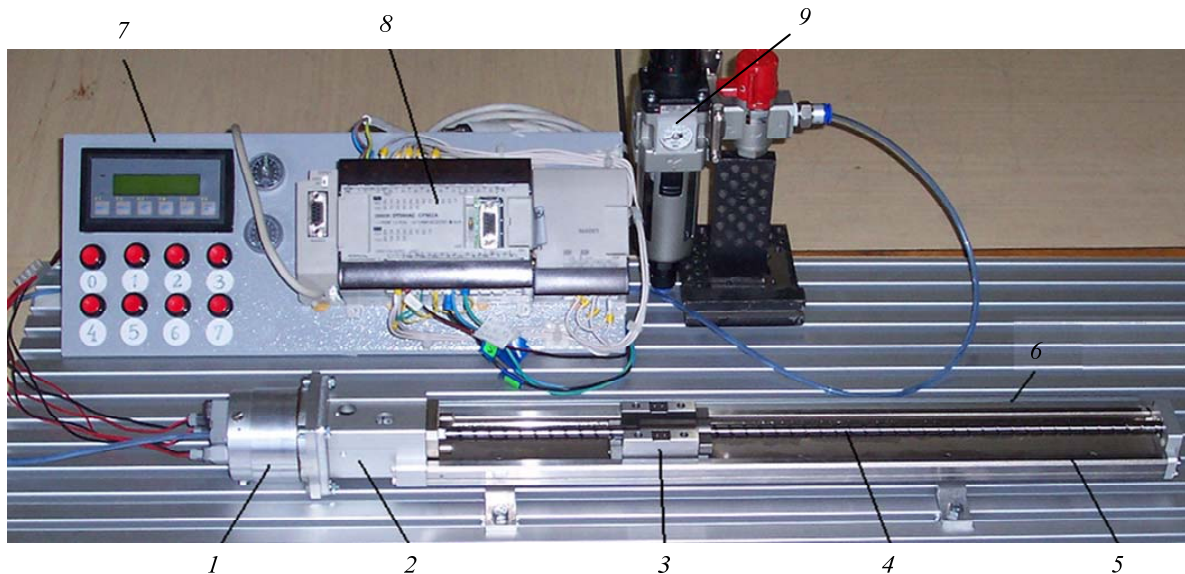


**Fig. 3.** A view of the experimental model of the pneumatic linear incremental positioning system using a pneumatic step by step rotational motor

The following steps were necessary in order to build the experimental model:

- designing and machining of the pneumatic step by step turning motor;
- choosing the mechanical components (screw and nut, guidings etc.) and also the pneumatic and electric components;
- building the mechanic subassembly;
- making the electric and pneumatic connections.

Figure 4 shows a longitudinal section through the pneumatic step by step turning motor. The motor has the following characteristics:

- it is a three phased motor, with six pistons/pegs 4 diametrically opposed, that are simultaneously supplied through some circuits machined in the lid 8, in order to double the couple of the motor; the axial and unilateral placement of the pistons/pegs was chosen in order to minimize the size of the motor;

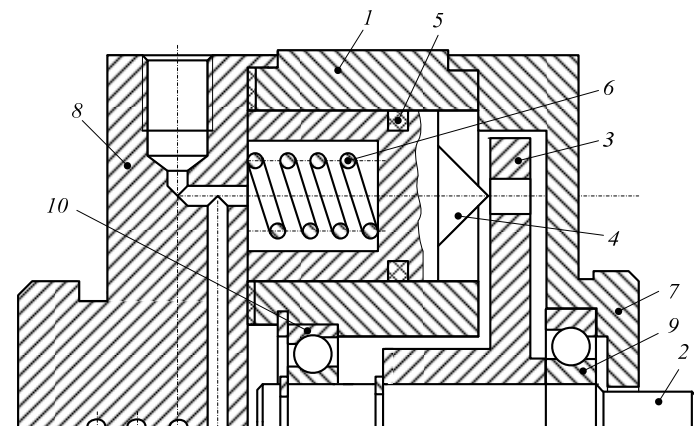


**Fig. 4.** A longitudinal section through the pneumatic step by step rotational motor

- 16 holes are machined on the frontal surface of the disc 3; they are calibrated and equidistant, resulting an angular step of  $7.5^\circ$ ;

- the rotor, consisting of the disc 3 and the shaft 2, can rotate against the stator due to the ball bearings 9 and 10;
- the stator consists of the lids 7 and 8 and the intermediate body 1.

The motor has a compact structure, with the three way valves mounted directly on the distribution plate; this way the working frequency was increased by reducing the length of the signal lines and the dead volumes.

The screw and nut mechanism is of the type LTF6 produced by SMC.

A programmable controller type CPM2A-30 produced by OMRON was used to control the system.

### References

- [1] Anghel, S., Matache, G., Popescu, A-M., Girleanu, I-C., Applications of proportional pneumatic equipment in industry, *Hidraulica*, no. 2/2013, pp. 90-95;
- [2] Avram, M., Acțiunări hidraulice și pneumatice, Echipamente și sisteme clasice și mecatronice, University Publishing House, Bucharest, 2005;
- [3] Avram, M., Bucșan, C., Sisteme de acțiunare pneumatice inteligente, Politehnica PRESS Publishing House, Bucharest, 2014;
- [4] Demian, T., Banu, G. V., Micromotoare Pneumatice liniare și Rotative, Technical Publishing House, Bucharest, 1984.

## Hydrostatic Transmissions Used to Drive a Collapsible Solar Thermal Collector

PhD. eng. **Corneliu CRISTESCU**<sup>1</sup>, PhD. eng. **Radu RADOI**<sup>1</sup>, PhD. eng. **Catalin DUMITRESCU**<sup>1</sup>

<sup>1</sup> Hydraulics and Pneumatics Research Institute INOE 2000-IHP, Bucharest; cristescu.ihp@fluidas.ro

**Abstract:** *This paper presents some considerations regarding the use of renewable energy, and also some results obtained by the institute INOE 2000-IHP Bucharest in promoting advanced technologies and equipment for solar thermal panel technologies, in order to use the renewable energy resources for individual users. There are presented some results obtained in ROMANIA regarding the development of actuation/guidance devices, named hydraulic solar tracking systems, used in construction of equipment for conversion of solar energy directly into thermal energy. Finally, there is presented an experimental model of an collapsible solar thermal collector, developed in the institute INOE 2000-IHP, with hydraulic tracking systems, which allows optimizing the working regimes, in order to increase the efficiency of collecting the solar energy and its adaptation to the variations of thermal loads during the day. The obtained results can be transferred to industry.*

**Keywords:** *renewable energy, solar energy, solar thermal panel, solar tracking systems, hydraulic orientation/guidance system*

### 1. Introduction

The Romanian government has developed the **Romanian Energy Strategy** for the period 2007 - 2020 updated for the period 2011 - 2020, in which, for the country's **sustainable development**, there have been set a number of objectives including: increasing the energy efficiency; promoting energy production based on renewable resources; promoting the production of electric and **thermal energy** in cogeneration plants; supporting research, development and dissemination of applicable research results; reducing the negative impact of the energy sector on the environment; rational and efficient use of primary energy resources [1]. For **sustainable development of the country, it is necessary to promote** energy production from renewable sources, so that the share of electricity produced from these sources of the total gross electricity consumption to be 35% in 2015 and respectively 38-40 % in 2020. **24%** of the gross domestic **energy** consumption will be supplied from renewable sources in 2020.

In the Strategy there is stated that because conventional energy resources are exhaustible, the only possible way to ensure coverage of increasing energy demand in Romania will be by increasing the use of renewable energy.

Also, in this Strategy there are presented the Renewable energy sources in Romania, mentioned in the National Action Plan for Renewable Energy (*PNAER*) – 2010 [2].

**Solar energy** is the energy emitted by the Sun, being a renewable energy source (Wikipedia). At European level, respectively, in Romania, the distribution of solar radiation is shown in Figures 1 and 2. The sun is a source of free and environmentally friendly energy. The average annual solar radiation in Romania varies from 1100 to 1300 kWh /m<sup>2</sup> for more than half of the country territory.

**The use of solar energy potential** is done by solar thermal and photovoltaic systems (photovoltaic conversion). Solar thermal systems are used for the production of heat and domestic hot water for individual households and centralized small power units. For use with high efficiency of solar energy, it is recommended that these systems operate in hybrid mode along with other conventional or non-conventional heating systems. The potential usable in solar thermal systems is estimated at about 1.434 million Toe (tones of oil equivalent).

Considering the European strategy on increasing the contribution of **renewable energy sources** to achieve **the goal of 20%** renewable energy contribution of the total energy used by each EU Member State, by 2020, through the **European Solar Thermal Industry Federation** (ESTIF) it was established that, **by 2020, 50% of energy** used for heating /cooling should be obtained from solar thermal systems.

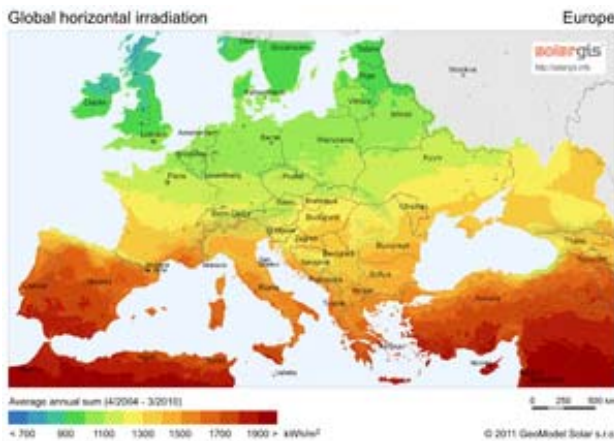


Fig. 1. Solar map of Europe

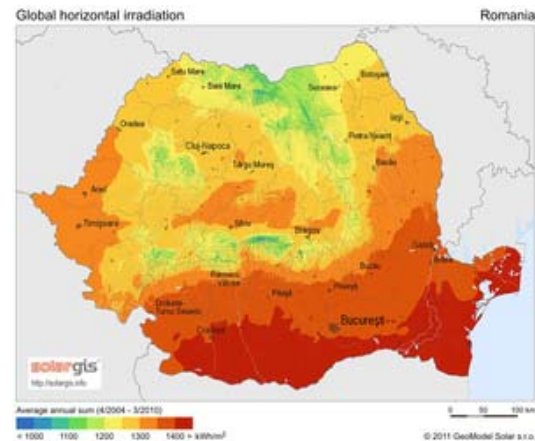


Fig. 2. Solar map of Romania

The use of renewable energy sources required continuous development of manufacturing and implementation technologies of renewable energy conversion systems in order to identify solutions characterized by high efficiency, low cost, reliability and adaptability to implementation conditions. The solar thermal energy is the cleanest source of energy and is practically inexhaustible. It can be captured using **solar thermal panels** that directly absorb the heat of the sun and deliver it to some hot water tanks, to provide domestic hot water or for contribution to heating a house or a pool. Therefore, in our institute there have been also conducted a number of projects at national level for the development of solar thermal energy collecting technologies, which bring great economic benefits to the users.

## 2. Conversion of solar energy into thermal energy

**The sun** is the source of life on Earth. Earth captures about  $2.8 \cdot 10^{21}$  kJ of total solar radiation emitted [3]. Direct radiation, received on the earth's surface, is influenced by the coverage of the sky with clouds. Another important factor influencing the **intensity of solar radiation** is the relative position. Majority of the energy from the sun, about 95%, has **wavelengths between 0.3 and 2.6 mm**, and only 1% has wavelengths greater than 4.0 mm. In **solar thermal applications** the spectrum of interest is the **infrared** one for direct heating and the **visible spectrum** for solar-thermal conversion.

Among the types of solar energy conversion, **photothermal conversion** presents a particular interest in all branches of activity, as the heat generated can be used directly (stored in various fluid, gas or solid environments) or indirectly (electricity, thermo-chemical transformations etc.). Solar energy is converted by means of solar-thermal collectors (CST) into clean thermal energy used for heating space and domestic water. Harnessing solar energy is achieved by **passive or active systems** [4].

Any black surface exposed to beams, called **absorbing surface**, converts solar energy into heat. This absorbent surface presents the simplest example of **direct converter of solar radiation into thermal energy**, called **flat plate solar collector**. Thermal conversion of solar energy includes several technologies: water heating with flat plate or evacuated tube collectors.

Usually, a solar heat collector looks as in Figure 3.

The main components of a flat plate solar collector, presented in Figure 4, are: black case-5, with thermo-insulation of three walls-4, covered on the front with transparent surface-3. The heat exchanger is of type metal plate-pipe, namely absorbent surface-1 and pipes 2.

**The functioning of the solar collector** is based on the two physical phenomena: the **absorption** by a black body of solar radiation incident on the absorbent surface **and the greenhouse effect** achieved on the transparent surface. In the case of a solar collector there is achieved an artificial greenhouse effect. A surface is transparent to sunlight and opaque for the infrared radiation. Temperature of the absorbent surface increases and heat is conveyed to the water flowing through the pipes 2.



Fig. 3. Flat plate solar heat collector

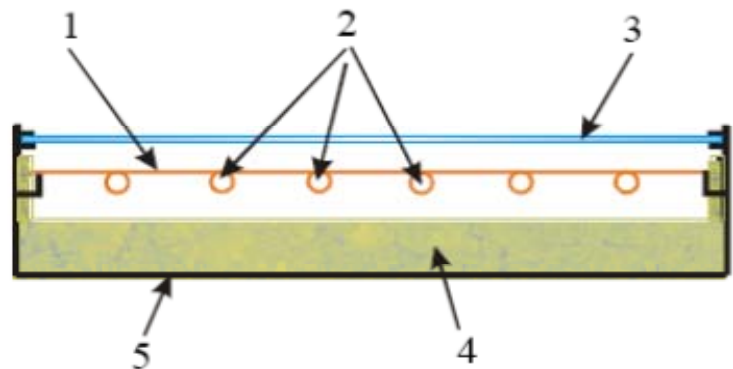


Fig. 4. The components of the solar heat collector

### 3. The hydrostatic transmissions used in actuating solar thermal collectors

In order to increase the efficiency of collecting solar radiation, through guidance around the Sun, in our country there have been developed various guidance means of uniaxial and biaxial mechanisms, based on hydraulic systems, similar to those used for orientation of photovoltaic systems. Moreover, optimization of diurnal orientation of thermal collectors has also the goal of achieving adequate correlation between variations of heat load and solar energy collected.

Sun position is given with reference to the azimuth angle ( $\alpha$ ) and elevation angle ( $\theta_z$ ). In determining the position of the solar radiation collector against the sun, so the yield be maximum, the following angles are important:  $\theta_z$  -zenith angle and solar azimuth angle - $\gamma_s$ , Figure 5, where the  $\gamma_s$  is solar azimuth angle,  $\alpha$  -elevation angle of the sun, zenith angle - $\theta_z$  and hour angle - $\omega$ , [5], [6].

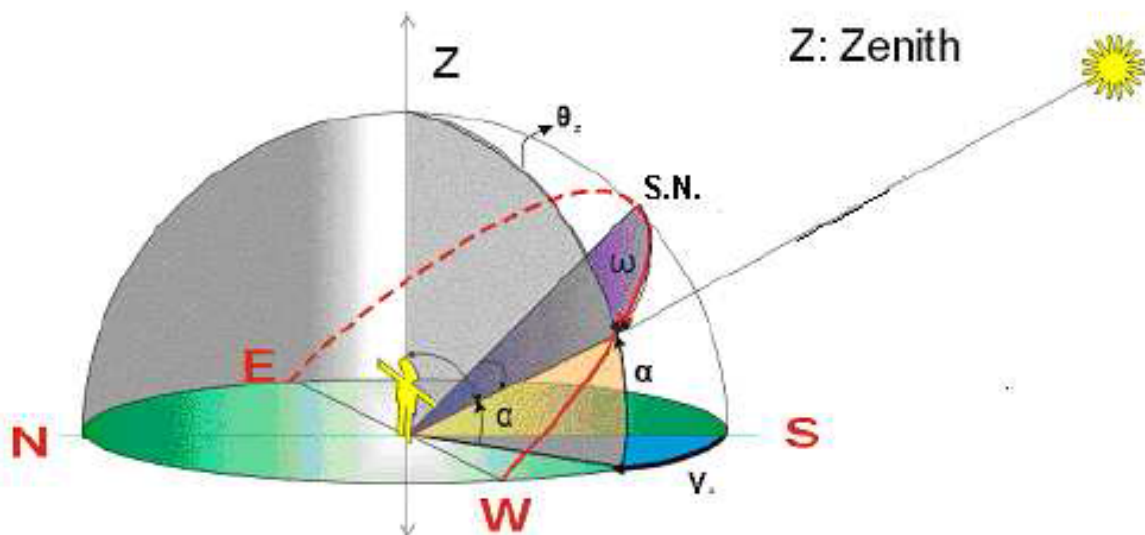


Fig. 5. Trajectory of the sun in the sky- important angles

For orientation around the Sun, in our country there have been analyzed various constructive variants, both uniaxial and biaxial mechanisms, but sometimes in the end the research was focused on the hydraulic uniaxial mechanism, Figure 6.

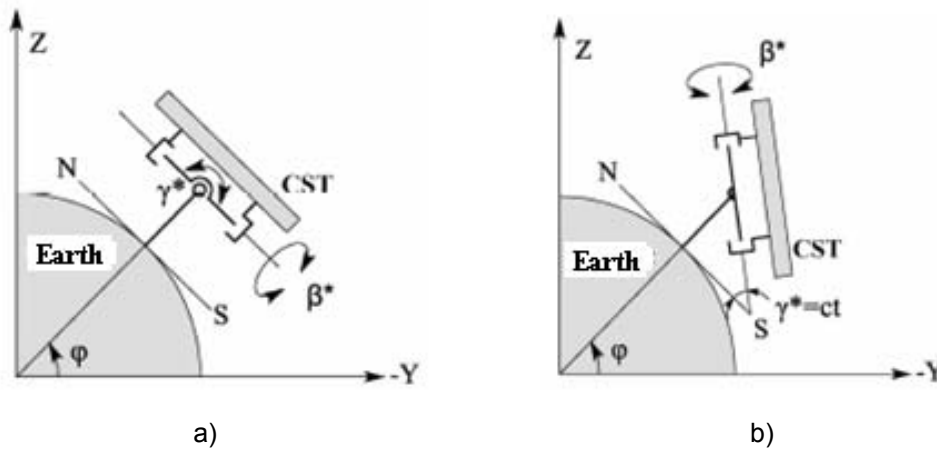


Fig. 6. Pseudo-equatorial guidance systems a) biaxial, b) uniaxial

For example, in a doctoral thesis developed at Transilvania University of Brasov [7], there has been developed a research for understanding and analyzing the hydraulic systems in the structure of equipment for direct conversion of solar energy into thermal energy. They used a common solution to increase the efficiency of collecting solar radiation, through **guidance around the Sun**, by means of mechanisms/**uniaxial hydraulic systems**, similar to those used for orientation of photovoltaic systems.

In **Figure 7**, there is presented the structural diagram of the mechanism **with uniaxial inclined guidance** (a), triangle type with one side adjusted by a linear actuator (hydraulic cylinder), and also **the physical model** (b) of a demonstrator solar thermal system.

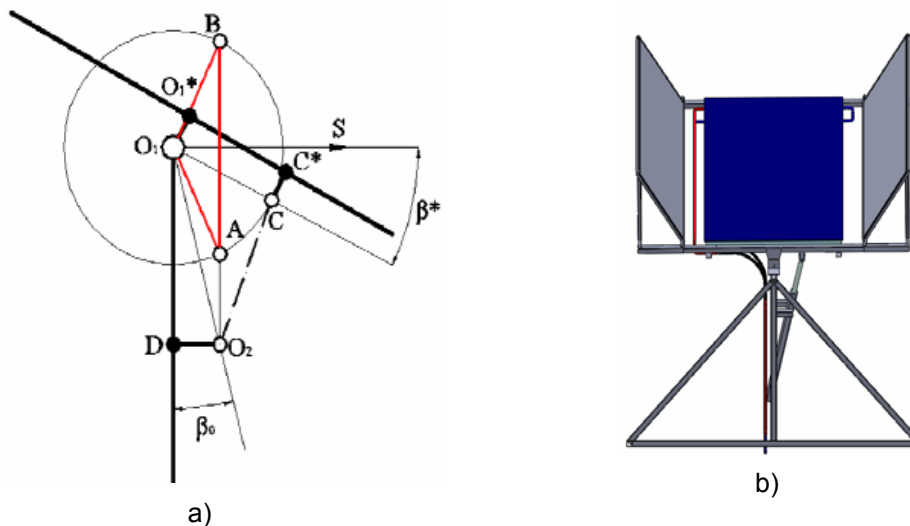


Fig. 7. Uniaxial mechanism for solar thermal panel guidance

In another doctoral thesis, also developed at Transilvania University of Brasov [8], there is proposed a pseudoazimuthal guidance mechanism to perform (diurnal) movement of the solar thermal collector, mechanism shown in Figure 8.

Diurnal movement is performed around an horizontal axis which contains the hinge of the base A, the thermal solar collector being mounted inclined along annual optimal angle of elevation,  $p^*=21^\circ$ .

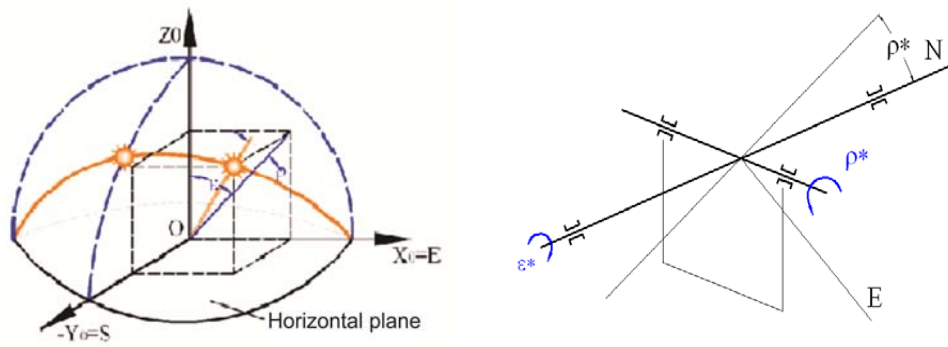


Fig. 8. Pseudoazimuthal guidance system

In Figure 9 there is presented a guidance mechanism with two linear actuators (hydraulic cylinders), arranged in triangle, having an articulated rod with one end hinged to the two actuators (hydraulic cylinders), and the other end hinged to a beam joined with a solar panel. Structural diagram is shown in Figure 9a, and constructive solution in Figure 9b.

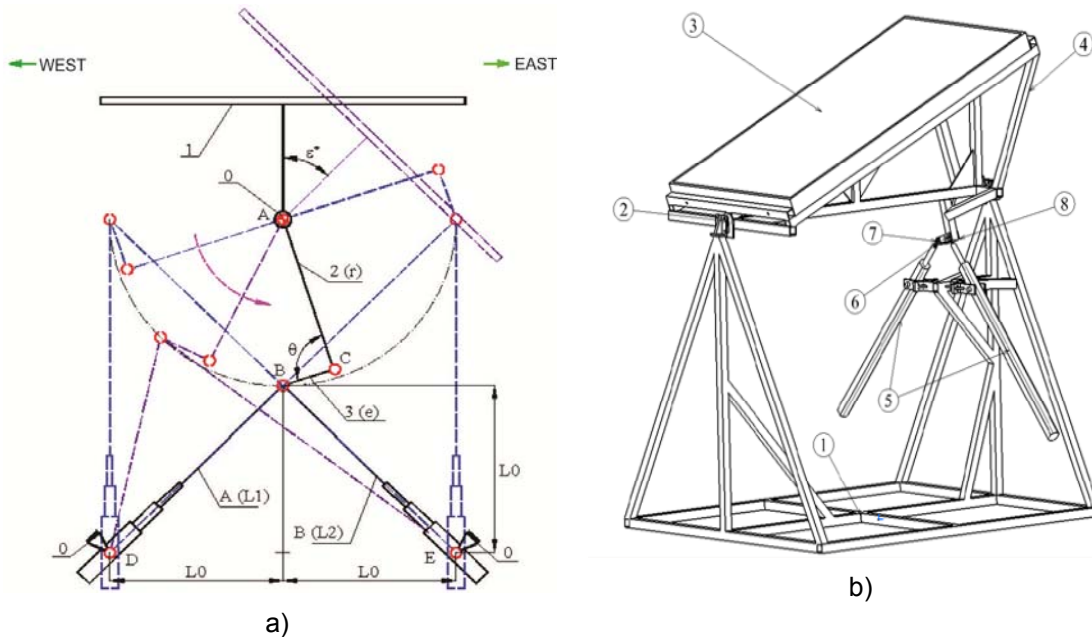


Fig. 9. The guidance mechanism with two linear actuators

Unlike in photovoltaic systems, where controlled guidance is used exclusively in order to increase the efficiency of collecting solar radiation, in the case of thermal collectors, which in addition have large sizes and weight having also to face strong wind, hydraulic drive of guidance trackers proves to be necessary and the best one.

**4. New solution for a solar thermal system with hydraulic drive developed in INOE 2000-IHP**

One of the most difficult problems in the operation of solar thermal collectors is that of the water temperature control, closely related to the thermal load required. Because the commonly used methods of orientation (for example, those in counter phase), do not manage to control strictly the difference between the heat energy delivered by the solar thermal collector and the actual heat load, it has been taken into consideration the development of one new tracking system for solar thermal collectors, which will be able to manage this issue, under more favorable conditions.

Starting from these considerations, in INOE 2000-IHP, there has been developed a novel technical solution for a hydraulic tracker, which consists in achieving a complex movement of the solar thermal collector, tracking as close as possible the position of the sun in the sky by using hydraulic drive mechanisms, both for performing the diurnal movement from east to west (the hourly angle) and for performing the raising movement of the sun in the sky (the elevation angle), in order to maximize the solar energy collected at operation under maximum thermal load, and by using a collapsible solar thermal collector, driven by a special mechanical-hydraulic mechanism, to be able to change the angle of incidence of the solar rays, depending on the thermal load (hot water consumption) [9].

The new solar thermal collector system, which is presented in Figure 10, is made up of a fixed support frame (0), on which there are mounted the 4 basic subsystems / mechanisms, namely: a collapsible solar thermal collector (CSTP), consisting of two semi-collectors / conventional semi-panels (1 and 2), hinged to one another by a tubular shaft (3) with some rotating joints (4), a collapsing mechanism (MPC), Figure 10a, consisting of a hydraulic cylinder (CH1), fixed on the upper underside of the support frame (0), the cylinder rod braket (5) being hinged with a bolt (6) to some thimble bars (7), which are hinged at the other end by bolts (8), to some eyelets (9), mounted on the back side of the two semi-panels (1 and 2) of the collapsible solar thermal collector (CSTP), a mechanism for performing the movement of elevation (MME), Figure 10b, comprising a tilting platform (10) that rotates vertically by means of a joint (11) mounted on the fixed frame (0) and driven by a hydraulic cylinder (CH2), and also a mechanism for performing the diurnal / hourly movement (MMD), similar to that shown in Figure 10a, also driven by a hydraulic cylinder (CH3).

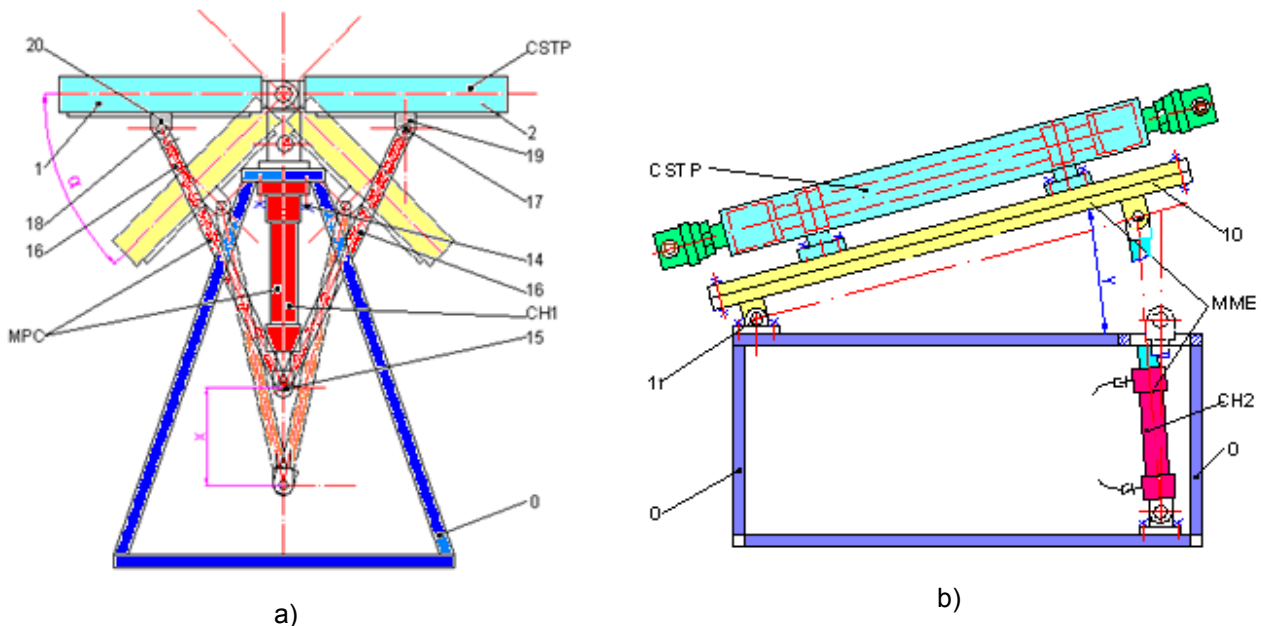


**Fig. 10.** Collapsible solar thermal collector with hydraulically actuated tracker

## 5. Conclusions

The article presents some specific elements of the strategy of Romania on use of renewable energy; it mentions the special solar energy potential that Romania has and briefly presents some concerns of the research work in the Institute INOE 2000-IHP on this matter.

Also, there are presented some concerns in Romania regarding the development of solar thermal collectors, and especially the development of guidance systems (trackers), based on linear actuators (hydraulic or pneumatic cylinders).

There is presented a new technical solution that helps increase the energy efficiency of solar thermal panels by using collapsible panels operated by hydraulic trackers, solution which is under a patenting process.

This new technical solution offers better control on the difference between thermal energy supplied by solar thermal collectors and the actual thermal load.

#### References

- [1] Strategia RO Strategia energetică a României pentru perioada 2007 – 2020, actualizată pentru perioada 2011 – 2020. / *Romanian Energy Strategy for the period 2007 – 2020, updated for the period 2011-2020*. In: [http://www.mmediu.ro/protectia\\_mediului/evaluare\\_impact\\_planuri/2011-11-07/2011-11-07\\_evaluare\\_impact\\_planuri\\_strategiaenergeticaactualizata2011.pdf](http://www.mmediu.ro/protectia_mediului/evaluare_impact_planuri/2011-11-07/2011-11-07_evaluare_impact_planuri_strategiaenergeticaactualizata2011.pdf);
- [2] Planul Național de Acțiune în Domeniul Energiei din Surse Regenerabile/ *National Action Plan for Renewable Energy (PNAER)*. In: [http://www.minind.ro/energie/PNAER\\_final.pdf](http://www.minind.ro/energie/PNAER_final.pdf);
- [3] Studiu privind evaluarea potențialului energetic actual al surselor regenerabile de energie în România / *Study on assessing current energy potential of renewable energy in Romania*. In: [http://www.minind.ro/domenii\\_sectoare/energie/studii/potential\\_energetic.pdf](http://www.minind.ro/domenii_sectoare/energie/studii/potential_energetic.pdf);
- [4] Croitoru, A-M., Analiza posibilităților de utilizare a energiei termice dezvoltate de sistemele fotovoltaice/ *Analysis of the possibility of use of thermal energy developed by the photovoltaic systems*. Doctoral thesis, Politehnica University of Bucharest, 2014.
- [5] Rusănescu C.O., Paraschiv G., Murad E., Dutu M.F., Monitoring solar radiation intensity with sun-earth angle in the year 2011 in the north-west of Bucharest. In: INMATEH –Agricultural Engineering, Vol. 40, No. 2 / 2013, pp. 97-102.
- [6] Cofas D. T., Cofas P. A., Cojocariu C., Costinescu L., Samoila C. (2008), Solar Tracker cu algoritm matematic - National Conference of Virtual Instrumentation, 5th Edition, Bucharest;
- [7] Dombi V.E., Optimizarea orientării colectoarelor solar termice plane funcție de necesarul energetic al unei clădiri/ *Optimization of flat solar thermal collectors orientation depending on the energy load of a building*. Doctoral thesis, Transilvania University of Brasov, 2011;
- [8] Șerban C., Adaptarea sistemului de orientare a colectoarelor solar-termice la necesarul termic al unei clădiri / *Adjusting the tracking system of solar-thermal collectors to the heating load of a building*. Doctoral thesis, Brasov, Romania, 2012;
- [9] Cristescu C., Dumitrescu, C., Ilie, I., Dumitrescu, L., Increasing energy efficiency of the solar thermal panels through the use of hydraulic tracking systems. In: Proceedings of International Multidisciplinary Scientific Geo-Conference SGEM-2014, June 17 – 26, 2014, Albena Co., Bulgaria, Vol.: „Energy and clean technologies”, pp. 291–298, ISBN 978-619-7105-15-5, ISSN 1314-2704, URL: [www.sgem.org](http://www.sgem.org).



<http://hidraulica.fluidas.ro>